



ADDITIONAL MATERIALS AVAILABLE ON THE HEI WEBSITE

Research Report 210

Global Burden of Disease from Major Air Pollution Sources

(GBD MAPS): A Global Approach

Erin McDuffie et al.


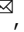






Additional Materials 2: McDuffie EE, Martin RV, Spadaro J, Burnett R, Smith SJ, O'Rourke P, et al. 2021. Source sector and fuel contributions to ambient PM2.5 and attributable mortality across multiple spatial scales. Nat Commun 12:3594; doi:10.1038/s41467-021-23853-y.

Additional Materials 2 was not formatted or edited by HEI. It is distributed under the Creative Commons Attribution 4.0 License. This document was part of the HEI Special Review Panel's review process.

Correspondence concerning the Investigators' Report may be addressed to Dr. Michael Brauer, The University of British Columbia, School of Population and Public Health, 366A – 2206 East Mall, Vancouver, BC V6T1Z3, Canada; e-mail: michael.brauer@ubc.ca, guxens@isglobal.org.

© 2021 Health Effects Institute, 75 Federal Street, Suite 1400, Boston, MA 02110

Source sector and fuel contributions to ambient PM_{2.5} and attributable mortality across multiple spatial scales

Erin E. McDuffie ^{1,2}, Randall V. Martin ^{1,2}, Joseph V. Spadaro³, Richard Burnett⁴, Steven J. Smith ⁵, Patrick O'Rourke⁵, Melanie S. Hammer^{1,2}, Aaron van Donkelaar^{2,1}, Liam Bindle ^{1,2}, Viral Shah^{6,10}, Lyatt Jaeglé⁶, Gan Luo⁷, Fangqun Yu ⁷, Jamiu A. Adeniran⁸, Jintai Lin ⁸ & Michael Brauer ^{4,9}

Ambient fine particulate matter (PM_{2.5}) is the world's leading environmental health risk factor. Reducing the PM_{2.5} disease burden requires specific strategies that target dominant sources across multiple spatial scales. We provide a contemporary and comprehensive evaluation of sector- and fuel-specific contributions to this disease burden across 21 regions, 204 countries, and 200 sub-national areas by integrating 24 global atmospheric chemistry-transport model sensitivity simulations, high-resolution satellite-derived PM_{2.5} exposure estimates, and disease-specific concentration response relationships. Globally, 1.05 (95% Confidence Interval: 0.74–1.36) million deaths were avoidable in 2017 by eliminating fossil-fuel combustion (27.3% of the total PM_{2.5} burden), with coal contributing to over half. Other dominant global sources included residential (0.74 [0.52–0.95] million deaths; 19.2%), industrial (0.45 [0.32–0.58] million deaths; 11.7%), and energy (0.39 [0.28–0.51] million deaths; 10.2%) sectors. Our results show that regions with large anthropogenic contributions generally had the highest attributable deaths, suggesting substantial health benefits from replacing traditional energy sources.

¹Department of Energy, Environmental, and Chemical Engineering, Washington University in St. Louis, St. Louis, MO, USA. ²Department of Physics and Atmospheric Science, Dalhousie University, Halifax, NS, Canada. ³Spadaro Environmental Research Consultants (SERC), Philadelphia, PA, USA. ⁴Institute for Health Metrics and Evaluation, University of Washington, Seattle, WA, USA. ⁵Joint Global Change Research Institute, Pacific Northwest National Laboratory, College Park, MD, USA. ⁶Department of Atmospheric Sciences, University of Washington, Seattle, WA, USA. ⁷Atmospheric Sciences Research Center, University at Albany, Albany, NY, USA. ⁸Department of Atmospheric and Oceanic Sciences, School of Physics, Peking University, Beijing, China. ⁹School of Population and Public Health, University of British Columbia, Vancouver, BC, Canada. ¹⁰Present address: Harvard John A. Paulson School of Engineering and Applied Sciences, Harvard University, Cambridge, MA, USA. ✉email: erin.mcduffie@wustl.edu

Long-term exposure to ambient (outdoor) fine particulate matter less than 2.5 μm in diameter ($\text{PM}_{2.5}$) is the largest environmental risk factor for human health, with an estimated 4.1 million attributable deaths worldwide (7.3% of the total number of global deaths) in 2019¹. Outdoor $\text{PM}_{2.5}$ mass is primarily composed of inorganic ions, carbonaceous compounds (black and organic carbon, including secondary organic aerosol), and mineral dust. Sources include direct emissions such as forest fires and agricultural waste burning^{2,3}, windblown mineral dust from arid regions⁴, and inefficient fuel combustion⁵, as well as secondary emissions from atmospheric chemical reactions between primary gas-phase pollutant precursors. These precursors are emitted from both combustion and non-combustion processes that include residential energy use, on- and off-road vehicles, energy generation, solvent use, industrial processes, and agricultural fertilizer application⁶. Once emitted, the chemical production of $\text{PM}_{2.5}$ mass in the atmosphere is highly non-linear^{7,8}. Due to its myriad of sources and complex formation chemistry, both the total mass and chemical constituents of $\text{PM}_{2.5}$ depend on local environmental conditions, dominant sources, and the magnitude of those source-specific emissions. In addition, as air pollution and atmospheric chemistry do not adhere to political boundaries^{9–11}, mitigation efforts require consideration of transboundary effects across multiple locations, informed by studies of $\text{PM}_{2.5}$ source contributions and the attributable disease burden across a range of sub-national to global scales.

Source contribution studies across multiple spatial scales help to inform specific mitigation strategies and prioritize limited resources for effective action¹². A large number of previous studies have used chemical observations or dispersion-based models to quantify sources of $\text{PM}_{2.5}$ mass, but have largely focused on specific locations or short-term events^{13–15}. In comparison, comprehensive assessments of the sources and impacts of $\text{PM}_{2.5}$ across large spatial scales have been relatively limited by available long-term $\text{PM}_{2.5}$ surface measurements. A recent study, for example, found that most countries between 2010 and 2016 had fewer than 10 long-term ground-based $\text{PM}_{2.5}$ monitors per million people, while 60% of all countries had no long-term monitors¹⁶. Therefore, to assess the global and regional $\text{PM}_{2.5}$ disease burden and its source contributions, recent studies have employed 3D chemical transport models as a means to relate changes in surface emissions to atmospheric $\text{PM}_{2.5}$ concentrations. These studies typically use adjoint models, tagged-tracer, or zero-out (brute-force) approaches to assess the influence of individual surface sources on $\text{PM}_{2.5}$ mass and attributable mortality and morbidity. These previous studies, however, have largely focused on individual cities, countries, regions^{11,17–24}, or source sectors^{3,25–35}, often with relatively coarse spatial resolution and emissions that may not reflect current conditions. In contrast, global-scale studies that account for transboundary effects using both consistent methodologies and sectoral definitions across all world regions help to place air pollution in a global context and allow for comparability of the disease burden and its source contributions across multiple locations. Relatively few of these previous global studies, however, have provided an assessment of the contributions from more than one source sector or aggregate fuel category in recent years^{36–40}, thereby limiting their ability to inform or prioritize specific air quality management policies under current global conditions.

In today's rapidly changing society, the accuracy and policy relevance of such global studies is contingent on (1) the availability of contemporary and detailed emission inventories, (2) scientifically rigorous chemical transport models, (3) global fine resolution $\text{PM}_{2.5}$ exposure estimates, and (4) disease-specific concentration-response functions (CRFs) derived from contemporary air pollution epidemiologic studies. First, emission

datasets that capture recent trends are particularly important in highly polluted regions, such as China, India, and Africa, that have experienced large and rapid changes in $\text{PM}_{2.5}$ precursor emissions in the last decade^{6,41,42}. Disaggregation of these emissions across multiple sectors, fuel types, and regions also increases their policy relevance, as detailed source contribution studies can quantify the health benefits from specific and achievable strategies such as transitions away from coal use for energy generation or solid biofuel for residential cooking and heating. Second, to accurately reflect current $\text{PM}_{2.5}$ chemical production regimes under various emission scenarios, 3D atmospheric-chemical transport models require state-of-the-science chemical and physical mechanisms, evaluated against surface observations of $\text{PM}_{2.5}$ mass and composition. Third, to capture and compare national and sub-national impacts across all world regions, these studies additionally require high-resolution $\text{PM}_{2.5}$ exposure estimates, such as those that utilize recent advances in satellite retrievals, chemical transport models, and ground-based monitoring⁴³. Lastly, integration of these source simulations and exposure estimates with updated disease-specific CRFs can motivate policy action by refining previous $\text{PM}_{2.5}$ disease burden estimates^{37,38,44,45}, incorporating spatial variation in the underlying health status and cause of death composition, and by comparably quantifying the dominant sources of this burden across global, national, and sub-national scales.

In this study, we integrate the emissions, modeling, $\text{PM}_{2.5}$ exposure, and CRF components described above to provide a globally comprehensive and contemporary source categorization of $\text{PM}_{2.5}$ mass and the attributable disease burden. In this work, we identify residential energy use, industrial processes, and energy generation as dominant sectors contributing to global $\text{PM}_{2.5}$ exposure and its attributable mortality. We also find that eliminating fossil fuel combustion emissions would substantially reduce (>25%) the global disease burden attributable to annual $\text{PM}_{2.5}$ exposure, with over half of this contribution from the combustion of coal. While the relative contributions from individual sectors and fuels vary across national and sub-national scales, the comprehensive nature of this work provides detailed source information relevant to developing $\text{PM}_{2.5}$ mitigation strategies and predicts a large potential health benefit from replacing traditional energy sources.

Results

In this work, we couple emission sensitivity simulations using the GEOS-Chem 3D global chemical transport model with newly available high-resolution (1 km \times 1 km) satellite-derived $\text{PM}_{2.5}$ exposure estimates⁴³, national-level baseline burden data, and updated CRFs from the 2019 Global Burden of Disease (GBD)¹. We use these data and methods to quantify the relative contributions from 24 individual emission sectors and fuel categories to annual population-weighted mean (PWM) $\text{PM}_{2.5}$ mass concentrations and the attributable disease burden across 21 world regions, 204 countries (defined in Supplementary Table 1), and 200 sub-national areas.

$\text{PM}_{2.5}$ exposure and attributable disease burden. In 2017, the global PWM $\text{PM}_{2.5}$ mass concentration was 41.7 $\mu\text{g m}^{-3}$, with 91% of the world's population experiencing annual average concentrations higher than the World Health Organization (WHO) annual average guideline of 10 $\mu\text{g m}^{-3}$. As shown in Fig. 1a and b, exposures were highest in countries throughout Asia, the Middle East, and Africa. To maintain consistency with the GBD¹, we use the same gridded ($\sim 10 \times 10$ km) outdoor $\text{PM}_{2.5}$ concentration estimates^{43,47,48}, further downscaled to a spatial resolution of $0.01^\circ \times 0.01^\circ$ ($\sim 1 \times 1$ km) using a newly and publicly

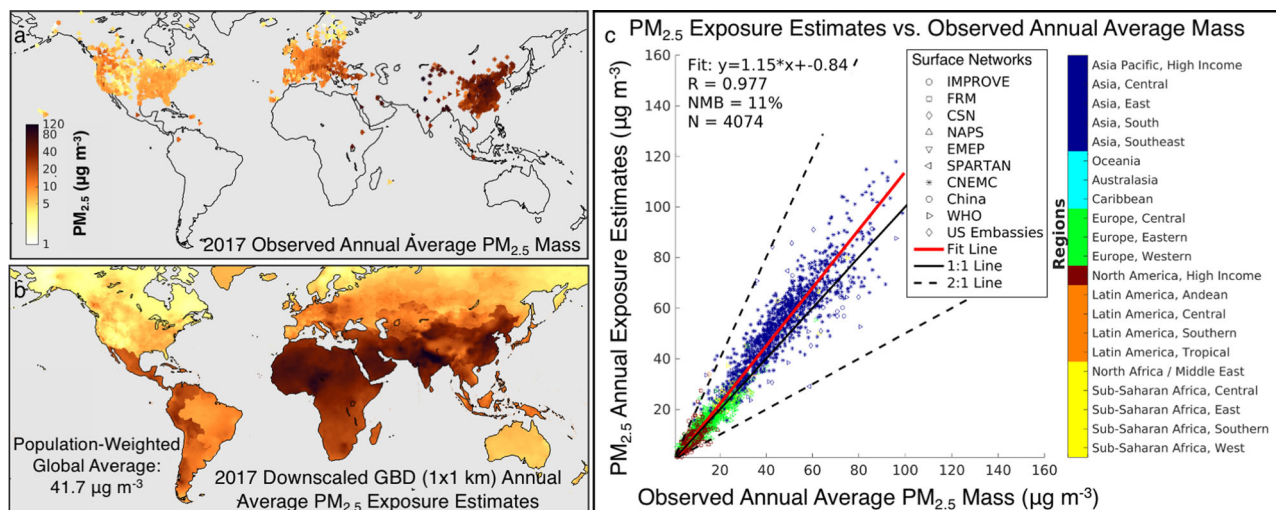


Fig. 1 Evaluation of $\text{PM}_{2.5}$ exposure estimates relative to surface observations. **a** Annual average observations of total $\text{PM}_{2.5}$ mass in the year 2017; symbol shapes correspond to monitor network. **b** Annual $\text{PM}_{2.5}$ exposure estimates for 2017, downscaled to $0.01^\circ \times 0.01^\circ$ resolution. **c** Correlation between the 2017 exposure estimates and observed annual average concentrations, colored by Global Burden of Disease (GBD) region (Supplementary Table 1); symbol shape corresponds to the observation network; correlation slope, intercept, coefficient, normalized mean bias (NMB), and number of observation points are provided. ($\text{NMB} = 100 \cdot \Sigma (\text{exposure estimate} - \text{observations}) / \Sigma \text{ observations}$).

available high-resolution satellite-derived product⁴³ (Methods). Figure 1c compares the resulting downscaled ($\sim 1 \times 1$ km) $\text{PM}_{2.5}$ concentrations to all readily available 2017 annual surface observations ($N = 4074$) of total $\text{PM}_{2.5}$ mass. Though annual surface observations are largely limited to regions in North America, Europe, and Asia, the downscaled estimates in Fig. 1c are consistent with co-located annual average observations, with a correlation coefficient (r) of 0.977 and a normalized mean bias of +11% or $4.6 \mu\text{g m}^{-3}$.

The global ambient $\text{PM}_{2.5}$ disease burden was estimated by integrating national-level annual PWM $\text{PM}_{2.5}$ concentrations with CRFs⁴⁹ and national baseline data consistent with the 2019 GBD¹ (GBD2019 CRF). These updated CRFs better reflect the uncertainty of health effects at high $\text{PM}_{2.5}$ concentrations. Globally, we estimate that 3.83 million deaths (95% Confidence Interval: 2.72–4.97 million) were attributable to annual ambient $\text{PM}_{2.5}$ exposure in the year 2017 (Fig. 2: top left panel). Attributable deaths were primarily from ischemic heart disease (IHD) and Stroke (63%; Fig. 2: top left, right pie chart), followed by chronic obstructive pulmonary disease (COPD), lung cancer (LC), lower respiratory infections (LRI), and type II diabetes (DM). In addition, there were a total of 2.07 (95% CI: 0.02–5.02) million attributable incidences of neonatal disorders (low birth weight (LBW) and pre-term births (PTB)) worldwide (Supplementary Data 1). National-level results for 204 countries are provided in the center map of Fig. 2 (and Supplementary Data 1). The largest numbers of attributable deaths occurred in China (~ 1.4 [95% CI: 1.05–1.70] million) and India (0.87 [95% CI: 0.68–1.04] million), together accounting for 58% of the global total ambient $\text{PM}_{2.5}$ mortality burden. The larger burden in China, despite a lower national $\text{PM}_{2.5}$ exposure level reflects differences in population age distribution and the relative baselines associated with each disease in each country (Supplementary Fig. 1). Figure 2 also shows a large $\text{PM}_{2.5}$ disease burden in countries such as the U.S. where country-level PWM $\text{PM}_{2.5}$ exposure levels are below the WHO guideline, highlighting the risks associated with $\text{PM}_{2.5}$ exposures below $10 \mu\text{g m}^{-3}$ but above the GBD counterfactual⁵⁰ (Supplementary Fig. 2; Methods). Supplementary Data 1 provides all national exposure and disease burden estimates, as well as fractional disease contributions.

As an additional sensitivity test, exposure and burden estimates for the year 2019 were additionally calculated with publicly available 2019 exposure estimates and national-level baseline burden data (Supplementary Text 1). No change was found in the global PWM $\text{PM}_{2.5}$ concentration (Supplementary Data 3), however due to changes in population characteristics (i.e., size and age decomposition in a particular country), the attributable deaths increased from 3.8 (95% CI: 2.72–4.97) million to 4.1 (95% CI: 2.9–5.3) million in 2019 (consistent with GBD2019¹) (Supplementary Text 1; Supplementary Data 3). Disease burden estimates were also calculated using CRFs from an updated version of the Global Exposure Mortality Model (GEMM)⁴⁴ (Supplementary Text 2; Supplementary Fig. 2). While the fractional disease contributions predicted by the updated GEMM were similar to those from the GBD2019 CRFs (Supplementary Fig. 3), the absolute number of attributable deaths in each country/region were nearly always larger when the GEMM was applied.

Global and national sector and fuel-type contributions.

Figure 2 also provides the relative (fractional) contributions of emission sectors and fuel types to annual $\text{PM}_{2.5}$ exposure levels and the attributable disease burden. As described in the Methods, fractional contributions are quantified using a recently updated version of the 3D GEOS-Chem chemical transport model⁴⁶ (Supplementary Text 3), evaluated against available surface observations (Supplementary Text 4; Supplementary Figs. 4, 5) in a series of 24 sensitivity simulations (Supplementary Table 2) with a newly released global anthropogenic emissions dataset (CEDSGBD-MAPS⁶) that includes sector- and fuel-specific emissions for the year 2017 (Supplementary Text 5; Supplementary Fig. 6).

Results in Fig. 2 (and Supplementary Data 1) show that on the global scale, roughly 40% of the $\text{PM}_{2.5}$ disease burden was attributable to residential (19.2%; 0.74 [95% CI: 0.52–0.95] million deaths), industrial (11.7%; 0.45 [0.32–0.58] million deaths), and energy (10.2%; 0.39 [0.28–0.51] million deaths) sector emissions, which are typically associated with fuel combustion⁶. To investigate combustion contributions across all sectors, the middle pie chart in Fig. 2 (and Supplementary Data 2) illustrates the potential health benefits from eliminating specific

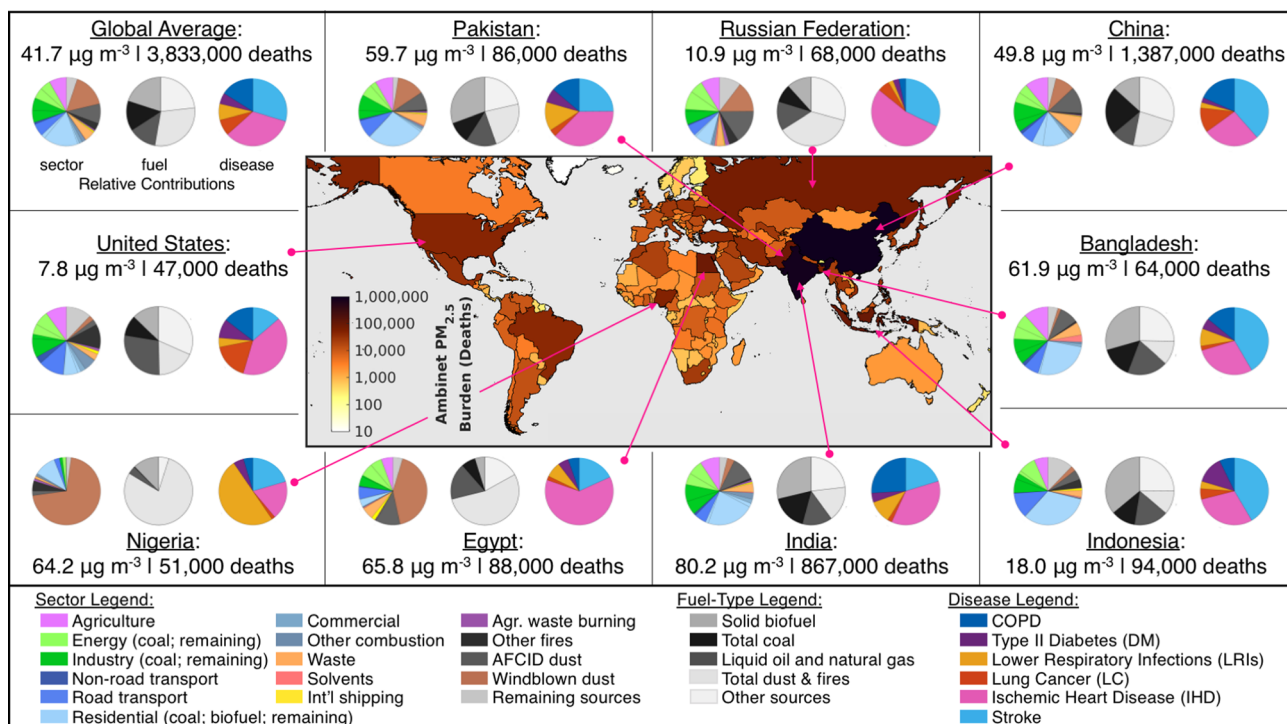


Fig. 2 Absolute ambient $PM_{2.5}$ burden and fractional sector, fuel, and disease contributions for the global average and top nine countries. Map: National-level outdoor $PM_{2.5}$ disease burden in 2017 (from the 2019 Global Burden of Disease concentration-response relationships). Panels: Annual average population-weighted $PM_{2.5}$ exposure levels and attributable mortality (rounded to the nearest 1000). (Left pie charts) fractional sectoral source contributions. ‘Other fires’ include deforestation, boreal forest, peat, savannah, and temperate forest fires. ‘Remaining sources’ include volcanic SO_2 , lightning NO_x , biogenic soil NO , aircraft emissions, and oceanic and biogenic sources (Supplementary Table 2). Energy and industry sectors also include separate contributions from coal use (first wedge, counterclockwise). The residential sector separates the contributions from coal (first wedge) and solid biofuel (second wedge). (middle pie charts) fuel-type contributions. The ‘total dust & fires’ category is the sum of windblown and AFCID (anthropogenic fugitive, combustion, and industrial) dust, agricultural waste burning, and other fires. Other sources are primarily from non-combustion or uncategorized combustion sources (agriculture, solvents, biogenic SOA, waste incineration, etc.). (Right pie charts) Relative disease contributions (not including pre-term birth and low birth weight). Supplementary Data 1 and 2 provide all data in this figure, including the number of neonatal incidences.

types of combustible fuels. For example, Fig. 2 shows that nearly 1.05 (95% CI: 0.74–1.36) million or 27.3% of total $PM_{2.5}$ attributable deaths could be avoided by eliminating emissions from fossil-fuel combustion (coal = 14.1%, O&NG = 13.2%), with an additional 20% or nearly 0.77 (95% CI: 0.54–0.99) million deaths avoidable by eliminating solid biofuel combustion, primarily used for residential heating and cooking. The remaining sources in the middle pie charts largely correspond to non-combustion and natural sources, such as windblown dust, which was the second single largest sectoral source of $PM_{2.5}$ exposure at the global scale (16.1%) (Fig. 2). This source was estimated to lead to 0.62 (95% CI: 0.44–0.80) million attributable deaths worldwide under the assumption of equal toxicity of all $PM_{2.5}$ sources and components (Discussion). Other $PM_{2.5}$ sources such as on-road transportation, non-combustion agriculture emissions, and anthropogenic dust each had relatively smaller global contributions ranging between 6.0 and 9.3% (0.23 [95% CI: 0.16–0.30] to 0.36 [0.25–0.46] million deaths). Additional global source sectors, including solvents, shipping, and natural sources such as fires, biogenic, and soil emissions each contributed to less than 5.2% of the annual global PWM $PM_{2.5}$ mass. Supplementary Data 1 and 2 provide a complete data set of the global fractional sector and fuel contributions.

While global contributions provide a snapshot of globally important sectors and fuel-types, regional and country-level contributions provide information more relevant to local sources of ambient $PM_{2.5}$ mass. Therefore, Fig. 2 additionally shows the relative contributions for nine countries with the largest number

of attributable deaths associated with long-term ambient $PM_{2.5}$ exposure (from the GBD2019 CRFs). These top countries differ from those with the highest PWM $PM_{2.5}$ concentrations (Supplementary Data 1), highlighting the importance of demographic factors and disease-specific baseline estimates in calculating the total burden of disease. The majority of attributable deaths in these countries were from Stroke and IHD, except for Nigeria, where childhood LRIs were the largest cause of mortality attributable to ambient $PM_{2.5}$ exposure. Sectoral pie charts in Fig. 2 show that source contributions varied between countries, with residential contributions ranging from 4.0% in Egypt to 33.1% in Indonesia, while the sum of energy and industry emissions ranged from 3.2% in Nigeria to 27.3% in India. Windblown dust was the most variable sector within these countries, ranging from 1.5% in Bangladesh to 70.6% in Nigeria. Of the three anthropogenic fuel categories (coal, oil & natural gas, and solid biofuel), coal was the largest source of $PM_{2.5}$ attributable mortality in China (22.7%; 315,000 [95% CI: 239,000–385,000] deaths), O&NG was the largest contributor in Egypt, Russia, and the United States (13.7–27.9%; 9000 [4000–16,000] to 13,000 [4500–24,000] deaths), and solid biofuel combustion was largest in the remaining five countries (12.3–36.0%; 6000 [4500–8000] to 250,000 [196,500–300,000] deaths). Results further show that use of these fuels in China and India alone each contribute to roughly 10% of the global ambient $PM_{2.5}$ disease burden (Supplementary Data 2).

For a more holistic world view, bar charts in Fig. 3 show the relative sector and fuel contributions for all 21 world regions and

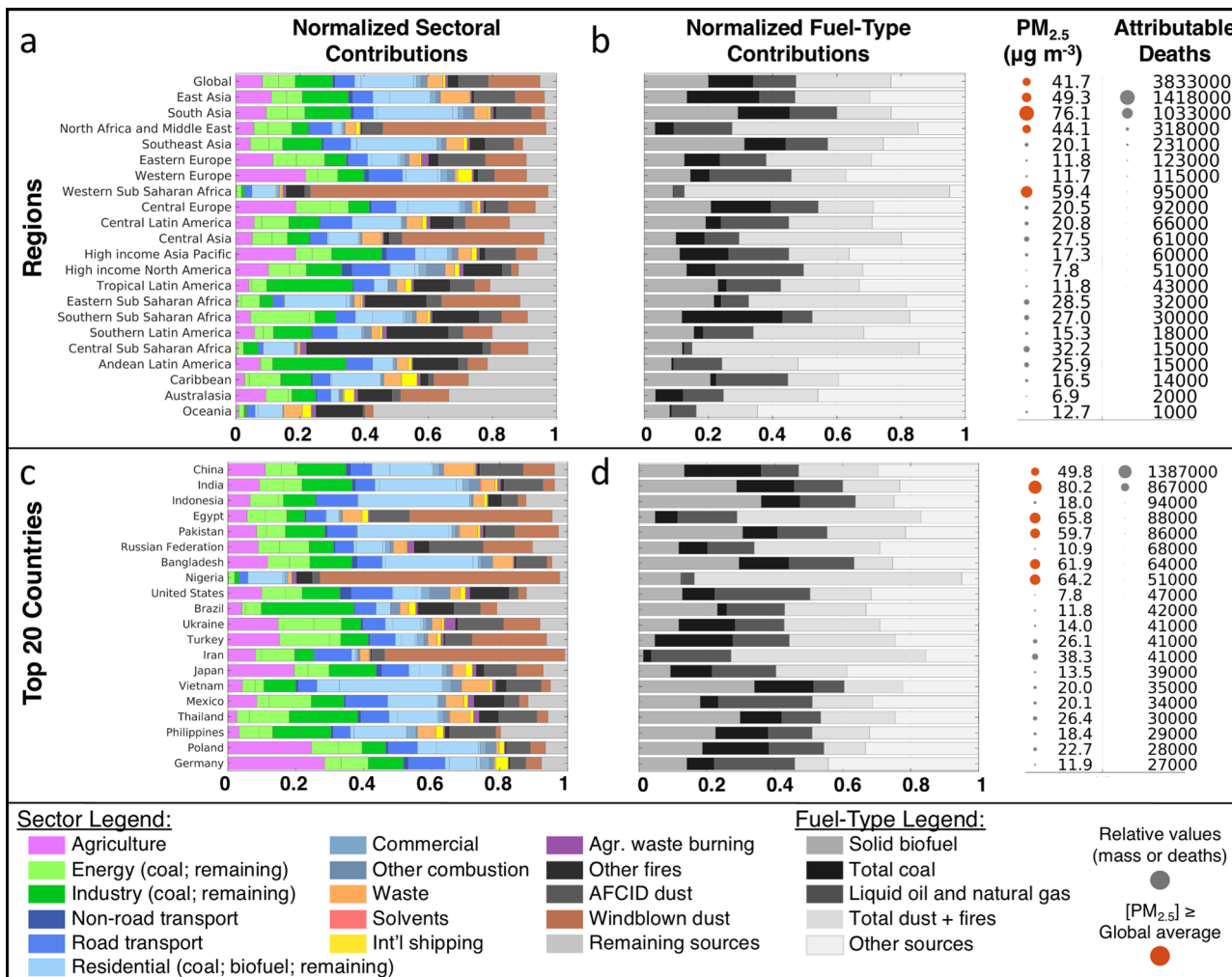


Fig. 3 Relative (fractional) source and fuel contributions to annual population-weighted mean PM_{2.5} mass and attributable deaths in 2017. **a, c** Normalized sectoral source contributions for 21 world regions and the global average (**a**) and top 20 countries (**c**). Sorted by decreasing number of ambient PM_{2.5}-attributable deaths (rounded to the nearest 1000). **b, d** Normalized contributions from the combustion of three fuel categories and remaining PM_{2.5} sources. To the right of **b** and **d**, annual population-weighted mean PM_{2.5} concentrations and associated attributable deaths are provided for each region/country. Relative amounts are illustrated by relative dot sizes. Concentrations above or equal to the global average are colored red.

the top 20 countries with the largest number of PM_{2.5}-attributable deaths. The relative contributions of PM_{2.5}-disease pairs for these same regions and countries are shown in Supplementary Fig. 3. The color scheme to the right of panels b and d in Fig. 3 shows that four of the 21 regions and six of the top 20 countries each had PWM PM_{2.5} concentrations higher than the global average. Similar to the pie charts in Fig. 2, Fig. 3 panels a and c show that residential energy use was the largest contributing sector in South, East, and Southeast Asia, largely driven by trends in India, Indonesia, Pakistan, Bangladesh, and Vietnam. Other notable features include the dominant contribution from windblown dust throughout North Africa, the Middle East, Central Asia, and Western Sub-Saharan Africa, as well as dominant fire contributions in Southern Latin America, Central Sub-Saharan Africa, Oceania, and North America. Large agricultural contributions were found in Western and Central Europe and Pacific Asia, along with dominant contributions from industrial processes in Andean and Tropical Latin America. Comparing all world regions, Fig. 3a shows that areas with the lowest number of PM_{2.5} attributable deaths generally had the smallest relative contributions from non-natural PM_{2.5} sources. Similarly, Fig. 3b shows that regions with greater attributable deaths had relatively larger contributions from anthropogenic fuel combustion emissions. Exceptions include

Western and Central Sub-Saharan Africa, where combined contributions from windblown dust and fires were greatest (81.0 and 68.4%).

Figure 4a provides a map of the dominant contributing fuel type in each country to further highlight the national-level variability in relative fuel contributions. For example, Fig. 4a shows that despite a recent decline in global coal emissions⁶, coal was the dominant combustible fuel type contributing to the PM_{2.5} disease burden in 20 countries, including China, Eswatini, South Africa, and countries throughout Central and Eastern Europe. At the national level, South Africa and neighboring Eswatini both had the largest relative coal contributions of all countries at more than 36.5% each (~9000 [95% CI: 6000–12,500] attributable deaths in total). Countries with the lowest relative coal contributions (<0.1%) included those in other regions of Africa, as well as small island nations. O&NG combustion typically dominated in more developed countries throughout North America, Australasia, and Western Europe, as well as parts of North Africa, the Middle East, Central Asia, and Eastern Europe. Of all world regions, North America and Western Europe had the largest relative O&NG contributions at ~25% each (43,000 [95% CI: 19,500–72,500] deaths total), while the lowest was in Central Sub-Saharan Africa at 2.5% (<1000 deaths total). Third, regional

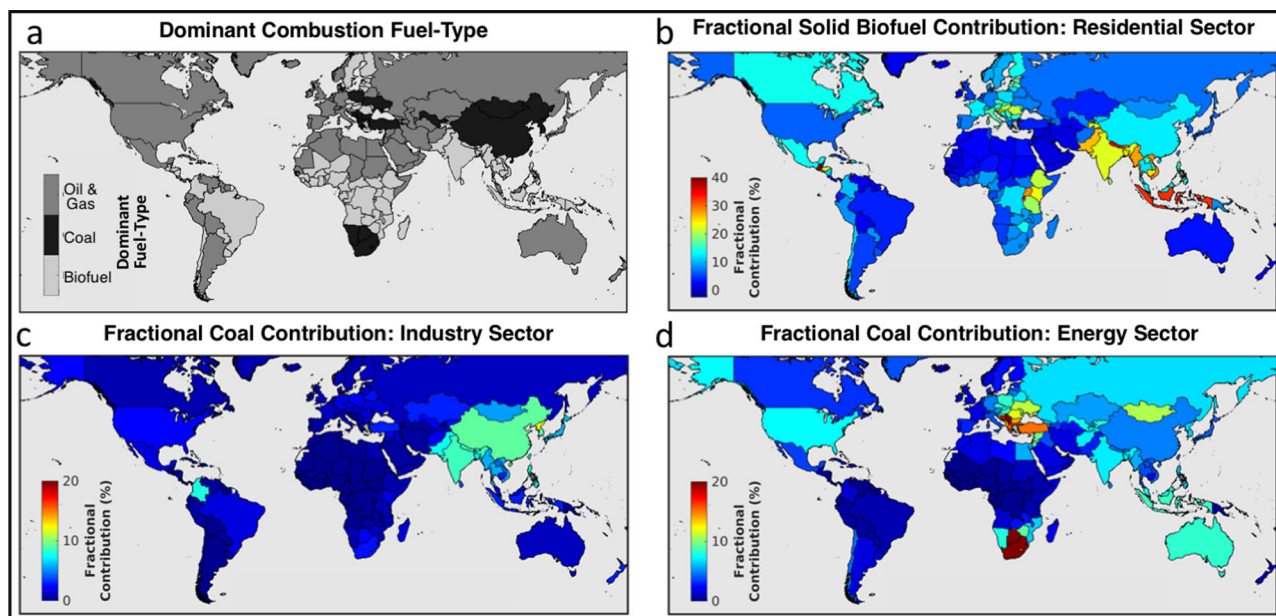


Fig. 4 Fractional contributions from select combustion fuel types and sectors. **a** The combustion fuel-type with the largest relative contribution to $PM_{2.5}$ mass and mortality in each country. **b–d** The fractional contributions from solid biofuel combustion in the residential sector (**b**), coal combustion in the industry sector (**c**), and coal combustion in the energy sector (**d**). Note the color scale change between (**b**) and (**c**, **d**).

solid biofuel contributions (largely from the residential sector) were largest in South and Southeast Asia at between 29.2 and 31.2% each (373,500 [95% CI: 279,500–465,000] deaths total). Solid biofuel was the dominant contributing combustible fuel in 76 countries including throughout Central, Eastern, and Sub-Saharan Africa, parts of Central and Western Europe, Asia, and Tropical Latin America. National-level fractional contributions ranged from 0.2% in small island nations to at least 40% in Guatemala, Nepal, and Rwanda (8500 [95% CI: 6500–11,000] total deaths).

Figure 4b–d additionally provides an assessment of three detailed emission reduction strategies that test policy-relevant scenarios of select fuel and sector combinations. These panels show the fractional contributions of $PM_{2.5}$ mass and attributable mortality avoidable by eliminating the use of (b) residential biofuel, (c) industrial sector coal combustion, and (d) coal combustion for energy generation. Figure 4a reveals that while coal is the dominant fuel type in both China and South Africa, coal from the energy sector contributes to a greater fraction of attributable deaths (20.5%) in South Africa than does the industry sector (2.7%), while the opposite is true for China (4.7% energy coal, 9.1% industry coal). Similarly, in countries throughout Central and Eastern Europe where coal is the dominant contributing fuel, the targeted reduction of coal use in the energy sector may lead to immediately larger air quality benefits than targeting coal use in the industrial sector (Fig. 4c and d). For residential biofuel use, the relative contributions are generally largest in regions where residential emissions are the dominant source sector (Fig. 3a). At the national scale, the combustion of solid biofuel for home heating and cooking contributed up to 46.1% of the total $PM_{2.5}$ mass and attributable deaths in Guatemala (Supplementary Data 1). These examples highlight the potential air quality benefits from specific and achievable reduction strategies. Detailed comparisons across countries in Fig. 4 and Supplementary Data 1 can further identify opportunities with the greatest potential health gains and identify countries who have successfully managed reductions from these select sources.

Sub-national source contributions. To investigate sub-national variability in $PM_{2.5}$ mass and its sources, we leverage the high-resolution downscaled exposure estimates ($0.01^\circ \times 0.01^\circ$) to estimate PWM $PM_{2.5}$ mass for 200 sub-national areas. We additionally apply gridded model sensitivity simulation results ($0.5^\circ \times 0.625^\circ$ in North America, Europe, and East Asia, $2^\circ \times 2.5^\circ$ elsewhere) to the sub-national exposure levels to estimate the relative source contributions in these same areas. Sub-national area boundaries are identified by the nearest dominant city and are defined using T3 urban extent data from the Atlas of Urban Expansion⁵¹. This dataset provides urban boundaries for 200 metropolitan areas that had more than 100,000 inhabitants in 2010.

$PM_{2.5}$ exposure estimates reveal a large public health benefit from reducing $PM_{2.5}$ exposure in urban areas. For example, Supplementary Data 1 shows that more than 65% of the select 200 areas experienced higher PWM $PM_{2.5}$ concentrations than their corresponding national averages. In a few extreme cases in India, for example, average PWM $PM_{2.5}$ concentrations exceeded $150 \mu g m^{-3}$, nearly twice that of the national average and over 15 times larger than the WHO guideline.

Figure 5 shows that both PWM $PM_{2.5}$ mass and dominant $PM_{2.5}$ surface sources vary at the sub-national scale, highlighting the importance of developing region-specific air quality strategies. For example, while residential emissions are the largest source of average $PM_{2.5}$ exposure and attributable mortality in China and India, areas surrounding Beijing and Singrauli (Madhya Pradesh, India) have relatively larger contributions from the energy and industry sectors. Similarly, while the transportation sector was the largest PWM $PM_{2.5}$ source in the U.S., Fig. 5c illustrates regionally varying sources, with dominant contributions from forest fires in the west, windblown dust in the arid southwest, agricultural, on-road transportation, and energy throughout the midwest and east coast, and highly uncertain sources such as secondary organic aerosol (SOA) in the southeast. In Europe, the non-combustion agriculture sector is a dominant source of PWM $PM_{2.5}$ mass and mortality across large portions of the region, however pie charts in Fig. 5d also illustrate areas with relatively

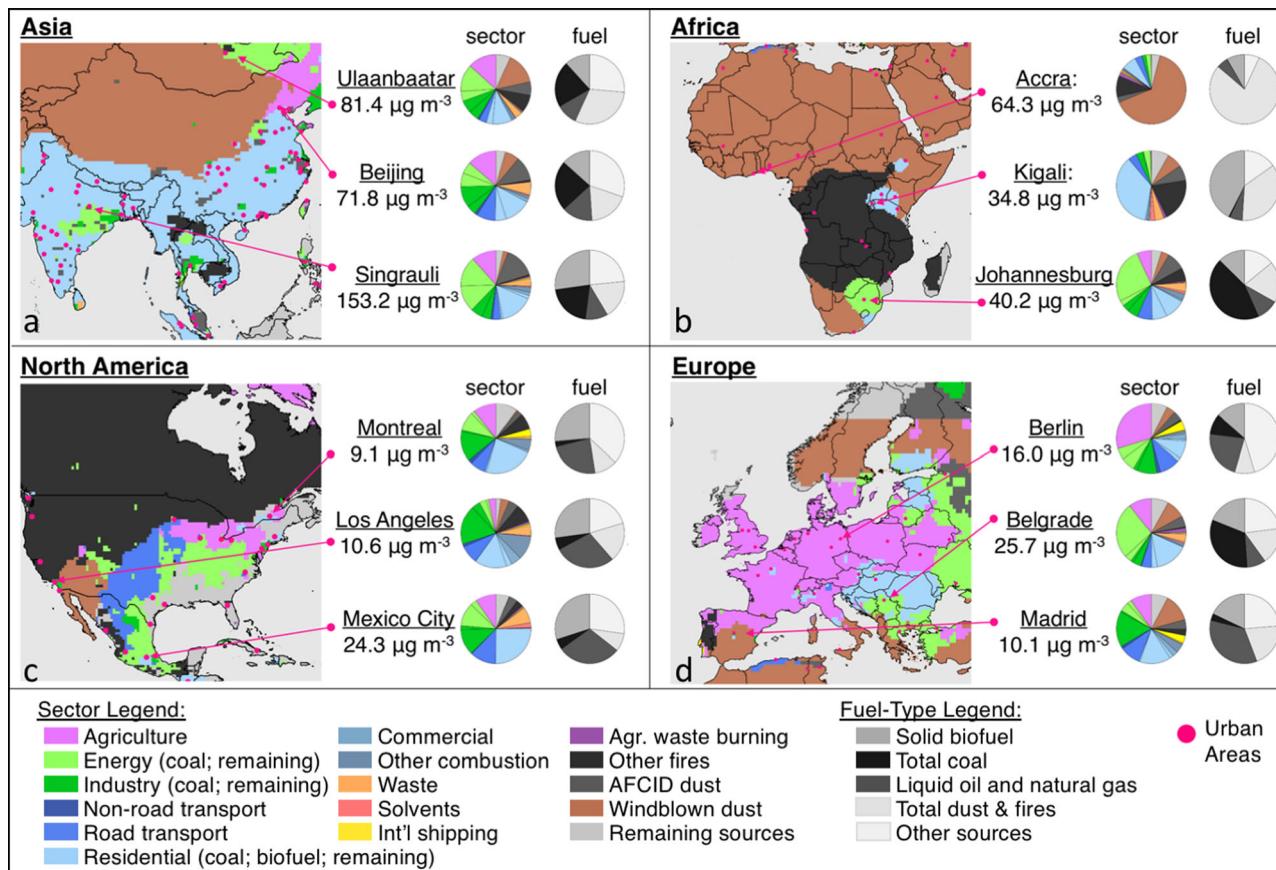


Fig. 5 Sub-national sources of PM_{2.5} mass and attributable mortality. Results are shown for (a) Asia, (b) Africa, (c) North America, and (d) Europe. Maps illustrate the single source with the largest contribution in each model grid cell (0.5° × 0.625°). Population-weighted mean PM_{2.5} concentrations (calculated from 0.01° × 0.01° PM_{2.5} exposure estimates) and regional fractional source contributions are also shown for a select sub-set of sub-national regions, identified by the name of the nearest major city.

large contributions from the energy, industry, and residential sectors. For Africa, energy generation from coal combustion was the largest source of PM_{2.5} attributable deaths in South Africa (Supplementary Data 1), though Fig. 5b shows that this influence was centered around Johannesburg (26.1%), while the area around Port Elizabeth was dominantly influenced by windblown dust and other non-combustion sources (Supplementary Data 1). Pie charts in all panels of Fig. 5 highlight that in all regions, a large number of sources collectively contribute to sub-national PM_{2.5} mass formation, not only the largest sources illustrated in the map panels.

While annual PM_{2.5} exposure estimates in Fig. 5 were derived from urban-relevant spatial scales (i.e., 0.01° × 0.01°), we note that the source contributions here are limited by the resolution of the GEOS-Chem model (above) and of the emissions dataset (0.5° × 0.5°). As a result, source contributions maps in Fig. 5 are effective at highlighting sub-national source contributions, but urban-level contributions would be improved with more spatially resolved simulations and emissions. Sub-national and urban scale PM_{2.5} exposure estimates and fractional source contributions are vital for identifying reduction strategies with the greatest public health benefit, which will become increasingly important as ~65% of the world’s population is projected to live in urban areas by 2050⁵².

Discussion

We provide a comprehensive and quantitative evaluation of the individual sector and fuel contributions to annual PWM PM_{2.5} mass and its disease burden, relevant to the development and

prioritization of effective mitigation strategies. We find that over 1 million (27.3%) attributable deaths were avoidable by eliminating PM_{2.5} mass associated with emissions from fossil-fuel combustion (total coal + O&NG). These results add to the growing evidence of the public health benefit achievable from global decarbonization strategies⁵³. While global total coal contributions (14.1%) were slightly larger than those from O&NG (13.2%), the relative balance between these two fuel categories varied at the regional, country (Figs. 2 and 3), and sub-national levels (Fig. 5). As the largest number of PM_{2.5} attributable deaths occurred in China and India, complete elimination of coal and O&NG combustion in these two countries could reduce the global PM_{2.5} disease burden by nearly 20% (Supplementary Data 2).

Comparisons here with prior analyses are limited by differences in estimation years as well as differences in spatial resolution and input data, including chemical transport models, CRFs, and emissions, population, exposure, and burden datasets. Fractional fossil-fuel contributions to the PM_{2.5} disease burden (27.3%) for the year 2017 were lower than the only previous global fractional estimate of 41% for the year 2015³⁶. Observed differences are largely driven by countries that have experienced recent reductions in fossil-fuel emissions⁶, such as China, the U. S., and Western European countries, including Germany and Italy. Absolute contributions in this work were also lower than recent fossil fuel attributable mortality estimates derived using different CRFs⁵⁴. Compared to two previous national-level studies, fractional coal contributions in 2017 were also 17% smaller than a 2013 estimate for China¹⁷, but generally consistent to

within 1% for a 2015 estimate for India¹⁸ (Supplementary Text 6). Emission inputs suggest that PM_{2.5} precursor emissions from coal combustion (e.g., SO₂) have decreased by up to 60% between 2013 and 2017 in China, while these same emission sources in India have increased by up to 7% between 2015 and 2017⁶. Fossil-fuel contributions in our analysis may also be lower limits as some sub-sectoral emission categories such as flaring and fossil-fuel fires were not assigned to a fuel category in the emissions dataset⁶, but rather were included in the ‘other sources’ category in this analysis (Supplementary Text 5).

The use of solid biofuel across all sectors in 2017 contributed to an additional 767,000 (95% CI: 543,000–994,500) attributable deaths worldwide (20%), with this source in India and China again responsible for roughly 11% of the global PM_{2.5} disease burden. Solid biofuel emissions in countries throughout South and Southeast Asia, as well as Central and Western Sub-Saharan Africa were largely associated with residential solid biofuel use for household heating and cooking (Fig. 5b). Large fractional contributions of this source were consistent to within 4% of the only previous global estimate²⁵. Results in 2017 were also consistent to within 3% of two previous national-level estimates of fractional PM_{2.5} disease burden contributions from residential heating and cooking in China in 2013¹⁷ and in India in 2015¹⁸ (Supplementary Text 6). While emissions from biofuel combustion have recently decreased in China, other world regions are experiencing a simultaneous increase⁶, highlighting the continued importance of considering residential solid biofuel emissions for future air quality improvement strategies. Considerations of net air quality benefits will also be important in regions where a transition from residential solid biofuel use to fossil fuel energy sources may lead to immediate indoor and outdoor air quality improvements and health benefits⁵⁵, while at the same time increasing the relative fossil fuel contributions.

For major contributing global source sectors (Fig. 2), relative contributions were generally consistent with previous global studies, though differences again may arise due to real temporal changes or differences in input datasets, chemical transport models, or sectoral definitions used. Comparisons with previous national-level studies are more variable, with summaries provided in Supplementary Text 6. At the global scale, the residential energy sector was the single largest contributing source to the 2017 global PM_{2.5} disease burden and had a relative contribution (~20%) similar to previous global estimates of 8–31% in 2000–2014^{37–39,56}. In addition, the global 2017 contribution from the combined energy (10.2%) and industry (11.7%) sectors was consistent with two previous global combined estimates of 21 and 33% in 2010–2014^{37,39}. Different reported relative contributions between the energy and industry sectors may be driven by differences in sectoral definitions. Global estimates for fractional contributions from dust and the transport sector were also generally consistent with previous global estimates. The total 2017 dust contribution (windblown and anthropogenic) of 25% was similar to two previous global studies of 18–24%^{37,39}. Similarly, previous estimates for the transportation sector of between 5–12% in 2005–2015^{32,37–39} encompass the 2017 value of 7.6%. In contrast, contributions from the agriculture sector (8%) were slightly lower than previous global estimates of 9–25% in 2010–2015^{37,39,57}, even when 2017 contributions from agricultural waste burning (+1%) were included.

Smaller global sectors include waste, fires, solvent use, and international shipping, which each contributed to <5% of the 2017 global PM_{2.5} disease burden. These sources however may be important to consider for national and sub-national control strategies (Fig. 5; Supplementary Text 6). The number of global attributable deaths from the waste sector (184,000; 95% CI: 130,500–238,500 deaths) in 2017 was 30% lower than the only

previous estimate of domestic waste burning²⁹. Global contributions from solvent use have not been previously reported. For international shipping, global mortality estimates (27,000; 95% CI: 19,000–35,000 deaths) fell within the range of a previous 2002 estimate³³, but were 75–95% lower than a more recent study, largely due to differences in the CRFs⁵⁸. In contrast to anthropogenic sources, annual open fire contributions are expected to vary strongly with annual fire activity³, and may increase in regions where the number and severity of wildfires is projected to increase⁵⁹. The global 2017 total fire contribution was 4.1%, consistent with two previous estimates of ~5% in 2010 and 2014^{37,39}. Figure 5, however, shows that fires were the single largest contributor to the PM_{2.5} disease burden in select regions throughout North America, Southeast Asia, and Africa. These relative contributions are generally consistent with a previous global-scale estimate³, though mixed agreement with previous national-level estimates likely highlights the interannual variability of this source. For example, 2017 contributions in India and China (~1%) were lower than previous estimates of 1–8% for 2013–2015^{17,18,28,37}, contributions in the U.S. (~13%) were more than double a previous 2010 estimate³⁷, and contributions in Canada (18.9%) were consistent with a previous 2013 study¹¹. All remaining PM_{2.5} sources (Supplementary Table 2) contributed to 5.2% or less at the global scale.

Similar to previous studies, fractional and absolute source contributions to PWM PM_{2.5} mass and the attributable disease burden are subject to uncertainties in the emissions dataset, PM_{2.5} exposure estimates, 3D chemical-transport model, national-level baseline mortality estimates, and the disease-specific GBD2019 CRFs. Following methods from previous similar studies^{36,37,60}, the 95% CI of the 2017 PM_{2.5} disease burden is derived from uncertainties in the GBD2019 CRFs, resulting in a range of 2.72 million–4.97 million global attributable deaths. An additional sensitivity study is presented in Supplementary Text 7 to test the impact of uncertainties associated with the baseline mortality data, which for the majority of world regions results in smaller uncertainty bounds than those associated with CRF uncertainties (Supplementary Fig. 7). As described in the Methods, the GEOS-Chem model is evaluated against available surface observations and uncertainties in the emissions dataset are discussed elsewhere⁶. In addition, sub-national fractional source contributions (Fig. 5) are limited to the resolution of the model and emissions, while the urban exposure estimates are further subject to greater uncertainties in the satellite-derived products for small spatial scales^{43,47}. Future developments of global high-resolution simulations, as well as increasing the accuracy and precision of satellite-derived PM_{2.5} estimates will serve to reduce these uncertainties in PM_{2.5} mass and source contributions at both the national and sub-national scales.

In addition to uncertainties in the general methodology, this work also assumes equitoxicity of aerosol mass and its sources, including from windblown mineral dust⁶¹. This assumption is necessary for use with the GBD2019 and GEMM CRFs and is consistent with US EPA⁶² and WHO⁶³ assessments. This assumption may under- or over-estimate the relative PM_{2.5} burden contributions from select sectors provided they contribute to more or less toxic components of total PM_{2.5} mass. We additionally note that by simultaneously reducing emissions across all geographic regions, this study did not explicitly investigate national contributions from long-range or regional transport^{11,64}. As the implementation of mitigation policies is typically constrained to political borders, specific policies may need to consider the regional influence on local pollution levels. We lastly note that results from the sensitivity simulations (Methods) largely reflect changes in PM_{2.5} mass associated with the complete elimination of each individual emission source. Therefore, the

same relative contributions may not be expected from studies that test more moderate reduction strategies or simultaneous reductions of multiple sources (Supplementary Text 8).

The comprehensive nature of our analysis provides detailed source information to inform PM_{2.5} mitigation strategies and provides potential health benefit estimates to further motivate action. Results show that residential, energy, industry, and total dust sources are among the largest contributing sectors to the global PM_{2.5} disease burden, while the relative contributions from individual sources and fuels vary at the national and sub-national levels. Roughly 1 million deaths could be avoided by the global elimination of fossil-fuel combustion, with 20% of this burden associated with fossil-fuel use in China and India alone (Fig. 2). Despite recent global reductions in air pollutant emissions from coal, this fuel was still the dominant contributing combustible fuel type to the PM_{2.5} disease burden in 20 countries, including China and countries throughout Southern Sub-Saharan Africa and Central Europe (Fig. 4). The use of solid biofuel was a primary source of emissions from the residential sector and was the dominant contributing combustible fuel in 78 countries, especially throughout the tropics (Fig. 4). While natural sources of PM_{2.5} mass dominantly contributed in more arid regions (Fig. 3), countries with the greatest PM_{2.5} disease burden generally had the largest relative contributions from anthropogenic sources, demonstrating a clear path towards attaining global air quality improvements.

Methods

This study integrates newly available high-resolution satellite-derived PM_{2.5} exposure estimates, CRFs from the 2019 GBD, and fractional source contribution results from 24 emission sensitivity simulations to provide the most comprehensive global source contribution results to-date. This work also provides global estimates of PM_{2.5}-attributable deaths from the use of coal, O&NG, and solid biofuel. The following sections describe the details of the high-resolution PM_{2.5} exposure estimates, attributable disease burden calculations, set-up and evaluation of the chemical transport model, sector- and fuel-specific emissions dataset, and fractional simulated source contribution calculations. A schematic of this overall process is provided in Supplementary Text 9 and Supplementary Fig. 8.

High-resolution PM_{2.5} exposure estimates. To maintain consistency with the GBD project, while also improving the accuracy of the population-exposure estimates, we downscale the 2019 GBD exposure estimates^{1,47,48} to a 0.01° × 0.01° (~1 km × 1 km) grid using a newly available high-resolution PM_{2.5} dataset from Hammer et al.⁴³. Supplementary Text 10 (Supplementary Fig. 9) describes this process of spatial downscaling by incorporating the spatial information from the Hammer et al.⁴³ product. This downscaling process is independent of the modeled fractional source contribution results and maintains the average PM_{2.5} mass concentration (area average only) from the original GBD product. The sensitivity of the PM_{2.5} exposure estimates to the downscaling process are evaluated in Supplementary Text 10 and Supplementary Fig. 10. Exposure estimates for the year 2019 were derived using these same methods with both GBD and Hammer et al.⁴³ data for the year 2019.

National-level PM_{2.5} disease burden. The total disease burden from six mortality endpoints and two neonatal disorders associated with exposure to annual average outdoor PM_{2.5} mass (from the downscaled GBD-product) was calculated following a similar methodology as the 2019 GBD project¹. First, Eq. (1) was used to derive cause-specific population attributable fractions (PAFs) for each endpoint using national-level PM_{2.5} concentrations (population-weighted) from the downscaled GBD exposure estimates and recently updated relative risk curves (RR*), derived using a Meta Regression-Bayesian, Regularized, Trimmed (MR-BRT) spline from the 2019 GBD (Supplementary Fig. 2)¹. MR-BRT curves use splines with Bayesian priors, which avoids using relative risk estimates for active smoking, previously necessary to avoid over-estimation of risks at high exposure levels. These meta-regressions were applied to the latest observational cohort and case-control studies of mortality or disease incidence from outdoor PM_{2.5} pollution cohort and case-control studies; cohort, case-control, and randomized-controlled trials of household use of solid fuel for cooking; as well as cohort and case-control studies of secondhand smoke.

$$\text{PAF}_{\text{age, disease, country}} = 1 - \frac{1}{\text{RR}^*_{\text{age, disease, [PWM PM}_{2.5}]_{\text{country}}}} \quad (1)$$

Consistent with the 2019 GBD, the resulting RR* (or CRF) values from the MR-BRT splines in Eq. (1) are gender-independent and describe the excess risk of

non-accidental mortality from adult (25 years and older) IHD, Stroke, COPD, LC, DM, and childhood and adult (under 5 years and 25 years and older) acute LRIs. Consistent with the 2019 GBD, RR*s for each disease in Eq. (1) are also a function of annual PWM PM_{2.5} mass exposure in each country and the difference between this exposure level and the Theoretical Minimum Risk Exposure Level (TMREL). The TMREL in this work, as in the GBD2019, is assumed to have a uniform distribution ranging between 2.4 and 5.9 µg m⁻³. Thus, RR* = RR(age, PWM PM_{2.5})/RR(age, TMREL). RR* values were also stratified by quinquennial age group (25–29, ..., 95+), with age-specific RR* values applied to IHD and stroke outcomes. In contrast, age-independent RR*s were applied to the other health outcomes (age group 25 and over for COPD, LC, and type II DM, and the combined age groups under 5 and 25 and over for LRI). Supplementary Fig. 2 provides an illustration of select RR* (or CRF) values for these diseases as a function of annual PM_{2.5} mass exposure, as well as the CRFs for two neonatal disorders, which include the number of preterm (PTB; gestational age less than 37 weeks) and low birth weight (LBW; below 2.5 kg) incidences. The 95% CI for the CRF values was determined from the distribution of 2000 randomly selected values of the TMREL.

As shown in Eq. (2), the PAFs for each age group, disease, and country were then multiplied by the age- and country-specific baseline mortality data for each disease and summed over all relevant age groups (*m*) and diseases (*n*) to obtain the total national-level PM_{2.5} burden associated with exposure to both outdoor and household (indoor) PM_{2.5} mass. National cause- and age-specific baseline mortality data for the years 2017 and 2019 were extracted from the GHDx database⁶⁵. The national-level baselines for PTB and LBW were calculated from the 2019 GBD statistics of the number of annual live births and the percentage of LBW and PTB cases at the national and regional levels^{66,67}.

$$\text{PM}_{2.5} \text{ Attributable Mortality}_{\text{country}} = \sum_{\text{disease}} \sum_{\text{age}} \text{PAF}_{\text{age, disease, country}} \times \text{Baseline Mortality}_{\text{age, disease, country}} \quad (2)$$

Finally, to separate the contributions from outdoor and indoor household co-exposure, the national-level total PM_{2.5} attributable mortality values from Eq. (2) were scaled using Eq. (3) to account for the risk of co-exposure to household air pollution included in the CRFs. Country-specific adjustment factors were derived from a comparison of national-level burdens in Eq. (2) to those derived for outdoor exposure only in the 2019 GBD study. As a result of these adjustments, the PM_{2.5} attributable mortality and source contribution results presented in this analysis reflect contributions from indoor sources of air pollution (e.g., biomass combustion for residential heating and cooking) to the extent that they impact ambient PM_{2.5} concentrations.

$$\text{Outdoor PM}_{2.5} \text{ Attributable Mortality}_{\text{country}} = \text{PM}_{2.5} \text{ Attributable Mortality}_{\text{country}} \times \text{Adjustment Factor}_{\text{country}} \quad (3)$$

The overall approach described here generally follows that of the 2019 GBD, but deviates in part by calculating national-level PAFs rather than PAFs for each grid cell, and by using publicly available national baseline data from the IHME⁶⁵, rather than both national and sub-national baseline estimates. We find that the aggregate-country level method used in this work is consistent to within 5% of the grid-cell methodology used in the GBD.

As discussed in Supplementary Text 2, we also calculate the PAFs for each PM_{2.5}-disease pair (plus two neonatal disorders) using an updated version of the GEMM⁴⁴. To aid in the comparison with GBD2019 CRF estimates, the original GEMM was updated to include CR curves for Type-II Diabetes, PTBs, and LBWs as well as newly available observational studies (described in Supplementary Text 2). For the neonatal outcomes, only the number of PTB and LBW cases were estimated, whereas the 2019 GBD estimated neonatal death mediated by the impact of PM_{2.5} on birthweight and short gestation. As the GEMM is exclusively developed from studies of outdoor PM_{2.5} exposure, total outdoor PM_{2.5} attributable deaths in Supplementary Data 1 and 2 were taken directly from Eq. (2) and did not require scaling factors to remove the risk associated with indoor PM_{2.5} exposure.

Simulated fractional sector and fuel-type contributions. Fractional sector and fuel-specific contributions were derived from a series of emission sensitivity simulations, using the 3D GEOS-Chem chemical transport model⁴⁶. As described in Supplementary Text 3, we used the GEOS-Chem v12.1.0 source code, updated to account for scientific updates to physical deposition, reactive nitrogen chemistry, and surface emissions (https://github.com/emcduffie/GC_v12.1.0_EEM). Model simulations were run from December 2016 to January 2018 to allow for one month of spin-up. The model was run globally at a resolution of 2° × 2.5° and was supplemented with three nested simulations with resolutions of 0.5° × 0.625° over North America, Europe, and Asia.

Gridded emission datasets are the backbone of any modeling source contribution study. In this work, we leverage a newly developed emissions dataset developed from the Community Emissions Data System that has been updated for the GBD-MAPS project (<https://sites.wustl.edu/acag/datasets/gbd-maps/>)⁶. This dataset provides global gridded (0.5° × 0.5°) emissions of key PM_{2.5} components (black and organic carbon) and gas-phase precursors from 11 individual

anthropogenic source sectors and multiple fuel types for the year 2017. Supplementary Fig. 6 illustrates these global emissions as a function of source sector and chemical compound. Additional emission inputs used for model sensitivity simulations largely include those from fires (forest fires and agricultural waste burning)⁶⁸, biogenic sources, and anthropogenic⁶⁹ and windblown dust. Supplementary Text 5 provides further emission details.

In source sensitivity simulations, it remains vital to evaluate the model's ability to predict total PM_{2.5} concentrations as well as regional chemical production regimes. Comparisons to total PM_{2.5} mass provide confidence in the model's ability to accurately simulate total mass production. Additional comparisons to PM_{2.5} chemical components imply accuracy in the model's ability to capture PM_{2.5} formation chemistry and provide confidence in the model's ability to accurately predict chemical changes in response to specific emission scenarios. In this work, we evaluated the base GEOS-Chem simulation (including all emission sources) against all available long-term surface observations of both PM_{2.5} mass and its chemical composition. As described in Supplementary Text 4, the observational dataset was compiled from more than 10 long-term observation networks and over 4000 individual sites (Supplementary Figs. 4 and 5a).

The comparisons in Supplementary Fig. 5 indicate that individual components in the base GEOS-Chem simulation agree to within -0.3 to $0.6 \mu\text{g m}^{-3}$ of the observed annual average concentrations for all PM_{2.5} chemical components. These observations ($N < 230$) were largely limited to North America, Europe, and China, however, Supplementary Fig. 5 also demonstrates the large improvement in the long-standing bias of aerosol nitrate in our updated version of the GEOS-Chem model⁷⁰ relative to the default version. Supplementary Fig. 5 also demonstrates relative improvements in the updated model in concentrations of sulfate, ammonium, and dust. In terms of total PM_{2.5} mass, Supplementary Fig. 10a shows that the base model predictions were consistent with the 2017 observations (NMB of +5%, and correlation (r) of 0.89).

For the 24 individual emission sensitivity simulation sets (1 global +3 nested per set), we employed a zeroing out (brute force) method^{20,36–38}, where fractional PM_{2.5} mass contributions from each source were calculated from simulations that systematically remove individual source sectors or fuel-specific emissions. Supplementary Table 2 provides a detailed list of the 24 individual sensitivity tests. Resulting simulated spatially resolved PM_{2.5} mass contributions from each source category were calculated following Eq. (4) and Eq. (5), where simulated gridded total PM_{2.5} mass concentrations from each sensitivity study were first compared to the total gridded PM_{2.5} mass in the base simulation (4), and then were compared to the sum of PM_{2.5} mass from all j simulations (5) to calculate the gridded fractional contributions.

$$[\text{PM}_{2.5}]_{\text{source}} = [\text{PM}_{2.5}]_{\text{base simulation}} - [\text{PM}_{2.5}]_{\text{source sensitivity simulation}} \quad (4)$$

$$(\% \text{PM}_{2.5})_{\text{source}} = \frac{[\text{PM}_{2.5}]_{\text{source}}}{\sum_{j=1}^{24} [\text{PM}_{2.5}]_j} \quad (5)$$

Lastly, Eq. (6) was used to calculate the fractional source contributions to PWM PM_{2.5} mass in 200 sub-national areas, 204 countries, 21 world regions, and for the global average. First, absolute contributions from each source were calculated from the product of the spatially resolved fractional PM_{2.5} source contributions from Eq. (5) and the spatially resolved downscaled GBD exposure estimates from Fig. 1, averaged over i grid boxes and weighted by the total population in a given region or country. Fractional contributions were then calculated by dividing these absolute source contributions by the total PWM PM_{2.5} concentration in a given region, country, or area. In Eq. (6), variable i represents individual grid boxes to distinguish the use of spatially resolved vs. spatially averaged products. Population-weighted fractional source contributions were calculated at the spatial resolution of the GEOS-Chem model. Supplementary Data 1 and 2 provide the resulting population-weighted fractional source contributions from Eq. (6).

$$(\% \text{Contribution})_{\text{source}} = \frac{\sum_{i=1}^n (\% \text{PM}_{2.5})_{\text{source}} \times [\text{GBD PM}_{2.5}]_i \times \text{population}_i}{\sum_{i=1}^n \text{population}_i} \bigg/ \frac{\sum_{i=1}^n [\text{GBD PM}_{2.5}]_i \times \text{population}_i}{\sum_{i=1}^n \text{population}_i} \quad (6)$$

Following the approach of previous studies^{20,37}, fractional contributions from Eq. (6) are then applied to national-level PM_{2.5} exposure levels (population-weighted) and total disease burden estimates (provided in Supplementary Data 1 and 2) to calculate the absolute contributions from each source (reported in the Main Text). This method eliminates the sensitivity of the burden calculation to the order in which emission sectors are removed in model sensitivity simulations.

Data availability

Supplementary Data files 1 and 2 provide the global, regional, national, and sub-national fractional sector and fuel contributions to PM_{2.5} mass and disease burden for the year 2017. Supplementary Data files 1 and 2 also provide the total disease burden estimates determined by the GBD2019 and GEMM CRFs and the fractional disease-specific contributions to each (Supplementary Data 1 only). Supplementary Data 3 provides the 2019 PM_{2.5} exposure estimates. A data visualization tool for all Supplementary Data is

available at: <https://gbdmaps.med.ubc.ca/>. Gridded model fractional source contribution results are available at: <https://zenodo.org/record/4739100>. CEDS_{GBD-MAPS} emissions data are available at: <https://zenodo.org/record/3754964>. Input datasets required for this analysis (including high-resolution exposure estimates and GBD baseline burden data and CRFs) are available at: <https://zenodo.org/record/4642700>.

Code availability

The GEOS-Chem model source code used for sensitivity simulations is available at: https://github.com/emcduffie/GC_v12.1.0_EEM and <https://zenodo.org/record/4718622>. The CEDS source code used to develop the global emissions dataset is available at: <https://github.com/emcduffie/CEDS> and <https://doi.org/10.5281/zenodo.3865670>. The analysis scripts used in here are available at: <https://github.com/emcduffie/GBD-MAPS-Global> and <https://zenodo.org/record/4718618>.

Received: 20 January 2021; Accepted: 17 May 2021;

Published online: 14 June 2021

References

- GBD 2019 Risk Factor Collaborators. Global burden of 87 risk factors in 204 countries and territories, 1990–2019: a systematic analysis for the Global Burden of Disease Study 2019. *Lancet* **396**, 1223–1249 (2020).
- Yokelson, R. J. et al. Emissions from biomass burning in the Yucatan. *Atmos. Chem. Phys.* **9**, 5785–5812 (2009).
- Johnston, F. H. et al. Estimated global mortality attributable to smoke from landscape fires. *Environ. Health Perspect.* **120**, 695–701 (2012).
- Reid, J. S. et al. Comparison of size and morphological measurements of coarse mode dust particles from Africa. *J. Geophys. Res. Atmos.* <https://doi.org/10.1029/2002JD002485> (2003).
- Bond, T. C. et al. Historical emissions of black and organic carbon aerosol from energy-related combustion, 1850–2000. *Global Biogeochem. Cycles* <https://doi.org/10.1029/2006GB002840> (2007).
- McDuffie, E. E. et al. A global anthropogenic emission inventory of atmospheric pollutants from sector- and fuel-specific sources (1970–2017): an application of the Community Emissions Data System (CEDS). *Earth Syst. Sci. Data* **12**, 3413–3442 (2020).
- Womack, C. C. et al. An odd oxygen framework for wintertime ammonium nitrate aerosol pollution in urban areas: NOx and VOC control as mitigation strategies. *Geophys. Res. Lett.* **46**, 4971–4979 (2019).
- Lu, K. et al. Fast photochemistry in wintertime haze: consequences for pollution mitigation strategies. *Environ. Sci. Technol.* **53**, 10676–10684 (2019).
- Liang, C. K. et al. HTAP2 multi-model estimates of premature human mortality due to intercontinental transport of air pollution and emission sectors. *Atmos. Chem. Phys.* **18**, 10497–10520 (2018).
- Zhang, Q. et al. Transboundary health impacts of transported global air pollution and international trade. *Nature* **543**, 705–709 (2017).
- Meng, J. et al. Source contributions to ambient fine particulate matter for Canada. *Environ. Sci. Technol.* **53**, 10269–10278 (2019).
- West, J. J. et al. What we breathe impacts our health: improving understanding of the link between air pollution and health. *Environ. Sci. Technol.* **50**, 4895–4904 (2016).
- Watson, J. G., Antony Chen, L. W., Chow, J. C., Doraiswamy, P. & Lowenthal, D. H. Source apportionment: findings from the U.S. supersites program. *J. Air Waste Manag. Assoc.* **58**, 265–288 (2008).
- Pui, D. Y. H., Chen, S.-C. & Zuo, Z. PM_{2.5} in China: measurements, sources, visibility and health effects, and mitigation. *Particuology* **13**, 1–26 (2014).
- Karagulian, F. et al. Contributions to cities' ambient particulate matter (PM): a systematic review of local source contributions at global level. *Atmos. Environ.* **120**, 475–483 (2015).
- Martin, R. V. et al. No one knows which city has the highest concentration of fine particulate matter. *Atmos. Environ.: X* **3**, 100040 (2019).
- GBD MAPS Working Group. Burden of Disease Attributable to Coal-Burning and Other Major Sources of Air Pollution in China. Special Report 20. (Health Effects Institute. <https://www.healtheffects.org/publication/burden-disease-attributable-coal-burning-and-other-air-pollution-sources-china>) (2016).
- GBD MAPS Working Group. Burden of Disease Attributable to Major Air Pollution Sources in India. Special Report 21., Health Effects Institute. <https://www.healtheffects.org/publication/gbd-air-pollution-india> (2018).
- Caiazzo, F., Ashok, A., Waitz, I. A., Yim, S. H. L. & Barrett, S. R. H. Air pollution and early deaths in the United States. Part I: Quantifying the impact of major sectors in 2005. *Atmos. Environ.* **79**, 198–208 (2013).
- Gu, Y. et al. Impacts of sectoral emissions in China and the implications: air quality, public health, crop production, and economic costs. *Environ. Res. Lett.* **13**, 084008 (2018).

21. Liu, J. et al. Air pollutant emissions from Chinese households: a major and underappreciated ambient pollution source. *Proc. Natl Acad. Sci. USA* **113**, 7756 (2016).
22. Lacey, F. G. et al. Improving present day and future estimates of anthropogenic sectoral emissions and the resulting air quality impacts in Africa. *Faraday Discuss.* **200**, 397–412 (2017).
23. Kheirbek, I., Haney, J., Douglas, S., Ito, K. & Matte, T. The contribution of motor vehicle emissions to ambient fine particulate matter public health impacts in New York City: a health burden assessment. *Environ. Health* **15**, 89 (2016).
24. Thakrar, S. K. et al. Reducing mortality from air pollution in the United States by targeting specific emission sources. *Environ. Sci. Tech. Lett.* <https://doi.org/10.1021/acs.estlett.0c00424> (2020).
25. Chafe, Z. A. et al. Household cooking with solid fuels contributes to ambient PM2.5 air pollution and the burden of disease. *Environ. Health Perspect.* **122**, 1314–1320 (2014).
26. Chambliss, S. E., Silva, R., West, J. J., Zeinali, M. & Minjares, R. Estimating source-attributable health impacts of ambient fine particulate matter exposure: global premature mortality from surface transportation emissions in 2005. *Environ. Res. Lett.* **9**, 104009 (2014).
27. Gao, M. et al. The impact of power generation emissions on ambient PM2.5 pollution and human health in China and India. *Environ. Int.* **121**, 250–259 (2018).
28. Hu, J. et al. Premature mortality attributable to particulate matter in China: source contributions and responses to reductions. *Environ. Sci. Technol.* **51**, 9950–9959 (2017).
29. Kodros, J. K. et al. Global burden of mortalities due to chronic exposure to ambient PM 2.5 from open combustion of domestic waste. *Environ. Res. Lett.* **11**, 124022 (2016).
30. Saikawa, E. et al. The impact of China's vehicle emissions on regional air quality in 2000 and 2020: a scenario analysis. *Atmos. Chem. Phys.* **11**, 9465–9484 (2011).
31. Wu, R. et al. Air quality and health benefits of China's emission control policies on coal-fired power plants during 2005–2020. *Environ. Res. Lett.* **14**, 094016 (2019).
32. Anenberg, S., Miller, J., Henze, D. & Minjares, R. A global snapshot of the air pollution-related health impacts of transportation sector emissions in 2010 and 2015. The International Council on Clean Transportation (ICCT). <https://theicct.org/publications/health-impacts-transport-emissions-2010-2015> (2019).
33. Corbett, J. J. et al. Mortality from ship emissions: a global assessment. *Environ. Sci. Technol.* **41**, 8512–8518 (2007).
34. Marais, E. A. et al. Air quality and health impact of future fossil fuel use for electricity generation and transport in Africa. *Environ. Sci. Technol.* **53**, 13524–13534 (2019).
35. Lacey, F. G., Henze, D. K., Lee, C. J., van Donkelaar, A. & Martin, R. V. Transient climate and ambient health impacts due to national solid fuel cookstove emissions. *Proc. Natl Acad. Sci. USA* **114**, 1269 (2017).
36. Lelieveld, J. et al. Effects of fossil fuel and total anthropogenic emission removal on public health and climate. *Proc. Natl Acad. Sci. USA* **116**, 7192 (2019).
37. Lelieveld, J., Evans, J. S., Fnais, M., Giannadaki, D. & Pozzer, A. The contribution of outdoor air pollution sources to premature mortality on a global scale. *Nature* **525**, 367 (2015).
38. Silva Raquel, A., Adelman, Z., Fry Meridith, M. & West, J. J. The impact of individual anthropogenic emissions sectors on the global burden of human mortality due to ambient air pollution. *Environ. Health Perspect.* **124**, 1776–1784 (2016).
39. Weagle, C. L. et al. Global sources of fine particulate matter: interpretation of PM2.5 chemical composition observed by SPARTAN using a global chemical transport model. *Environ. Sci. Technol.* **52**, 11670–11681 (2018).
40. Lee, C. J. et al. Response of global particulate-matter-related mortality to changes in local precursor emissions. *Environ. Sci. Technol.* **49**, 4335–4344 (2015).
41. Marais, E. A. & Wiedinmyer, C. Air quality impact of diffuse and inefficient combustion emissions in Africa (DICE-Africa). *Environ. Sci. Technol.* **50**, 10739–10745 (2016).
42. Zheng, B. et al. Trends in China's anthropogenic emissions since 2010 as the consequence of clean air actions. *Atmos. Chem. Phys.* **18**, 14095–14111 (2018).
43. Hammer, M. S. et al. Global estimates and long-term trends of fine particulate matter concentrations (1998–2018). *Environ. Sci. Technol.* <https://doi.org/10.1021/acs.est.0c01764> (2020).
44. Burnett, R. et al. Global estimates of mortality associated with long-term exposure to outdoor fine particulate matter. *Proc. Natl Acad. Sci. USA* **115**, 9592 (2018).
45. GBD 2017 Risk Factor Collaborators. Global, regional, and national comparative risk assessment of 84 behavioural, environmental and occupational, and metabolic risks or clusters of risks for 195 countries and territories, 1990–2017: a systematic analysis for the Global Burden of Disease Study 2017. *Lancet* **392**, 1923–1994 (2018).
46. Bey, I. et al. Global modeling of tropospheric chemistry with assimilated meteorology: model description and evaluation. *J. Geophys. Res. Atmos.* **106**, 23073–23095 (2001).
47. Shaddick, G. et al. Data integration for the assessment of population exposure to ambient air pollution for global burden of disease assessment. *Environ. Sci. Technol.* **52**, 9069–9078 (2018).
48. Shaddick, G. et al. Data integration model for air quality: a hierarchical approach to the global estimation of exposures to ambient air pollution. *J. R. Stat. Soc. C-Appl.* **67**, 231–253 (2018).
49. Global Burden of Disease Collaborative Network. Global Burden of Disease Study 2019 (GBD 2019) Particulate Matter Risk Curves. (Seattle, United States of America: Institute for Health Metrics and Evaluation (IHME)), <https://doi.org/10.6069/KHWH-2703> (2021).
50. Pappin Amanda, J. et al. Examining the shape of the association between low levels of fine particulate matter and mortality across three cycles of the Canadian census health and environment cohort. *Environ. Health Perspectives* <https://doi.org/10.1289/EHP5204> (2019).
51. Angel, S. et al. (New York: New York University, Nairobi: UN-Habitat, and Cambridge, MA: Lincoln Institute of Land Policy, 2016).
52. United Nations. 2018 Revision of the World Urbanization Prospects. <https://population.un.org/wup/>
53. Shindell, D. & Smith, C. J. Climate and air-quality benefits of a realistic phase-out of fossil fuels. *Nature* **573**, 408–411 (2019).
54. Vohra, K. et al. Global mortality from outdoor fine particle pollution generated by fossil fuel combustion: results from GEOS-Chem. *Environ. Res.* **195**, 110754 (2021).
55. Grieshop, A. P., Marshall, J. D. & Kandlikar, M. Health and climate benefits of cookstove replacement options. *Energy Policy* **39**, 7530–7542 (2011).
56. Butt, E. W. et al. The impact of residential combustion emissions on atmospheric aerosol, human health, and climate. *Atmos. Chem. Phys.* **16**, 873–905 (2016).
57. Pozzer, A., Tsimpidi, A. P., Karydis, V. A., de Meij, A. & Lelieveld, J. Impact of agricultural emission reductions on fine-particulate matter and public health. *Atmos. Chem. Phys.* **17**, 12813–12826 (2017).
58. Sofiev, M. et al. Cleaner fuels for ships provide public health benefits with climate tradeoffs. *Nat. Commun.* **9**, 406 (2018).
59. Jolly, W. M. et al. Climate-induced variations in global wildfire danger from 1979 to 2013. *Nat. Commun.* **6**, 7537 (2015).
60. Achakulwisut, P., Brauer, M., Hystad, P. & Anenberg, S. C. Global, national, and urban burdens of paediatric asthma incidence attributable to ambient NO₂ pollution: estimates from global datasets. *Lancet Planet. Health* **3**, e166–e178 (2019).
61. Querol, X. et al. Monitoring the impact of desert dust outbreaks for air quality for health studies. *Environ. Int.* **130**, 104867 (2019).
62. U.S. EPA. (U.S. Environmental Protection Agency, Washington, DC, EPA/60/R-19/188, 2019).
63. WHO. Review of evidence on health aspects of air pollution - REVIHAAP. <https://www.euro.who.int/en/health-topics/environment-and-health/air-quality/publications/2013/review-of-evidence-on-health-aspects-of-air-pollution-revihaap-project-final-technical-report> (2013).
64. Lin, J. et al. Carbon and health implications of trade restrictions. *Nat. Commun.* **10**, 4947 (2019).
65. IHME. <http://ghdx.healthdata.org/gbd-results-tool> (2020).
66. Blencowe, H. et al. National, regional, and worldwide estimates of low birthweight in 2015, with trends from 2000: a systematic analysis. *Lancet Glob. Health* **7**, e849–e860 (2019).
67. Chawanpaiboon, S. et al. Global, regional, and national estimates of levels of preterm birth in 2014: a systematic review and modelling analysis. *Lancet Glob. Health* **7**, e37–e46 (2019).
68. van der Werf, G. R. et al. Global fire emissions estimates during 1997–2016. *Earth Syst. Sci. Data* **9**, 697–720 (2017).
69. Philip, S. et al. Anthropogenic fugitive, combustion and industrial dust is a significant, underrepresented fine particulate matter source in global atmospheric models. *Environ. Res. Lett.* **12**, 044018 (2017).
70. Heald, C. L. et al. Atmospheric ammonia and particulate inorganic nitrogen over the United States. *Atmos. Chem. Phys.* **12**, 10295–10312 (2012).

Acknowledgements

The research described in the article was conducted under contract (Grant Agreement: #4965/19-1) to the Health Effects Institute (HEI), an organization jointly funded by the U.S. Environmental Protection Agency (EPA; Assistance Award No. R-82811201) and certain motor vehicle engine manufacturers. The contents of this article do not

necessarily reflect the views of the HEI or its sponsors, nor do they necessarily reflect the views and policies of the EPA or motor vehicle and engine manufacturers. We would like to thank Chi Li, Jun Meng, Crystal Weagle, Brian Boys, and Colin Lee for support during the development of the GEOS-Chem simulations and analysis scripts.

Author contributions

M.B., R.V.M., and E.E.M. conceived the project. E.E.M. developed and conducted the model simulations and model analysis scripts, with computing support from L.B.. E.E.M. conducted the disease burden analysis, as directed by M.B. and J.V.S., with contributions from R.B., M.S.H. and A.v.D. provided high-resolution satellite-derived PM_{2.5} exposure estimates. J.L. and J.A.A. provided compiled observations of PM_{2.5} chemical components from China. E.E.M., S.J.S., and P.O. contributed to the development of the CEDS_{GBD-MAPS} dataset. V.S., L.J., G.L., and F.Y. supported the update of the GEOS-Chem model. E.E.M., M.B., and R.V.M. wrote the manuscript with contributions from all co-authors.

Competing interests

The authors declare no competing interests.

Additional information

Supplementary information The online version contains supplementary material available at <https://doi.org/10.1038/s41467-021-23853-y>.

Correspondence and requests for materials should be addressed to E.E.M.

Peer review information *Nature Communications* thanks Hao Guo, Stefan Reis, and the other, anonymous, reviewer(s) for their contribution to the peer review of this work. Peer reviewer reports are available.

Reprints and permission information is available at <http://www.nature.com/reprints>

Publisher's note Springer Nature remains neutral with regard to jurisdictional claims in published maps and institutional affiliations.



Open Access This article is licensed under a Creative Commons Attribution 4.0 International License, which permits use, sharing, adaptation, distribution and reproduction in any medium or format, as long as you give appropriate credit to the original author(s) and the source, provide a link to the Creative Commons license, and indicate if changes were made. The images or other third party material in this article are included in the article's Creative Commons license, unless indicated otherwise in a credit line to the material. If material is not included in the article's Creative Commons license and your intended use is not permitted by statutory regulation or exceeds the permitted use, you will need to obtain permission directly from the copyright holder. To view a copy of this license, visit <http://creativecommons.org/licenses/by/4.0/>.

© The Author(s) 2021

Supplementary Information for

Source Sector and Fuel Contributions to Ambient PM_{2.5} and Attributable Mortality Across Multiple Spatial Scales

Erin E. McDuffie^{1,2*}, Randall V. Martin^{1,2}, Joseph V. Spadaro³, Richard Burnett⁴, Steven J. Smith⁵, Patrick O'Rourke⁵, Melanie Hammer^{1,2}, Aaron van Donkelaar^{2,1}, Liam Bindle^{1,2}, Viral Shah^{6†}, Lyatt Jaeglé⁶, Gan Luo⁷, Fangqun Yu⁷, Jamiu Adeniran⁸, Jintai Lin⁸, Michael Brauer^{9,4}

¹Department of Energy, Environmental, and Chemical Engineering, Washington University in St. Louis, St. Louis, MO, USA

²Department of Physics and Atmospheric Science, Dalhousie University, Halifax, NS, Canada

³Spadaro Environmental Research Consultants (SERC)

⁴Institute for Health Metrics and Evaluation, University of Washington, Seattle, WA, USA

⁵Joint Global Change Research Institute, Pacific Northwest National Laboratory, College Park, MD, USA

⁶Department of Atmospheric Sciences, University of Washington, Seattle, WA, USA

⁷Atmospheric Sciences Research Center, University at Albany, Albany, New York, USA

⁸Laboratory for Climate and Ocean-Atmosphere Studies, School of Physics, Peking University, Beijing, China

⁹School of Population and Public Health, University of British Columbia, Vancouver, BC, Canada

[†]Now at: Harvard John A. Paulson School of Engineering and Applied Sciences, Harvard University, Cambridge, MA, USA

Corresponding Author: Erin E. McDuffie

Email: erin.mcduffie@wustl.edu

This file includes:

Supplementary Text 1 to 10

Supplementary Figures 1 to 10

Supplementary Tables 1 to 2

Other Supplementary Information for this manuscript include:

Supplementary Data 1-3

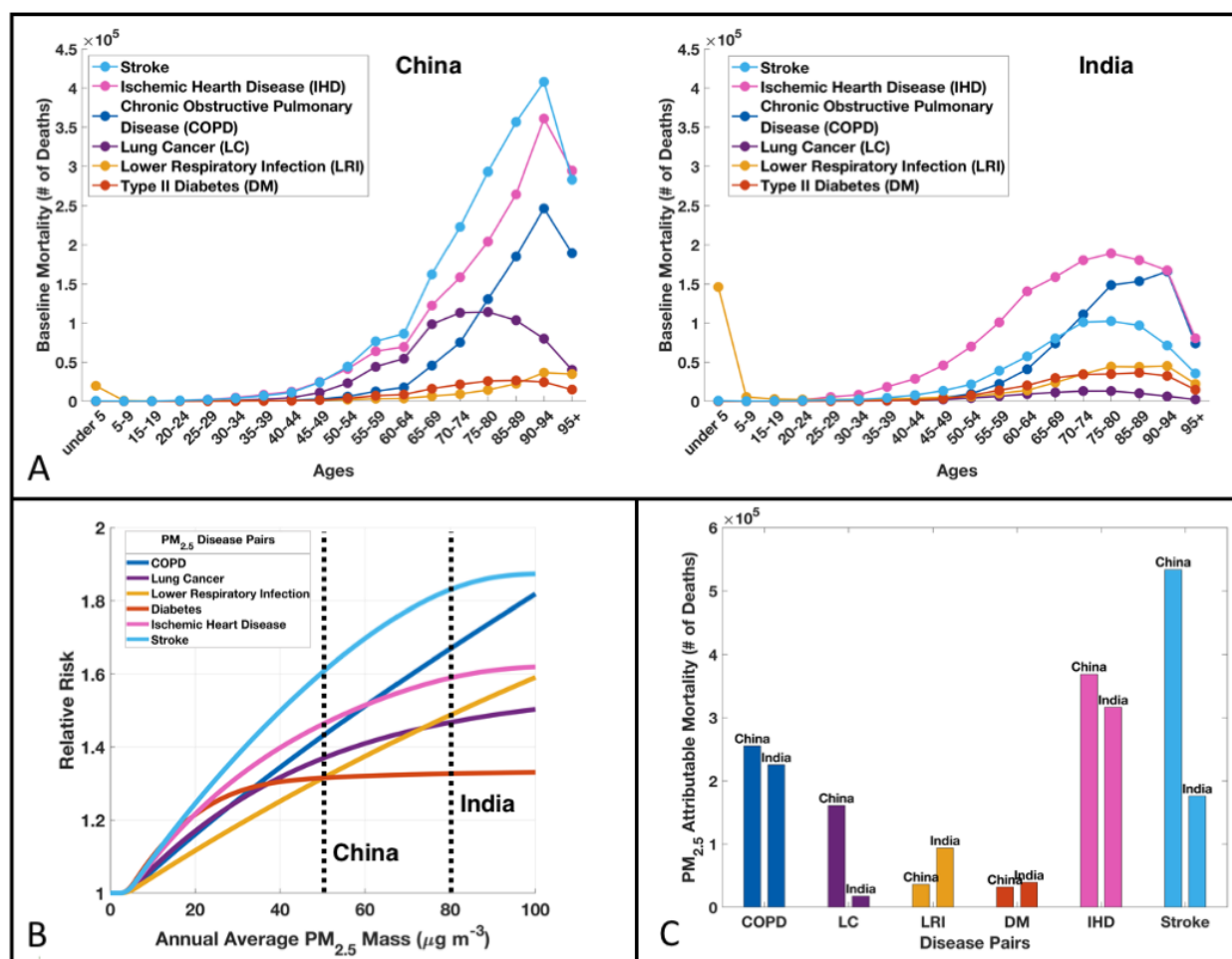
Additional Supporting Tables and Figures

This supplementary information file describes the details of the analysis configuration. A key objective of including these details is to promote transparency and reproducibility. In this work, world countries and regions follow those used in the Global Burden of Disease (GBD) Project, as shown in Supplementary Table 1.

Supplementary Table 1. Member countries and territories of the 21 GBD world regions.

GBD Region	Member Countries			
Asia Pacific, High Income	Brunei Darussalam	Japan	South Korea	Singapore
Asia, Central	Armenia	Azerbaijan	Georgia	Kazakhstan
	Kyrgyzstan	Mongolia	Tajikistan	Turkmenistan
	Uzbekistan			
Asia, East	China	Taiwan (Province of China)		
	North Korea (Democratic People's Republic of Korea)			
Asia, South	Bangladesh	Bhutan	India	Nepal
	Pakistan			
Asia, Southeast	Cambodia	Indonesia	Malaysia	Maldives
	Mauritius	Myanmar	Philippines	Sri Lanka
	Seychelles	Thailand	Timor-Leste	Vietnam
	Laos (Loa People's Democratic Republic)			
Oceania	American Samoa	Cook Islands	Fiji	Guam
	Kiribati	Marshall Islands	Nauru	Niue
	Palau	Papua New Guinea	Samoa	Solomon Islands
	Tokelau	Tonga	Tuvalu	Vanuatu
	Federated States of Micronesia		Northern Mariana Islands	
Australasia	Australia	New Zealand		
Caribbean	The Bahamas	Barbados	Belize	Bermuda
	Cuba	Dominica	Dominican Republic	Grenada
	Guyana	Haiti	Jamaica	Puerto Rico
	Saint Lucia	Suriname	Antigua and Barbuda	Saint Kitts and Nevis
	Trinidad and Tobago	US Virgin Islands	Saint Vincent and the Grenadines	
Europe, Central	Albania	Bulgaria	Croatia	Czech Republic (Czechia)
	Hungary	North Macedonia	Montenegro	Poland
	Romania	Serbia	Slovakia	Slovenia
	Bosnia and Herzegovina			
Europe, Eastern	Belarus	Estonia	Latvia	Lithuania
	Republic of Moldova	Russian Federation	Ukraine	
Europe, Western	Andorra	Austria	Belgium	Cyprus
	Denmark	Finland	France	Germany
	Greece	Iceland	Ireland	Israel
	Italy	Luxembourg	Malta	Monaco
	Netherlands	Norway	Portugal	San Marino
	Spain	Sweden	Switzerland	United Kingdom
North America, High Income	Canada	Greenland	United States	
Latin America, Andean	Bolivia (Plurinational State of)		Ecuador	Peru
Latin America, Central	Colombia	Costa Rica	El Salvador	Guatemala
	Honduras	Mexico	Nicaragua	Panama
	Venezuela (Bolivarian Republic of)			
Latin America, Southern	Argentina	Chile	Uruguay	
Latin America, Tropical	Brazil		Paraguay	
North Africa / Middle East	Afghanistan	Algeria	Bahrain	Egypt
	Iraq	Jordan	Kuwait	Lebanon
	Libya	Morocco	Palestine	Oman
	Qatar	Saudi Arabia	Sudan	Syrian Arab Republic
	Tunisia	Turkey	Yemen	United Arab Emirates
	Iran (Islamic Republic of)			

Sub-Saharan Africa, Central	Angola Central African Republic	Congo Democratic Republic of the Congo	Equatorial Guinea	Gabon
Sub-Saharan Africa, Eastern	Burundi Ethiopia Mozambique Uganda	Comoros Kenya Rwanda Zambia	Djibouti Madagascar Somalia United Republic of Tanzania	Eritrea Malawi South Sudan
Sub-Saharan Africa, South	Botswana Eswatini	Lesotho Zimbabwe	Namibia	South Africa
Sub-Saharan Africa, Western	Benin Chad Guinea Mauritania Sierra Leone	Burkina Faso Cote d'Ivoire Guinea-Bissau Niger Togo	Cameroon The Gambia Liberia Nigeria Sao Tome and Principe	Cape Verde Ghana Mali Senegal



Supplementary Figure 1. PM_{2.5} Disease Burden Comparison for India and China. (A) GBD2019 background baseline mortality data as a function of population age and disease. (B) GBD2019 concentration response functions (same as Supplementary Figure 2), with dashed lines showing population weighted mean PM_{2.5} concentrations for China and India. (C) Total PM_{2.5} attributable deaths in China and India as a function of disease.

Supplementary Text 1. 2019 Exposure Estimates – Additional Details

Following the downscaling procedure described in the Methods (and Supplementary Text 9), we apply high-resolution (gridded at $\sim 1 \text{ km} \times \sim 1 \text{ km}$) exposure estimates for the year 2019 (weighted by 2019 gridded population¹) to the GBD2019 CRFs with 2019 baseline mortality data to assess changes in the estimated disease burden between 2017 and 2019. Disease burden estimates are independent from model emission sensitivity simulations and do not require changes or projections in emissions. In both years, the same nine countries were estimated to have largest number of PM_{2.5} attributable deaths, though the annual number of deaths in each country was larger in 2019 than 2017, except for in Russia. Similarly, annual population-weighted mean (PWM) PM_{2.5} concentrations also increased in each of these top nine countries, except for in China and the United States. The complex relationship between annual national PM_{2.5} concentrations and resulting attributable deaths highlights the importance of multiple factors in disease burden estimations. For neonatal disorders, the incidence associated with outdoor PM_{2.5} exposure totaled to 2.07 (95% CI: 0.02-5.02) million worldwide, which increased marginally to 2.09 (95% CI: 0.02-5.06) million in 2019. At the sub-national level, the top four of the 200 select areas with the highest PM_{2.5} concentrations (Singrauli, Kanpur, Sitapur, and Ahmedabad, India) all experienced increases in PWM PM_{2.5} mass, persisting at levels between 14 and 16 times greater than the WHO annual average guidelines. Of the 200 sub-national areas, 45% experienced no change or an increase in PWM PM_{2.5} concentration between 2017 and 2019. The area surrounding Pune, India had the largest absolute increase from 57 to 63.2 $\mu\text{g m}^{-3}$, while the area surrounding Xingping, China had the largest absolute decrease from 68.4 to 60.1 $\mu\text{g m}^{-3}$. These changes serve to identify potential locations with effective mitigation strategies or those locations with the most to gain from pollution reductions. Supplementary Data 3 provides the PWM values for the global area, each of the 21 world regions, 204 countries, and 200 sub-national areas.

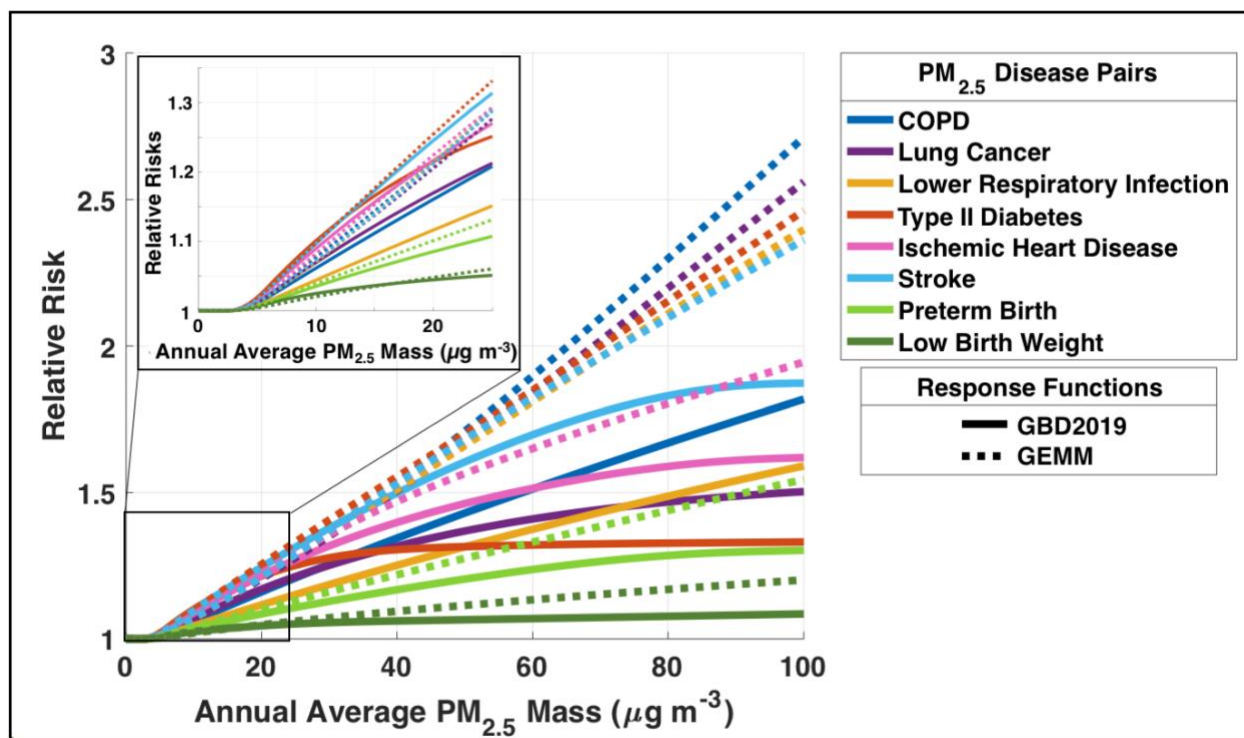
Supplementary Text 2. GEMM Sensitivity Study – Additional Details

As an alternative to the GBD estimates, previous global studies have used the GEMM. The GEMM exclusively incorporates risk information from cohort studies of outdoor air pollution (41 cohorts from 16 countries)² on non-accidental mortality and was highly sensitive to one particular cohort of Chinese men³ in the original version. Another feature of the GEMM is that

its non-accidental mortality estimate suggests a larger impact of PM_{2.5} exposure on mortality than the sum of cause-specific attributable mortality estimates. As new evidence on links between PM_{2.5} and other (e.g., chronic kidney disease, dementia) causes of death emerge, this difference between cause-specific and all-cause (non-accidental) attributable mortality will decrease.

Application of the GEMM-based disease-specific estimates to the disease burden, however, should also be employed with caution. As further discussed in Hystad, et al.⁴ the GEMM is based on analyses of non-accidental mortality primarily derived from epidemiologic studies conducted in high-income countries. When applied to disease burden estimates, this assumes similar distributions of causes of death, including the relative proportion of the specific diseases linked to air pollution and the population age distribution in high-income countries as in low and middle-income countries. This leads to uncertainty since the relative frequencies of the various causes of deaths differ markedly between countries of the world. In particular, application to Africa and South Asia is likely to lead to substantial uncertainty. As the GBD2019 CRFs are derived directly from studies of specific diseases, they can be more reliably applied to disease-specific mortality rates across countries. Other sources of uncertainty such as the assumptions of equitoxicity, variation in e.g., healthcare access and quality and population characteristics, and extrapolation to concentrations beyond those included in epidemiologic studies are common to the application of both the GBD2019 CRFs and the GEMM.

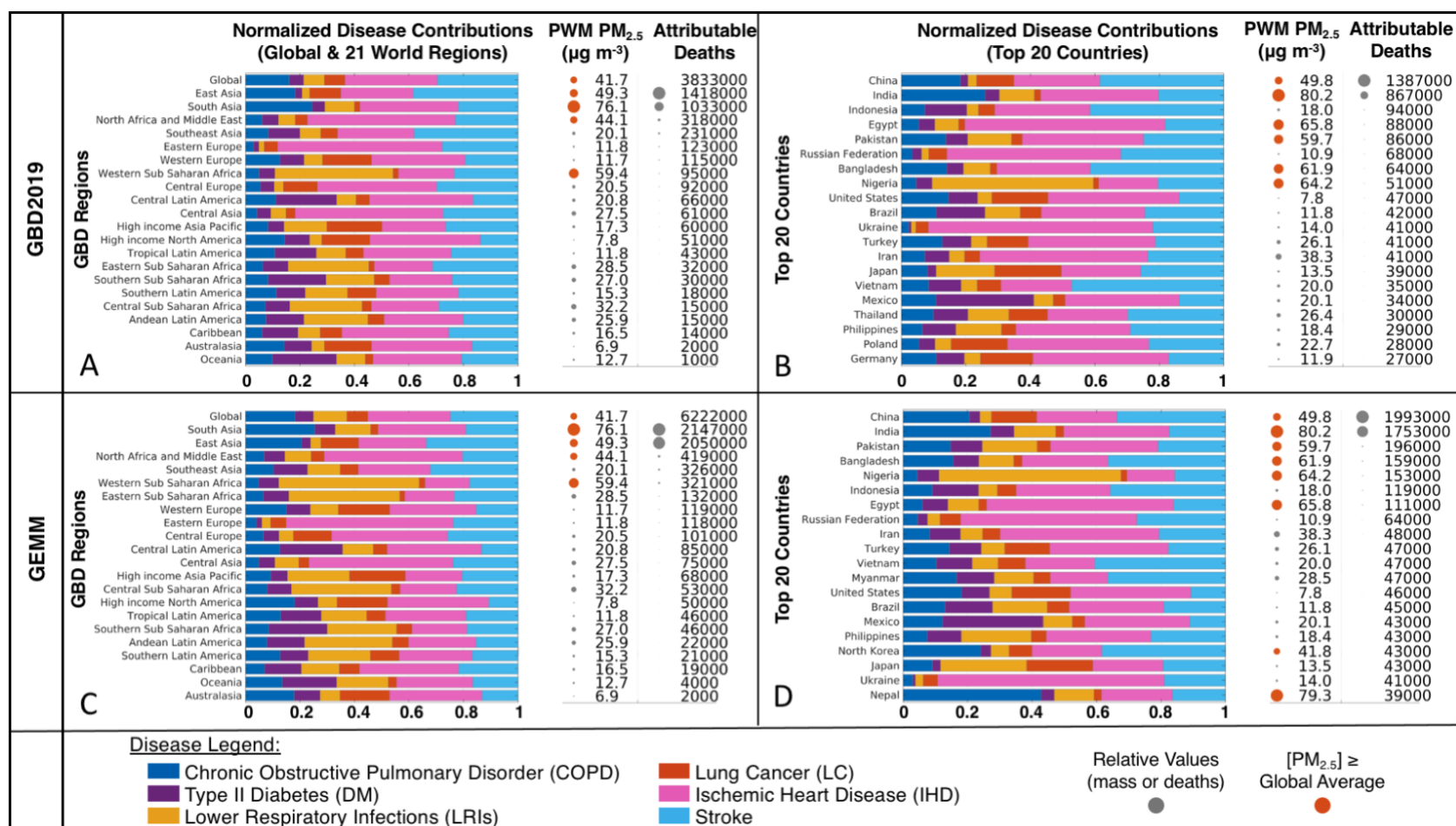
To address some of these uncertainties, the GEMM CRFs in this work were updated as described in the Methods to include the same ambient PM cohort studies that are inputs to the GBD2019 CRFs and to add functions for diabetes and reproductive outcomes. Supplementary Figure 2 compares the disease-specific CRFs for the GBD2019 and updated GEMM. With these updates, and when restricted to the five NCDs +LRI that are included in the GBD2019 CRFs, 2017 global GEMM attributable mortality estimates were lower than previous GEMM estimates for 2015 when only the four NCDs +LRI were included (6.2 million vs 6.9 million)². Globally, the updated GEMM CRFs estimated a PM_{2.5} attributable burden of 6.2 (95% CI: 4.4 to 7.8) million deaths in 2017. While satellite-based estimates have shown a recent decreasing trend in PWM PM_{2.5} mass across East Asia, Europe, and the Eastern U.S.⁵, a detailed analysis of differences (temporal trends vs. methodological differences) between the original and updated GEMM estimates is outside the scope of this work.



Supplementary Figure 2. Concentration response functions for the GBD2019 and updated GEMM. Solid Lines: GBD2019 CRFs, **Dashed Lines:** updated GEMM. Line colors correspond to the central values of eight disease-response pairs. For illustrative purposes, response curves for IHD and Stroke correspond to the 60-64 age group, COPD, LC, and DM responses are for all ages over 25 years, and LRIs are for ages under 5 years and greater than 25 years. Preterm births are at a gestational age less than 37 weeks (PTB) and weights below 2.5 kg (LBW). For illustrative purposes, the insert highlights the relative risks at exposure levels less than $25 \mu\text{g m}^{-3}$.

Supplementary Figure 3 shows the relative disease-specific contributions from both the updated GEMM and GBD2019 CFRs for 21 world regions (A, C), and the top 20 countries with the largest number of attributable deaths (B, D). S1-Fig. 2 shows that the relative disease contributions predicted by the updated GEMM were similar to those from the GBD2019 CRFs. For example, both predict that the largest number of attributable deaths at the global scale were from IHD, and then in decreasing order from Stroke, COPD, LRI, LC, and DM. The absolute number of attributable deaths, however, were nearly always larger from the GEMM (Supplementary Data 1). Two exceptions were for North America and Australasia. These regions had the lowest PWM $\text{PM}_{2.5}$ concentrations and the difference in relative predictions reflect the lower relative risks for IHD, Stroke, and Diabetes in the updated GEMM at $\text{PM}_{2.5}$ concentrations below $10 \mu\text{g m}^{-3}$ (Supplementary Figure 2). As a result of these and other differences in the CRFs, the GEMM and GBD2019 CRFs also predicted different relative

rankings of the top 20 countries. Supplementary Figure 3b and d show that both the GBD2019 CRFs and GEMM predicted the same top two countries (China and India), but that the relative rankings for the next 18 countries differ. In addition to ranking differences, the GBD2019 CRFs also included Thailand (16th), Poland (19th), and Germany (20th) in the top 20 countries, while the GEMM alternatively predicted that Myanmar (12th), North Korea (17th), and Nepal (20th) ranked in the top 20. This comparison closes a portion of the gap between previous GEMM and GBD disease burden results, however, the accuracy of both estimates are dependent on the availability of robust and high-resolution exposure data, particularly in high exposure areas.



Supplementary Figure 3: Normalized disease contributions to total attributable mortality in 2017 for 21 world regions (A, C) and 20 countries (B, D) with the highest outdoor PM_{2.5} disease burden. Panels show results estimated using the GBD2019 CRFs (A, B) and the updated GEMM (C, D). Bar charts show the relative contributions of six PM_{2.5}-disease pairs to regional and national-level outdoor PM_{2.5} attributable deaths, sorted by decreasing number of deaths. The number of LBW and PTB incidences are included in Supplementary Data 1. PWM PM_{2.5} concentrations and number of attributable deaths are additionally provided for each region/country. Relative amounts are illustrated by relative dot sizes (except for the global total disease burden). Red dots indicate regions/countries with PM_{2.5} exposure levels equivalent or larger than the global average.

Supplementary Text 3. Global Model Details

PM_{2.5} source sensitivity simulations for the year 2017 are shown in Supplementary Table 2 and are conducted with the GEOS-Chem 3D atmospheric chemical transport model⁶. The GEOS-Chem model solves for the evolution of atmospheric aerosols and gases using meteorological data, global and regional emission inventories, and algorithms that represent the physics and chemistry of atmospheric processes. Global simulations are conducted from December 2016 to January 2018 (1-month spin-up) at 2°×2.5° horizontal resolution and 47 vertical layers. Global simulations are supplemented with three additional one-way nested simulations at 0.5°×0.625° horizontal resolution that cover North America (10° N – 70° N, 140° W – 40° W), Europe (30° N – 70° N, 30° W – 50° E), and China and Southeast Asia (11° S – 55° N, 60° E – 150° E)⁷. Each simulation is driven by assimilated meteorological data from the Goddard Earth Observing System from the NASA Global Modeling and Assimilation Office (GMAO). We use the MERRA-2 historical reanalysis product, archived at a 3-hour temporal resolution for 3D fields and 1-hour for 2D fields. The transport and chemistry timesteps are set to 10 and 20 minutes respectively, to optimize simulation accuracy and computational efficiency⁸.

In this work, we use the GEOS-Chem ‘tropchem’ chemical mechanism that includes coupled aerosol-oxidant chemistry in the troposphere and stratosphere. The gas-phase mechanism includes detailed HO_x-NO_x-VOC-ozone chemistry⁶, coupled to aerosol chemistry for inorganic sulfate-nitrate-ammonium aerosol^{9,10}, as well as carbonaceous (black and organic carbon) aerosol^{10,11}, sea salt¹², and dust^{13,14}. Relative humidity dependent aerosol size distributions and optical properties are based on the Global Aerosol Data Set^{15,16}, with updates for organics and secondary inorganics from observations^{17,18}, mineral dust^{14,19,20}, and absorbing brown carbon²¹. Aerosol thermodynamic partitioning between sulfate-nitrate-ammonium is computed with the ISORORPIA II thermodynamic model²², while the BC mechanism is described by Wang, et al. ¹⁰. We use the simple, irreversible, direct yield scheme for secondary organic aerosol (SOA) from Kim, et al. ¹¹, as this mechanism has been shown to better reproduce available observations of global organic aerosol mass relative to the more complex scheme²³. For physical processes, GEOS-Chem uses the TPCORE advection algorithm²⁴ and computes convective transport from the convective mass fluxes in the meteorological data, as described by Wu, et al. ²⁵. In this work, boundary layer mixing uses the non-local mixing scheme as implemented by Lin and McElroy ²⁶.

The core source code for this work is GEOS-Chem v12.1.0²⁷, released Nov. 2018. To correct a long-standing bias in nitrate aerosol concentrations^{28,29}, the v12.1.0 source code has been updated here as part of the Global Burden of Disease – Major Air Pollution Sources project (<https://sites.wustl.edu/acag/datasets/gbd-maps/>). The code is available on GitHub: https://github.com/emcduffie/GC_v12.1.0_EEM. Major updates follow literature recommendations and include an updated parameterization for the heterogeneous uptake of N₂O₅ from McDuffie, et al.³⁰, the added heterogeneous production of ClNO₂ following Shah, et al.³¹ and recommended ClNO₂ yield reductions from McDuffie, et al.³², a reduction in the deposition of HNO₃ under cold conditions following Shah, et al.³¹, as well as an update to the wet deposition scheme following recommendations in Luo, et al.²⁹. In addition to the updates described in Luo, et al.²⁹, the rate of SO₂ removal in clouds is also reduced, and the rainout efficiencies for hydrophilic OC and BC species are reduced by 50% following recent recommendations³³. These and additional minor code updates are described in the GitHub README file.

To evaluate the impact of these model updates, Supplementary Figure 5b shows a bar chart of the normalized mean bias (NMB) in the simulated global annual averages of aerosol nitrate, sulfate, ammonium, total organic carbon, black carbon, fine dust, and sea salt in the default v12.1.0 GEOS-Chem source code and the updated model, compared to annual average observations (described in Supplementary Text 4). As shown in Supplementary Figure 5b, the mechanistic model updates described above reduce the NMB in the updated GEOS-Chem simulated concentrations of aerosol nitrate from 2 µg/m³ to 0.5 µg/m³ relative to observed values. Model updates additionally improve the model-observation agreement of ammonium, black carbon, and dust compared to the default model. In contrast, the negative bias in sea salt is enhanced in the updated base simulation relative to the default source code. The annual PWM mass concentrations of each observed compound are additionally provided in Supplementary Figure 5b (gridded population from the Gridded Population of the World Database¹). These indicate that the smallest model NMB's are found for the compounds that contribute to the largest fraction of total PM_{2.5} mass. As further shown in the right panel of Supplementary Figure 5b, there is general agreement in the fractional contributions of each chemical compound to total PM_{2.5} mass, providing confidence in the model's ability to accurately predict changes in the chemical production of PM_{2.5} under various emission sensitivity simulations.

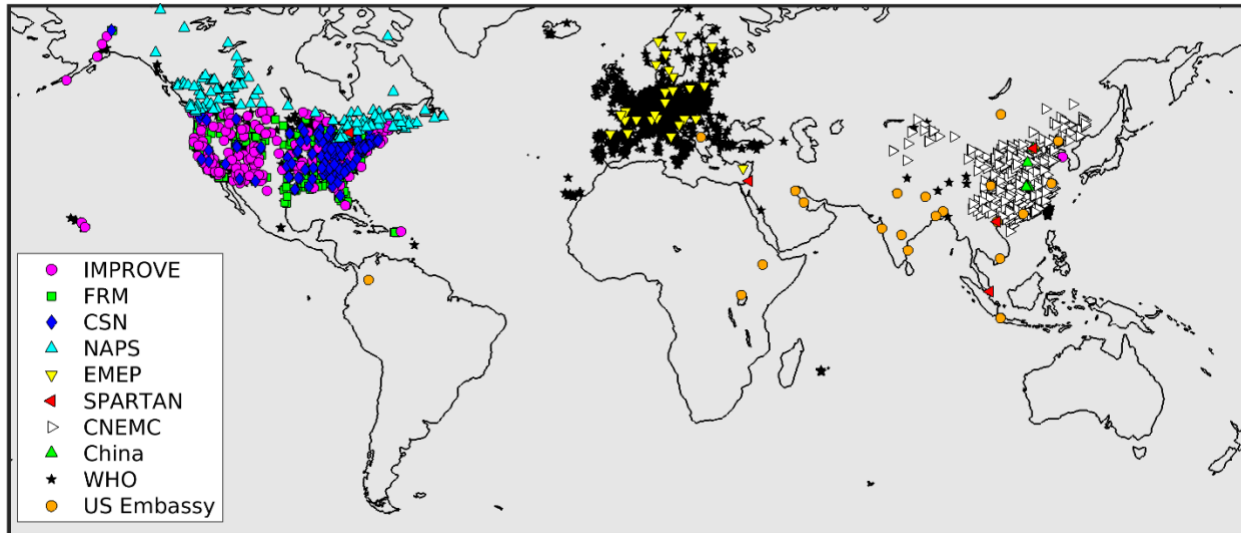
Lastly, total PM_{2.5} mass concentrations are calculated using modeled output mass concentrations of aerosol nitrate (NO₃⁻), sulfate (SO₄²⁻), ammonium (NH₄⁺), sea salt, dust, organic mass, and black carbon, as described in the analysis scripts package (<https://github.com/emcduffie/GBD-MAPS-Global>). In this work, spatially gridded annual total PM_{2.5} mass concentrations are calculated by averaging monthly PM_{2.5} concentrations. National-level PM_{2.5} concentrations are averaged over the grid cells within each country's geographical borders.

Supplementary Text 4. Observational PM_{2.5} Dataset for Model Evaluation

Evaluation of base model performance is a vital component of any analyses that derives results from modeled emission sensitivity simulations. In this work, the base 2017 GEOS-Chem PM_{2.5} simulation and downscaled PM_{2.5} exposure estimates (Fig. 1) are evaluated against a dataset of annual-average surface observations of total PM_{2.5} mass and PM_{2.5} chemical composition (where available). This section describes methods used to develop this observational dataset.

Supplementary Figure 4 provides a map of the individual measurement sites in this dataset, colored by their measurement networks. More extensive sampling and analysis details are reported from the North American networks than those from other regions, which have larger uncertainties due to a lack of consistent reporting on sampling and analysis protocols (particularly for EMEP and WHO datasets). Based on available reported metadata, some networks also provide mass concentrations derived from multiple sampling and analysis methods. Here we attempt to reduce sampling differences by selecting for consistent analysis methods between sites and networks when this information is available (described in detail below). Observational data also include uncertainties in the amount of aerosol water assumed in the gravimetric analysis of PM_{2.5} and degree of volatilization of PM_{2.5} and its chemical components (particularly ammonium nitrate and organics) during sampling and/or filter transport. Uncertainties in these observational datasets should be considered when comparing to modeled results.

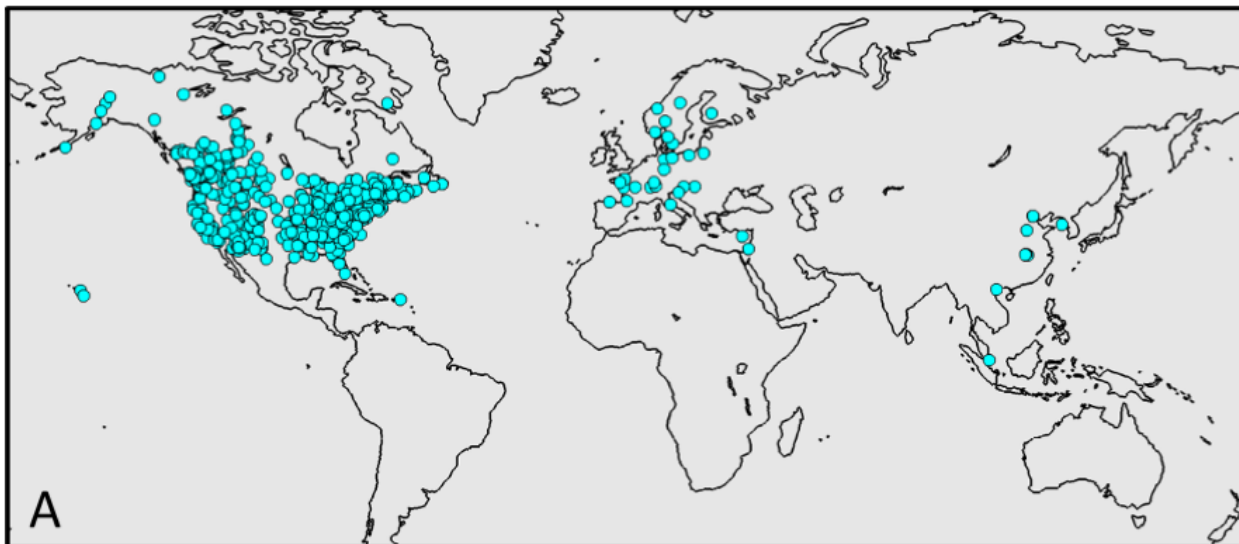
2017 PM_{2.5} Surface Observation Network Sites



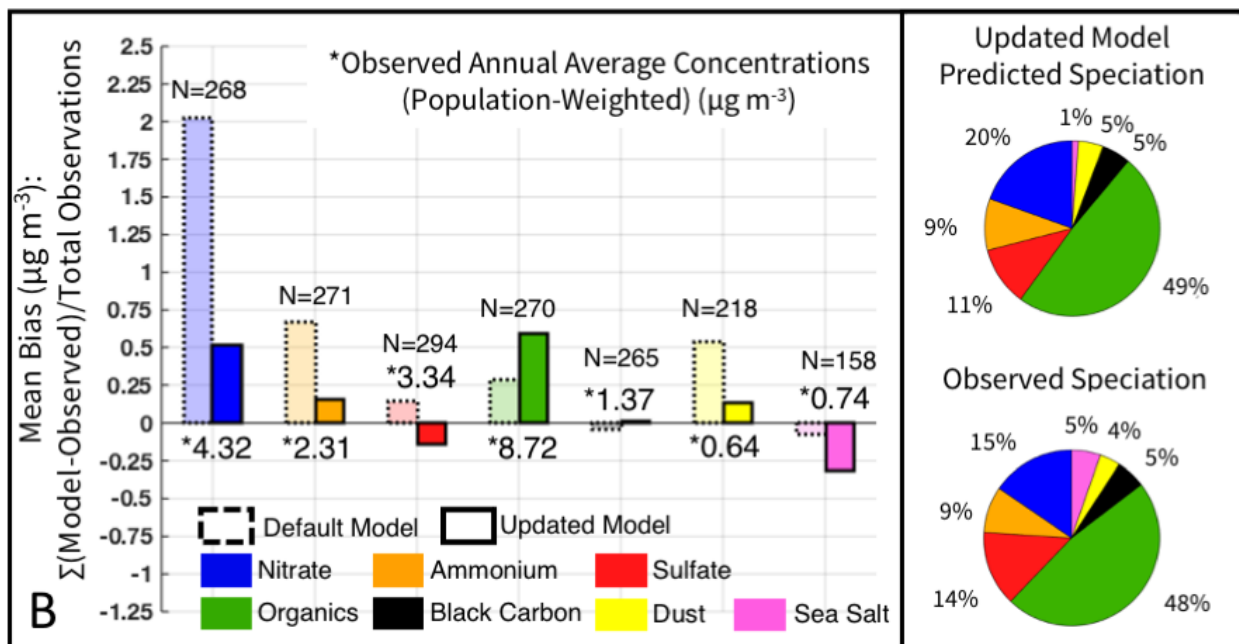
Supplementary Figure 4: Map of 2017 long-term PM_{2.5} sampling stations. Symbol colors and shapes reflect individual monitoring networks. This figure includes sites that are used both for the total PM_{2.5} mass and speciated PM_{2.5} mass model evaluations.

The following sub-sections describe the individual networks that provide long-term measurements of PM_{2.5} total mass and/or PM_{2.5} chemical components. Estimates of PM_{2.5} chemical composition in 2017 are available for a more select number of sites than total PM_{2.5} mass, as shown in Supplementary Figure 5a. These sites are primarily in populated regions throughout North America, Europe, select sites in China, and 5 international sites through the SPARTAN network^{34,35}. Data from the SPARTAN network and the compiled speciated inventory for China are used for the speciated comparison in Supplementary Figure 5b and are not used in Fig. 1. Annual average values from each site are calculated from the calculated monthly averages. Dataset development details can be found in the analysis scripts package at: <https://github.com/emceduffie/GBD-MAPS-Global>.

2017 Long-Term PM_{2.5} Composition Observation Sites



2017 Annual Simulated vs. Observed PM_{2.5} Speciation



Supplementary Figure 5: Evaluation of default and updated base model simulation of PM_{2.5} chemical components. (A) map of available long-term surface observations of PM_{2.5} chemical components. (B) Bar plot of the normalized mean bias between the simulated and observed concentrations of individual PM_{2.5} components (nitrate, ammonium, sulfate, organic aerosol, black carbon, dust, and sea salt). Light bars represent the values from the default v12.1.0 GEOS-Chem model. Darker bars show results from the updated model source code used here. Population-weighted average observed concentrations of each component are also provided. Pie charts illustrate the fractional distribution of PM_{2.5} components from the updated model (top) and the observations (bottom).

WHO (World Health Organization) Compilation – Global

The World Health Organization has compiled an extensive database of annual-average surface-level PM_{2.5} concentrations from around the world. In this work, these data are downloaded from <https://www.who.int/airpollution/data/cities/en/>. Only direct PM_{2.5} measurements are used here, not those calculated from PM₁₀ measurements (as in the GBD exposure calibration procedure), due to uncertainties in this conversion. This dataset is filtered to only include annual average measurements from 2017 for sites that report at least 75% measurement coverage. Data sources are available in the downloaded dataset, but measurement methods and analysis techniques are not readily available for the reported observations. We assume that data are reported at 35% RH and at local temperature and pressure. Observations from other regional networks may also be included in this compiled dataset, especially over North America and Europe. To ensure that these sites are not double counted in the model evaluation, we remove sites from the WHO dataset that are within 0.1° of other network sites.

US Embassy Measurements – Global

The U.S. Department of State collects air quality monitoring data from U.S. embassies and consulates around the world and has partnered with the U.S. Environmental Protection Agency to report data at AirNow.gov. Hourly observations from Beta-Attenuation Monitors (BAMs) are available for 28 sites in 2017 (55 sites by 2020). Hourly data for each site are downloaded from: <https://www.airnow.gov/international/us-embassies-and-consulates>. In this work, hourly raw concentrations are averaged into annual values and filtered to remove sites with <75% temporal data coverage. We assume that data are reported for local conditions (ambient pressure and temperature) and 35% RH.

CNEMC (China National Environmental Monitoring Centre) – China

The government of China has facilitated the deployment of nearly 2000 sites that measure PM_{2.5} mass and its chemical composition. At the time of this study, only total PM_{2.5} mass concentrations were publicly available. Data can be downloaded from: <http://www.cnemc.cn/en/> and are available from May 2014 onward. Both Thermo Fisher Tapered Element Oscillating Microbalance (TEOM) 1405F analyzers and BAMs are used for continuous sampling of PM_{2.5} mass, reported at each site at hourly time resolution. As

described in Wu, et al.³⁶, both methods use heaters to reduce the humidity in sampled air. This heating, however, can lead to mass loss due to the volatilization of PM_{2.5} components. As a result, previous studies have reported lower total PM_{2.5} mass measurements from TEOM instruments relative to US Federal Reference Methods (FRM)³⁷, largely as a result of the loss of semi-volatile compounds³⁸ and particularly in cold ambient temperatures³⁹. To minimize this potential under-reporting, the 1405F monitoring system additionally measures concentrations in the volatilized portion of air, while a smart heater is used with the BAMs to minimize heating while also controlling the RH of the sample at 35%³⁶. In this work, we assume that all CNEMC mass concentrations are reported at 35% RH and at local temperature and pressure, consistent with other networks. Monthly averages for January-December 2017 are then calculated for each site that reports a complete number of 24 measurements each day, for at least 20 days each month (~75% temporal coverage each month).

FRM Sites (Federal Reference Method) – United States

FRM sites follow protocols specified in Appendix L to Part 50 of Title 40 in the United States Code of Federal Regulations (CFR) – *Reference Method for the Detection of Fine Particulate Matter as PM_{2.5} in the Atmosphere*. These sites measure total PM_{2.5} mass by gravimetric analysis of a Teflon collection filter. Samples are collected on a filter for a 24-hour period every 3rd day, then transported to an analysis facility where filters are allowed to equilibrate for a minimum of 24 hours prior to weighing. The temperature and RH must be controlled between 20-23°C and 30-40%, respectively during the analysis. All data are reported at local ambient conditions (pressure and temperature). For this work, FRM data were downloaded from: <http://views.cira.colostate.edu/fed/QueryWizard/>, with additional details in the analysis scripts package. Data are saved as monthly averages for all sites with at least 10 measurements during the month (8 for February).

IMPROVE (Interagency Monitoring of Protected Visual Environments) – United States

Details about the IMPROVE network are reported elsewhere⁴⁰ and at <http://vista.cira.colostate.edu/Improve/>. IMPROVE sites are generally focused on rural areas and follow the same sampling procedures at each site. Briefly, each site has four measurement modules:

- 1) Teflon filter for gravimetric mass and X-ray fluorescence (XRF) analysis of trace elements
- 2) denuder + Nylon filter for anions by ion chromatography

3) Quartz filter for organic carbon by thermal optical reflectance (TOR) and calculation of elemental carbon using HIPS (Hybrid Integrating Plate and Sphere system).

4) Coarse mode sampler

Samples are collected for 24 hours, every 3rd day, after which they are transported to laboratories for analysis (without controlling for temperature or pressure). Samples are allowed to equilibrate for a few minutes prior to sampling. Data are reported at local, ambient conditions (pressure and temperature). For this work, IMPROVE data were downloaded from: <http://views.cira.colostate.edu/fed/QueryWizard/>, with additional file formatting details listed in the analysis scripts package. Data for each compound are saved as monthly averages for all sites with at least 10 daily measurements during the month (8 for February). In this work, spatially and seasonally varying OM:OC ratios are used to convert total monthly organic carbon measurements to total organic mass. Ammonium is re-constructed from sulfate and nitrate ion measurements, assuming pure ammonium nitrate and ammonium sulfate in the aerosol phase. Dust is reconstructed from trace elements assuming normal oxides in typically occurring soil dust following Supplementary Eq. 1. Sea salt is calculated as 1.8*chloride following White ⁴¹. Black carbon is taken as elemental carbon.

$$\text{Dust} = 2.2 \times \text{Al} + 2.49 \times \text{Si} + 1.63 \times \text{Ca} + 2.42 \times \text{Fe} + 1.94 \times \text{Ti} \quad (\text{S-Eq. 1})$$

CSN (Chemical Speciation Network) – United States

Details about the CSN network are reported elsewhere⁴². In contrast to IMPROVE, CSN sites focus primarily on urban areas and do not use the same sampling instrumentation/methods at each site. In general, collection and analysis methods are similar to those listed for the IMPROVE network, with the analysis of some species (i.e., organic and elemental carbon) following IMPROVE protocols. Similar to IMPROVE, samples are collected for 24 hours, every 3rd day. Samples are transported overnight, held at a temperature of $\leq 4^{\circ}\text{C}$ to minimize sample volatilization. Gravimetric analysis of PM_{2.5} follows the FRM protocol where the samples are allowed to equilibrate for 24 hours prior to analysis and measured in a controlled clean room between 20-23°C and 30-40% RH. All data are reported at local, ambient conditions (pressure and temperature). For this work, CSN data were downloaded from: <http://views.cira.colostate.edu/fed/QueryWizard/>, with additional details in the analysis scripts package. Data for each compound are saved as monthly averages for all sites with at least 10 daily measurements during the month (8 for February). The final calculation of

organic mass, black carbon, sea salt, and dust follow the procedures used for IMPROVE data, described above.

NAPS (National Air Pollution Surveillance Program) – Canada

The NAPS network was designed to provide long-term air quality data across populated regions in Canada. The NAPS network includes sites with 24-hour integrated measurements of PM_{2.5} mass and its components every 3-6 days, as well as sites with continuous, hourly PM_{2.5} measurements. Data are available at: <http://data.ec.gc.ca/data/air/monitor/national-air-pollution-surveillance-naps-program/Data-Donnees/2017/?lang=en>. In 2017, hourly measurements were reported from a variety of instruments including the TEOM, Scientific Synchronized Hybrid Ambient Real-time Particulate (SHARP) model 5030, and Met-One BAM. Additional integrated PM_{2.5} zip files contain Excel files for each monitoring site across Canada. Integrated daily filters are collected for 24 hours every 3-6 days and are allowed to equilibrate in the laboratory prior to sampling. The temperature and humidity are controlled during weighing between 20-26°C and 37-47% RH, respectively. Some sites have a dual Teflon-nylon filter collection system to collect nitrate loss during sampling. Due to known losses of ammonium nitrate on Teflon filters, only nitrate data from sites with a dual filter cartridge are used in this analysis. For these sites, total nitrate is calculated as the sum of nitrate measured by IC from the Teflon filter and nitrate and nitrite collected from the Nylon filter and analyzed by IC. Data for each compound are saved as monthly averages for all sites with at least 5 daily measurements during the month (4 for February). For continuous PM_{2.5} data, hourly data are also averaged for months with at least 5 sampling days and 24 hours of valid measurements each day. All data are reported at local, ambient conditions (pressure and temperature). In this work, concentrations of organic mass, dust, sea salt, nitrate, ammonium, and sulfate are calculated as for the IMPROVE and CSN data, described above. Black carbon is calculated from the difference between total carbon and organic carbon.

EMEP (European Evaluation and Monitoring Program) – Europe

Measurements collected by partner organizations across Europe are reported to the EMEP database. Despite standard metadata protocols, lack of consistent compliance has resulted in largely unknown sampling methods and analysis protocols for the data available from this network. For this work, the EMEP dataset was downloaded from <http://ebas.nilu.no>, with

additional details in the analysis script package. Due to limited measurements of silicon, dust is not calculated from this dataset. Reported sampling frequencies range from 1 hour to 1-month. Where metadata is available, measurements have been filtered for data greater than reported detection limits. Due to a lack of consistent reporting of meta-data, there are a large number of uncertainties in the data from this network including measurement methods, sample filter types, or whether data have been corrected to standard or local conditions. Here, we assume data are reported in local conditions for consistency in units with national ambient air quality standards and do not apply any other filters. Data for each compound are then standardized to a time series of daily averages and saved as monthly averages for all sites with at least 4 daily measurements during the month⁴³. In this work, concentrations of organic mass, sea salt, nitrate, ammonium, and sulfate are calculated as for the IMPROVE, CSN, and NAPS data, described above. Black carbon is taken as elemental carbon.

Compiled PM_{2.5} Mass and Chemical Components - China

Additional total PM_{2.5} mass and chemical composition data for select sites in 2017 in China have been compiled from literature sources. The data used in this work include measurements from⁴⁴⁻⁴⁸, which report data from 14 measurement locations throughout Beijing, Hebei, Zhejiang, Jiangsu, Shaanxi, and Inner Mongolia provinces, collected at various times during the period between August 2016 and February 2018. Measurement techniques for OC and BC include DRI- Thermal/optical carbon analyzers, while sulfate, nitrate, and ammonium measurement methods include IC. Additional sampling and analysis details for each study are provided in the above references. Available reported data were compiled into annual averages for each measurement site for comparison with model results.

SPARTAN (Surface Particulate Matter Network) – Global

An overview of the SPARTAN network is available in Snider, et al.³⁴, Weagle, et al.³⁵, and McNeill, et al.⁴⁹. The SPARTAN network provides publicly available data for PM_{2.5} total mass, chemical composition, and optical characteristics in populated regions of the world where air quality monitoring has been historically limited. SPARTAN reported complete yearly data from 5 sites in 2017 and has since grown to report data from 21 sites worldwide. SPARTAN monitors sample ambient air on a Teflon filter, intermittently for a total of 24 hours over a 9-day period, following protocols described in Snider, et al.³⁴. Filters are then shipped in sealed containers at ambient temperature to analysis labs in North America where

they undergo analysis for total gravimetric PM_{2.5} mass and concentrations of ions, equivalent black carbon, and trace elements. Particle bound water is calculated and residual mass (i.e., total PM_{2.5} – inorganic mass + particle bound water) is considered to be organic mass. Total PM_{2.5} mass is measured gravimetrically following EPA protocols under laboratory conditions where temperature and RH are controlled to between 20-23°C and 30-40%, respectively. Equivalent black carbon is measured by light absorbance with a smoke stain reflectometer, calibrated to co-located TOR measurements on a quartz filter. More recent analysis techniques for SPARTAN filters include XRF, HIPS, UV-Vis^{49,50}, the measurement of organics through FT-IR⁵¹, and ongoing research activities to measure organic spectra through Aerosol Mass Spectroscopy⁵². For this work, SPARTAN data have been downloaded from: <https://www.spartan-network.org/data>, with additional details in the analysis scripts package. Due to known loss of ammonium and nitrate on Teflon filters, these compounds are not used from SPARTAN. Data for each compound are saved as monthly averages for all sites with at least two reported measurements. Dust is reconstructed as $10 * ([Al] + [Mg] + [Fe])$ following Weagle, et al. ³⁵. Sea salt is calculated as $2.54 * [Na] - 0.1 [Al]$ following Weagle, et al. ³⁵. Black carbon is taken as equivalent black carbon.

Supplementary Text 5. Model Input Emission Details

Global input emissions for the GEOS-Chem model are primarily for the year 2017 from the Community Emissions Data System⁵³, updated for the GBD-MAPS project: CEDS_{GBD-MAPS}^{54,55}. The CEDS_{GBD-MAPS} emissions dataset is available on Zenodo⁵⁶ and uses contemporary energy consumption data from the International Energy Agency, source and fuel-specific emission factors, as well as a mosaic scaling approach to incorporate global emission estimates (such as the EDGAR v4.3.2⁵⁷ inventory and ECLIPSEv5a inventory from the GAINS model^{58,59}) with regional inventories to calculate monthly emission fluxes ($\text{kg m}^{-2} \text{ s}^{-1}$) of key atmospheric pollutants (NO_x, SO₂, CO, speciated NMVOCs, NH₃, BC, and OC). Emissions are disaggregated into contributions from 11 anthropogenic source sectors and 4 fuel categories (solid biofuel, total coal, the sum of liquid fuel and natural gas, and all other non-combustion sources). CEDS emissions are gridded at a 0.5°×0.5° spatial resolution and do not include vertical distribution information. Further details about this dataset are described in McDuffie, et al. ⁵⁴ and Hoesly, et al. ⁵³. CEDS_{GBD-MAPS} emissions for 2017 are incorporated into the GEOS-Chem model using the

HEMCO emissions module⁶⁰ and are systematically removed in sensitivity simulations by zeroing out individual sources. Monthly CEDS_{GBD-MAPS} emissions are additionally distributed over a 24-hr period using sector-specific diel scaling factors, calculated from the U.S. NEI 2011v1 dataset, implemented in HEMCO by Travis, et al. ⁶¹.

Supplementary Table 2 provides details about the CEDS and non-CEDS emission sources used for model emission sensitivity simulations in the main text. Non-CEDS emission sources include dust emissions from windblown, fugitive, combustion, and industrial sources (AFCID), as well as emissions from aircraft, open fires, volcanoes, lightning, the ocean, and biogenic sources. If emissions from 2017 are not available from a given source, the latest available year is used. Supplementary Figure 6 shows the total global annual emissions of NO_x, SO₂, CO, NH₃, OC, BC, total NMVOCs, and fine dust used in the base 2017 GEOS-Chem simulation. The categories shown in Supplementary Figure 6 correspond to the emission sensitivity simulation categories in Supplementary Table 2.

We also note that the fuel-specific contributions in this work may be lower estimates as some sub-sectoral emission categories were not assigned to a particular combustion fuel-type in the emissions dataset, as shown in Table 2 in McDuffie, et al. ⁵⁴. For example, contributions from fuel production, flaring, transformation, and fossil-fuel fires in the energy sector were not assigned to a combustion fuel-type. As a result, PM_{2.5} contributions from these sources were included in the ‘other sources’ fuel category in Figs. 2-5 rather than the O&NG category. These contributions, however, were included in the total energy sector fractional results in these same figures. In addition, the emissions dataset does not include primary emissions of PM_{2.5} associated with road, tire, and brake wear or ash from coal combustion. While the former source has been shown to have relatively small global PM_{2.5} contributions ⁵⁹, both sources may be important in regions with large fractional contributions from transportation and coal use.

Supplementary Table 2. Model emission sensitivity simulation descriptions. Includes emissions dataset references and descriptions. Note: “calculated” emissions depend on meteorological variables and are computed at the time of simulation.

#	Sector Sensitivity Simulation	Dataset	Year	Reference	Notes
1	Agriculture (AGR) includes manure management, soil fertilizer emissions, rice cultivation, enteric fermentation, and other agriculture	CEDS _{GBD-MAPS}	2017	54,56	-
2	Energy Production (ENE) Includes electricity and heat production, fuel production and transformation, oil and gas fugitive/flaring, and fossil fuel fires	CEDS _{GBD-MAPS}	2017	54,56	-
3	Industry (IND) Includes Industrial combustion (iron and steel, non-ferrous metals, chemicals, pulp and paper, food and tobacco, non-metallic minerals, construction, transportation equipment, machinery, mining and quarrying, wood products, textile and leather, and other industry combustion) and non-combustion industrial processes and product use (cement production, lime production, other minerals, chemical industry, metal production, food, beverage, wood, pulp, and paper, and other non-combustion industrial emissions)	CEDS _{GBD-MAPS}	2017	54,56	-
4	Road Transportation (ROAD) includes cars, motorcycles, heavy and light duty trucks and buses	CEDS _{GBD-MAPS}	2017	54,56	-
5	Non-Road/Off-Road Transportation (NRTR) Includes Rail, Domestic navigation, Other transportation	CEDS _{GBD-MAPS}	2017	54,56	-
6	Residential Combustion (RCO-R) includes residential heating and cooking	CEDS _{GBD-MAPS}	2017	54,56	-
7	Commercial Combustion (RCO-C) Includes commercial and institutional combustion	CEDS _{GBD-MAPS}	2017	54,56	
8	Other Combustion (RCO-O) Includes combustion from agriculture, forestry, and fishing	CEDS _{GBD-MAPS}	2017	54,56	-
9	Solvents (SLV) Includes solvents production and application (degreasing and cleaning, paint application, chemical products manufacturing and processing, and other product use)	CEDS _{GBD-MAPS}	2017	54,56	-
10	Waste (WST) Includes solid waste disposal, waste incineration, waste-water handling, and other waste handling	CEDS _{GBD-MAPS}	2017	54,56	-
11	International Shipping (SHP) Includes international shipping and tanker loading	CEDS _{GBD-MAPS}	2017	54,56,62,63	A
12	Agricultural Waste Burning (AGBURN) Includes open fires from agricultural waste burning	GFED4.1s	2017	64,65	B
13	Other Open Fires (OBURN) Includes deforestation, boreal forest, peat, savannah, and temperate forest fires	GFED4.1s	2017	64,65	B
14	Fugitive, Combustion, Industrial dust (AFCID)	AFCID	2012, 2013, 2015	66	C
15	Windblown Dust (WDUST)	DEAD model	calculated	67,68	D
16	Remaining Emission Sources (OTHER) Includes all remaining emission sources:				
	volcanic SO ₂	AeroCom	2017		E
	aircraft	AEIC	2005	69	
	lightning NO _x	LightNOx	calculated	70	F
	biogenic Soil NO	Soil NO _x	calculated	71	G
	ocean	SeaFlux, GEIA, SeaSalt, Inorg Iodine	calculated	12,72-77	H
	biogenic emissions	MEGANv2.1	calculated	78	I
	very short-lived iodine and bromine species	LIANG_BROMOCARB ORDONEZ_IODOCARB	2000	79,80	
	decaying plants	DECAYING PLANTS		73	
	Fuel Sensitivity Simulations	Dataset	Year	Reference	Notes
17	Total Coal Includes hard coal, brown coal, coal coke	CEDS _{GBD-MAPS}	2017	54,56	-
18	Solid Biofuel	CEDS _{GBD-MAPS}	2017	54,56	-

	Includes solid biofuel				
19	Liquid Oil and Natural Gas Includes light and heavy oil, diesel oil, and natural gas	CEDS _{GBD-MAPS}	2017	54,56	-
20	Process Includes non-combustion CEDS 'process' source emissions.	CEDS _{GBD-MAPS}	2017	54,56	-
	Sector & Fuel Sensitivity Simulations	Dataset	Year	Reference	Notes
21	Total Coal from Energy Production Includes hard coal, brown coal, coal coke; Includes electricity and heat production.	CEDS _{GBD-MAPS}	2017	54,56	J
22	Total Coal from Industrial Processes Includes hard coal, brown coal, coal coke; Includes Industrial combustion (iron and steel, non-ferrous metals, chemicals, pulp and paper, food and tobacco, non-metallic minerals, construction, transportation equipment, machinery, mining and quarrying, wood products, textile and leather, and other industry combustion)	CEDS _{GBD-MAPS}	2017	54,56	K
23	Total Coal from Residential Combustion (RCO-R) Includes hard coal, brown coal, coal coke; Includes residential heating and cooking	CEDS _{GBD-MAPS}	2017	54,56	-
24	Solid Biofuel from Residential Combustion (RCO-R) Includes solid biofuel; Includes residential heating and cooking	CEDS _{GBD-MAPS}	2017	54,56	-

^ACEDS International shipping emissions run with the PARANOX ship plume module, which calculates co-emitted concentrations of O₃ and HNO₃ in aged shipping plumes.

^BOfficial GFED4 emissions have been released through 2016. 2017 and 2018 emissions are available through a beta release (<https://www.geo.vu.nl/~gwerf/GFED/GFED4/>) that provides updates to estimated monthly emissions of dry matter (DM) and carbon (C) based on the relationship between MODIS active fire detections and the GFED4s inventory for the years 2013-2016. To distribute monthly emissions, these files also include daily variability based on active fire distributions and diurnal cycles based on climatological data following the approach of Mu, et al. ⁶⁵. Emission factors for individual species (kg or kg C/ kg DM) are from the original GFED4s release.

^CThe AFCID (Anthropogenic Fugitive, Combustion, and Industrial Dust) inventory is based on 2015 global monthly average primary particulate matter emissions from the ECLIPSEv5a inventory and regional monthly mean inventories for 2013 over India and 2012 over China.

^DGlobal windblown mineral dust emissions are calculated for the year 2017 using the dust entrainment and deposition (DEAD) model.

^EEmissions obtained from NASA/GMAO and include contributions from eruptive and degassing volcanic emissions in 2017, details are here: <http://ftp.as.harvard.edu/gcgrid/data/ExtData/HEMCO/VOLCANO/v2019-08/README>

^FLightning emissions of NO match OTD/LIS climatological observations of lightning flashes from May 1995 – December 2013, as described by Murray et al., 2012.

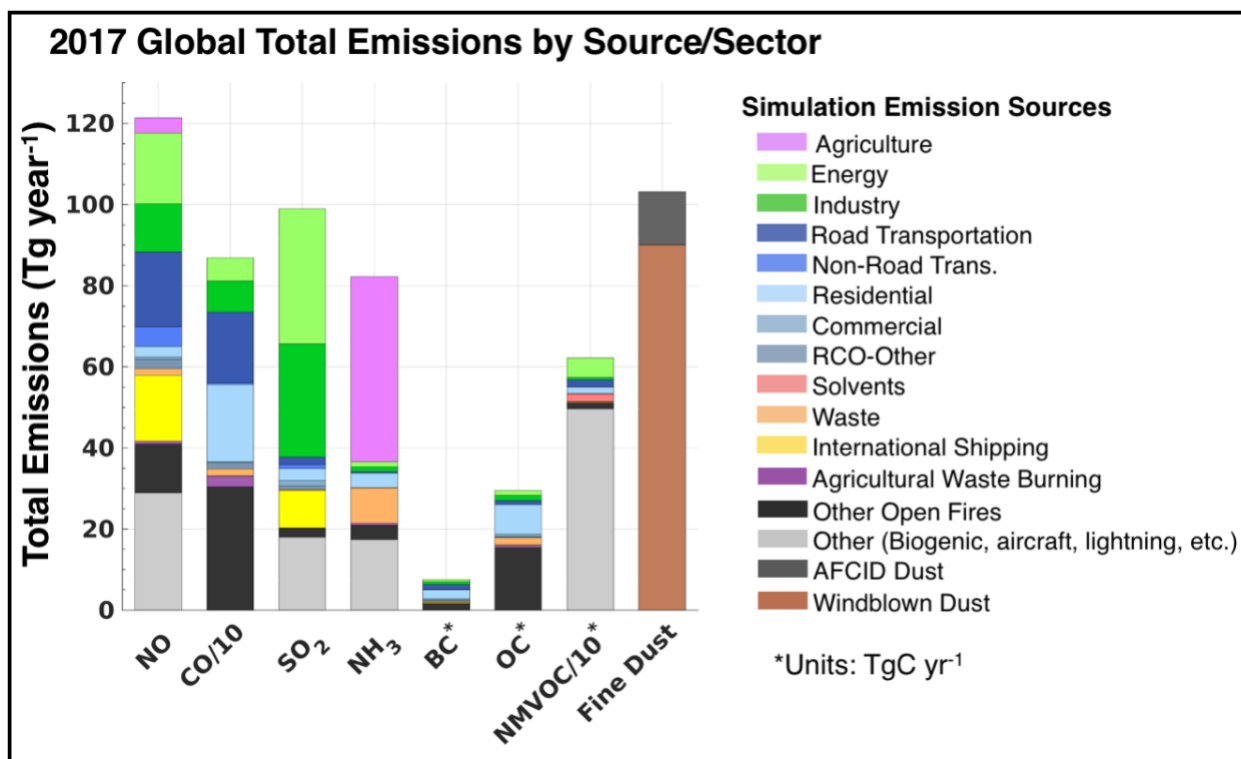
^GSoil NO_x emissions are calculated as a function of surface vegetation type, temperature, precipitation history, and a canopy reduction factor, following the parameterization described in Hudman, et al. ⁷¹. Note that fertilizer emissions are not included in this calculation as fertilized soil emissions are included in the CEDS_{GBD-MAPS} inventory.

^HOcean-air exchange fluxes for DMS, acetone, acetaldehyde, and inorganic iodine are from ⁷⁴, ⁷², ⁷³, and ⁷⁷, respectively. Ocean emissions of NH₃ from natural sources are set to 1990 levels from GEIA and NH₃ emissions from arctic seabirds are from ⁷⁶ and ⁷⁵. Sea salt emissions are calculated following ¹².

^IBiogenic emissions are calculated using the Model of Emissions of Gases and Aerosols from Nature (MEGAN) v2.1.

^JEnergy emissions from fuel production and transformation, oil and gas fugitive/flaring, and fossil fuel fire emissions are not assigned to specific fuel types

^KIndustry emissions from non-combustion industrial processes and product use (cement production, lime production, other minerals, chemical industry, metal production, food, beverage, wood, pulp, and paper, and other non-combustion industrial emissions) are not assigned to specific fuel types.



Supplementary Figure 6: Global total 2017 base simulation emissions. Emissions are colored by source sector category. BC, OC, and total NMVOCs are provided in units of Tg carbon yr⁻¹. Emissions of CO and NMVOCs are divided by 10 for illustration purposes only. Note: OC emissions do not include the GEOS-Chem chemical compound SOAP (secondary organic aerosol precursor), which is emitted from biogenic sources and co-emitted with CO. Emissions of this compound, however, are included in each model simulation.

Supplementary Text 6. Fractional Fuel and Sector Contributions – Additional Comparisons to Previous Nation-Level Studies

To provide further context for our results, this section provides further comparisons to previous national-level studies that have also used 3D chemical transport models to quantify PM_{2.5} source contributions and/or the associated ambient PM_{2.5} disease burden. Where available, we primarily compare the reported fractional contributions to minimize methodological and input data differences. As described in the main text, differences in sectoral definitions (e.g., including fires in the agricultural sector or waste in the residential sector) highlight the importance of clearly defining emission sector definitions in source contribution studies (e.g., Supplementary Table 2). This text is not an exhaustive review of previous studies.

Fuel Types

Previous studies using similar methodologies have typically combined all anthropogenic sources for global or regional scale analyses⁸¹⁻⁸³ or reported contributions from single or aggregate fuel-types⁸⁴, typically for select countries such as China and India⁸⁵⁻⁸⁷. Previous studies also provide estimates of years prior to 2017, which may not capture recent trends in PM_{2.5} chemical precursor emissions, such as recent reductions in China⁸⁸.

Previous national-level studies have only investigated the contribution from coal combustion emissions for select countries and sectors. For example, previous studies have discussed the importance of residential, energy, and industrial coal use on local and regional PM_{2.5} pollution in India⁸⁷ and China⁸⁶, particularly during winter^{89,90}. Emission reduction policies in China have also recently targeted coal use in these sectors. Fractional coal contributions in the residential, energy, and industry sectors in this study in 2017 were estimated to account for 5.3%, 4.7%, and 9.1% of total PM_{2.5} sources in China and 1.4%, 7.0%, and 8.2% in India. These are generally smaller than the corresponding contributions of 4%, 9%, and 17% in 2013 for China⁸⁶, but generally agree well with the 8% contributions from both energy and industrial coal use in India in 2015⁸⁷. When considering total coal use across all sectors, these previous studies have estimated contributions of 40% in China and 16% in India^{86,87}. In 2017, total coal contributions were lower in China (22.7%) and slightly larger in India (17.1%), which may be a result of different methodologies, but is also consistent with recent emission trends in these respective countries.

For solid biofuel, Chafe, et al.⁸⁴ previously investigated the contribution of residential cooking with biofuel to the PM_{2.5} mass and associated burden at both global and regional scales for the year 2010. Both studies predict large relative contributions in South and Southeast Asia, though Chafe, et al.⁸⁴ also predict fractional contributions from biofuel cooking in Southern Sub-Saharan Africa and Southern Latin America that were more than twice as large as those in this work. Reductions in the proportion of the population using solid fuels in these locations between 2010 and 2017 may partially explain these differences. In China and India, two previous studies found that solid biofuel combustion for residential heating and cooking contributed to 15% in China in 2013⁸⁶ and 24% in India in 2015⁸⁷. These fractional contributions were similar to those of 12.7% and 22.5% for China and India in 2017 and suggest that these relative contributions have been relatively constant in recent

years. Due to such persistent contributions, however, previous studies have also shown the potential for significant air quality benefits by addressing the fuels and combustion efficiencies of sources used for residential heating and cooking in China^{89,90}. For 2017, we estimate a total of nearly 250,000 (95% CI: 189,500-305,500) deaths avoidable by eliminating both solid biofuel and coal use in the residential sector in China.

Sectors

For the residential sector, previous studies for India estimated PM_{2.5} disease burden contributions between 27% and 50% in 2010 and 2015^{87,91}. Contributions in 2017 were comparable but slightly lower at between 23%-35% when comparable sub-sectors (e.g., residential + waste) were considered. In China, previous residential estimates ranged from 25%-32% in 2010^{91,92} and ~19%-22% in 2013^{86,93}, both consistent with 26% here in 2017 (Supplementary Data 1). Fig. 2 and Fig. 3 in the main text show that the fractional residential contributions were generally smaller in Canada and the U.S. than in Asia, also consistent with multiple previous studies^{91,94-98}. Emissions estimates from the residential sector, however, are particularly uncertain in emission inventories compared to those from other large anthropogenic emission sources^{54,99-101}.

For the energy and industry sectors, 2017 contributions were 10.2% and 11.7%, respectively. These sectors have been studied relatively extensively in past work compared to other PM_{2.5} sources, however, differences may arise due to differences in the detailed sub-sectoral categories used here, or recent emission changes. The more detailed sectors such as commercial, AFCID, and waste examined here isolate sources that may have either been lumped into the industry sector in prior work or neglected altogether. Over recent years, industrial and energy emissions have been decreasing in China, while these emission sources have been simultaneously increasing throughout other parts of Asia, Latin America, and Africa⁵⁴. Previous studies have specifically investigated these source contributions at the national level in China^{86,91-93}, India⁸⁷, Canada⁹⁴, the U.S.⁹⁸, and throughout Africa^{82,83}. In Canada, combined fractional energy and industry contributions in this work were similar to previous results⁹⁴. In China, previous energy contributions were consistent with this work, however industrial emissions in 2017 were close to half those previously reported for 2010 and 2013^{86,92,93}. In Africa, two recent studies found the greatest contributions from the energy sector in Egypt and Southern Sub-Saharan Africa^{82,83}, also consistent with this work (Fig. 3).

Two additional fuel and sector specific simulations for 2017 revealed that 91% of these energy contributions in South Africa were from coal, while only 46% were from coal in Egypt (Fig. 3, Supplementary Data 1). One additional study predicted a much smaller (3%) contribution from combined energy and industry sources in Egypt in 2010, predicting instead a 92% contribution from natural sources⁹¹. More detailed assessments of these differences between industry, energy, and other source contributions are largely limited by a lack of more detailed emission sector descriptions.

For dust, agriculture, transportation, and fires, agreement with previous national-level results were variable. For example, national-level fractional dust estimates in 2017 were much larger for North Africa, the Middle East¹⁰², and China⁹³, and smaller in India⁸⁷ compared to previous studies. For India specifically, updates to the model deposition²⁹ and dust size distribution schemes¹⁴, as well as interannual variability in dust emission fluxes and removal rates, likely contribute to the smaller total contribution from fine dust (< 2.5 μm diameter) in this work (~14.9%) relative to previous estimates (~38%), derived using an older version of the GEOS-Chem model. As shown in Supplementary Figure 5, the model updates in this work improved the agreement with surface dust observations, however, the measured PWM dust concentrations at surface monitors were < 1 $\mu\text{g}/\text{m}^3$, indicating that current surface monitor locations may not provide an accurate characterization of the total population exposure to dust. These uncertainties highlight the need for increased monitoring and continued improvement to the model treatment of dust to improve the accuracy of contribution estimates from this source.

For non-combustion agriculture, 2017 estimates were generally smaller than previous regional-level studies^{103,104}. For example, 2017 contributions in Europe, North America, and South and East Asia were less than 22%, 11%, and 12%, respectively, while the same source was estimated to contribute to 34%, 17%, and 10% in 2010¹⁰³. Global and regional NH_3 emissions have been increasing between 2010 and 2017⁵⁴, indicating that differences here are methodological (e.g., differences in emissions or chemical production), rather than real temporal trends. Our mechanistic updates to the ammonium nitrate simulation (Supplementary Text 3) both improved the agreement with observations and reduced the agricultural sources of $\text{PM}_{2.5}$ in this work.

For the transportation sector, relative contributions have also been previously investigated at the national scales¹⁰⁵⁻¹⁰⁷. Consistent with previous studies, total transportation contributions in this work were generally greater than the global average in North America, Europe, parts of Asia, Australia, and Latin America¹⁰⁵⁻¹⁰⁷. Comparisons with additional national-level results^{86,87,91-93,98,107} show that differences in fractional contributions generally follow recent trends in transportation emissions, with recent decreases in China and the U.S. and increases in India.

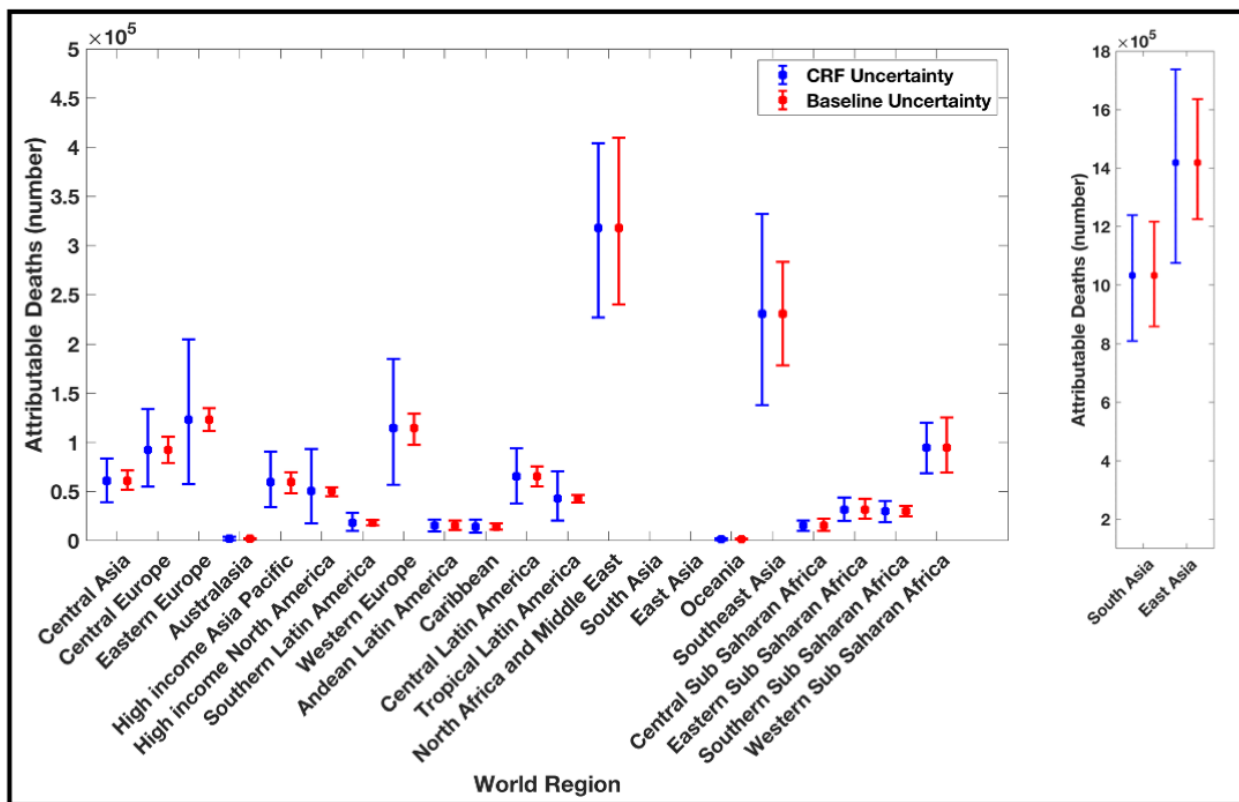
For fire emissions, comparisons to previous global and national level estimates are discussed in the main text.

Waste, solvent use, and international shipping sectors have relatively small contributions on the global scale but can significantly contribute to national and sub-national PM_{2.5} variation (e.g., up to 18% in Sri Lanka; Fig. 5). Contributions from waste combustion to the ambient PM_{2.5} disease burden have not been previously reported. The relative contribution from the solvent sector has only been reported in one previous national-level study⁸⁶. As a result of non-linear PM_{2.5} mass production, solvent emission reductions can result in an increase in total PM_{2.5} mass. This was shown previously for a study in China⁸⁶. Solvent emission reductions in 2017, however, resulted in a total mass decrease in this same country. As the solvent sector primarily emits NMVOCs (Supplementary Figure 6), this variable sign response demonstrates that decreases in these emissions can increase the availability of atmospheric oxidants, leading to increases in inorganic aerosol mass in NO_x-limited/VOC-saturated chemical regimes¹⁰⁸. Therefore, this negative response may be important to consider when developing air pollution reduction strategies in regions with large VOC/NO_x emission ratios. Solvent emissions, however, are also highly uncertain as NMVOCs may be underestimated in U.S. emissions inventories by a factor of 2-3¹⁰⁹. Relative national contributions from international shipping are generally consistent with previous studies^{110,111}, where the largest relative contributions are predicted in coastal countries such as Ireland, Portugal, and the Bahamas (more than 12% each in 2017).

Supplementary Text 7. Uncertainty Sensitivity Study

We conduct an additional sensitivity test to account for potential uncertainties in the PM_{2.5} disease burden associated with the age- and disease-specific baseline mortality data from the

2019 GBD. The 95% uncertainty ranges are calculated by applying lower and upper estimates of the baseline mortality data to the PAF in Equation 2, derived from the mean CRF. The resulting 95% confidence intervals for 21 world regions are shown in Supplementary Figure 7, compared to the 95% CIs derived from uncertainties in the mean CRFs (reported in the Main Text). As the upper and lower limits in the baseline and CRF datasets are both estimated from multiple draws of underlying distributions, propagating the uncertainties from these two input variables likely leads to an overestimate in the 95% CI for the total attributable disease burden. Supplementary Figure 7 shows that for most regions, the 95% CI associated with uncertainties in the CRFs encompass the 95% CIs associated with uncertainties in the baseline mortality estimates. Additional uncertainties in the PM_{2.5} exposure estimates and modeled fractional source contributions are not considered here to due computational limitations.



Supplementary Figure 7. Total disease burden estimates and confidence intervals for 21 world regions, derived from uncertainties in CRFs and baseline mortality data. Total disease burden estimates are from Supplementary Data 1. Uncertainty ranges illustrate the 95% CI derived from uncertainty estimates in the CRFs (blue) and baseline mortality data (red). The bounds for South and East Asia are shown on an expanded scale to the right.

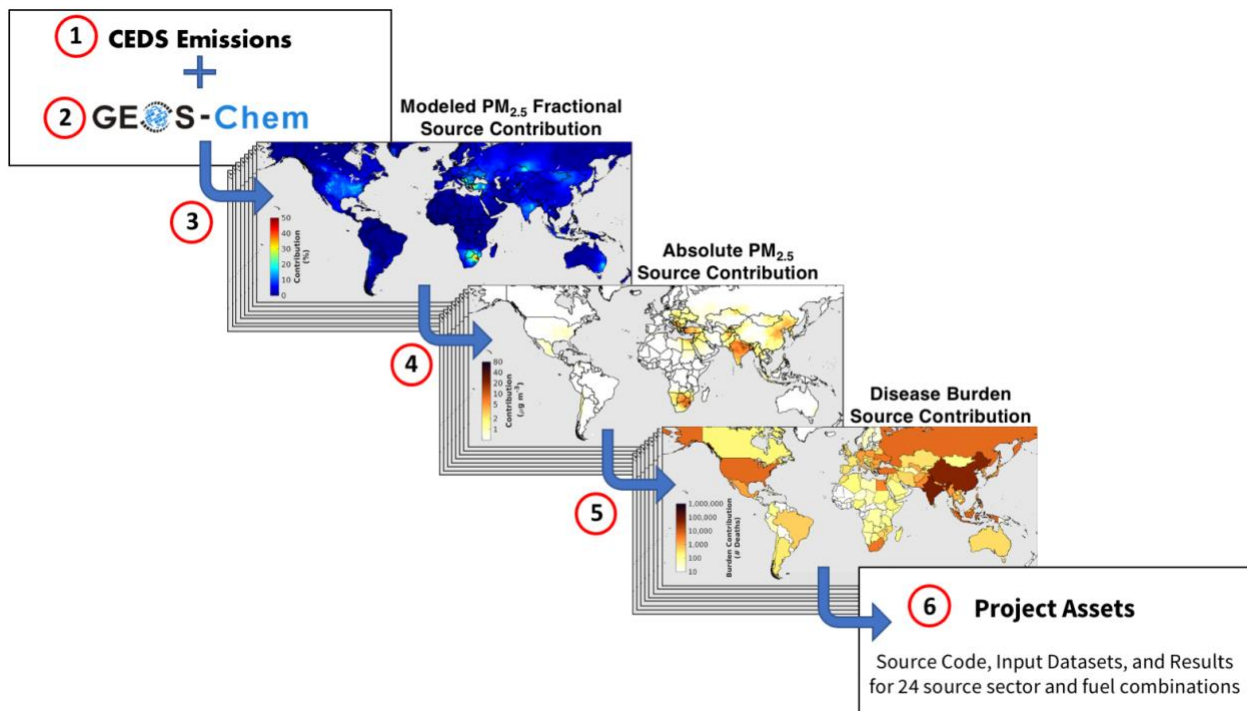
Supplementary Text 8. Consideration of the Zero-Out (Brute Force) Method

Similar to many other analyses of this type of work, our analysis uses a zero-out or brute force approach for model sensitivity simulations. This widely used approach is designed to quantify source contributions to the total PM_{2.5} disease burden under complete elimination of emissions from individual sources. As discussed in previous zeroing-out studies^{35,91,92,103}, the non-linear chemical production of PM_{2.5} will result in the sum of individual PM_{2.5} simulations to exceed the total PM_{2.5} mass predicted in the base simulation. By implementing Eq. (5) in the Main Text, we ensure that fractional contributions from individual source sectors sum to 100% in this work. Using this approach, the final fractional PM_{2.5} source contributions will be sensitive to the number of individual source sensitivity simulations that are included in the calculation, resulting in further differences between the detailed simulations in this work and previous similar studies. Due to this non-linearity, fractional and absolute contributions predicted from this method may not be consistent with simulations that implement more moderate reduction strategies (i.e., < 20-50% emission reductions), or strategies that simultaneously target multiple emission sectors (e.g., simultaneous reductions in both energy and industry sources).

Supplementary Text 9. Methodological Schematic

As described in the main text, results in this study are derived by integrating high-resolution satellite-derived PM_{2.5} exposure estimates, CRFs from the 2019 GBD, and fractional source contribution results from 24 emission sensitivity simulations with the GEOS-Chem chemical transport model. Supplementary Figure 8 illustrates the overall workflow of this methodology. In Step 1, gridded global emissions of PM_{2.5} precursors are developed as a function of source sector and fuel-type (Supplementary Table 5; anthropogenic emissions largely from the CEDS_{GBD-MAPS} inventory), as described in McDuffie, et al.⁵⁴. In Step 2, emissions are used as input in an updated version of the GEOS-Chem 3D chemical transport model (described in Supplementary Text 3), with the simulated PM_{2.5} concentrations validated against available mass and composition surface observations (described in Supplementary Text 4). In Step 3, a series of zero-out emission sensitivity simulations are conducted (Supplementary Table 2) with the GEOS-Chem model and emission inputs. The resulting PM_{2.5} concentrations from each simulation are compared to the base simulation (with all emission sources) to quantify the modeled fractional PM_{2.5} contributions (reported in Data Files 1 (sectors) and 2 (fuel-types)). In

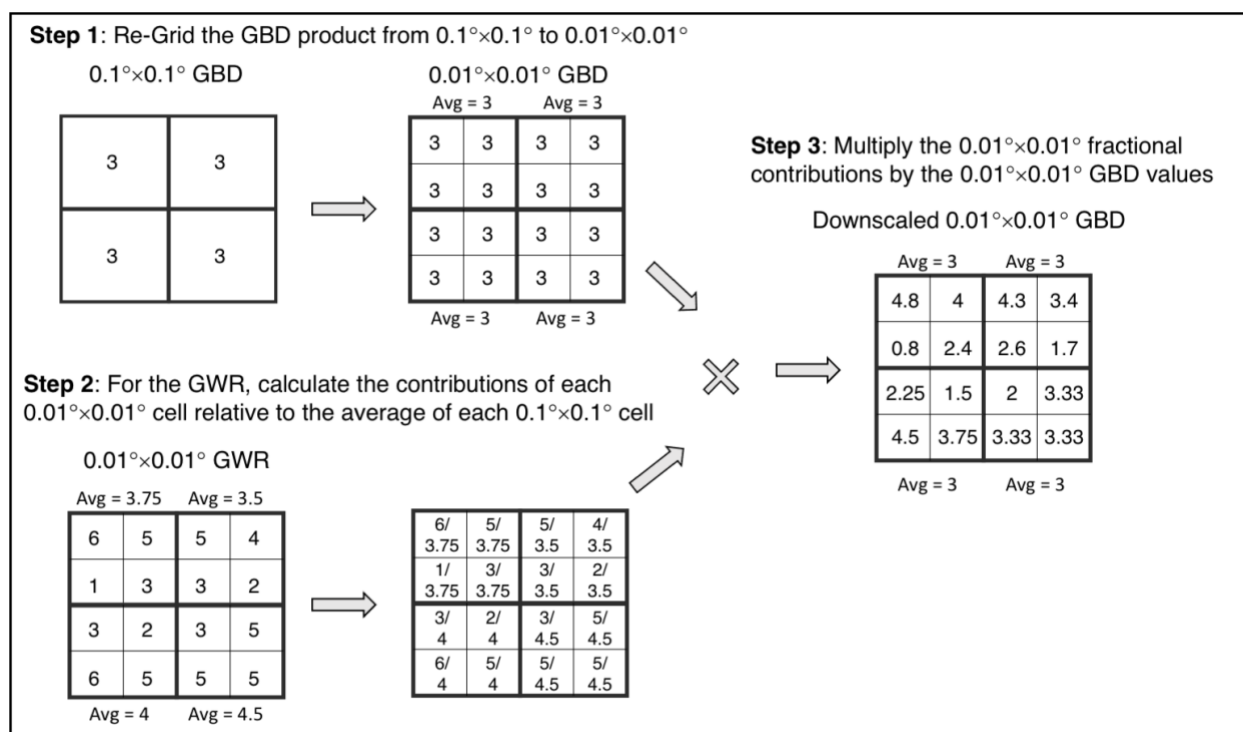
Step 4, high-resolution $PM_{2.5}$ exposure estimates are derived by downscaling exposure estimates from the 2019 GBD (described in Supplementary Text 10; reported in Supplementary Data 1 and 2) and are applied to the fractional model source contributions from Step 2 to quantify absolute source-specific contributions to ambient $PM_{2.5}$ mass. In Step 5, CRFs from the GBD2019 (Supplementary Figure 2) are combined with downscaled $PM_{2.5}$ exposure estimates from Step 4 to calculate the total ambient $PM_{2.5}$ disease burden (reported in Supplementary Data 1 and 2). The total burden is combined with modeled fractional source contributions from Step 3 to calculate source-specific burden contributions reported throughout the manuscript. Lastly, Step 6 highlights the data assets that are associated with this analysis and manuscript, including the analysis scripts, model source code, input emissions, CRFs, baseline burden and exposure estimate datasets (<https://github.com/emcduffie/GBD-MAPS-Global>), and the global, regional, national, and subnational source sector and fuel contribution results (Supplementary Data 1 and 2).



Supplementary Figure 8: Overall methodological workflow schematic. The relevant equations and data from Supplementary Text 9 are indicated in each step.

Supplementary Text 10. PM_{2.5} Exposure Estimates - Spatial Downscaling Procedural Details

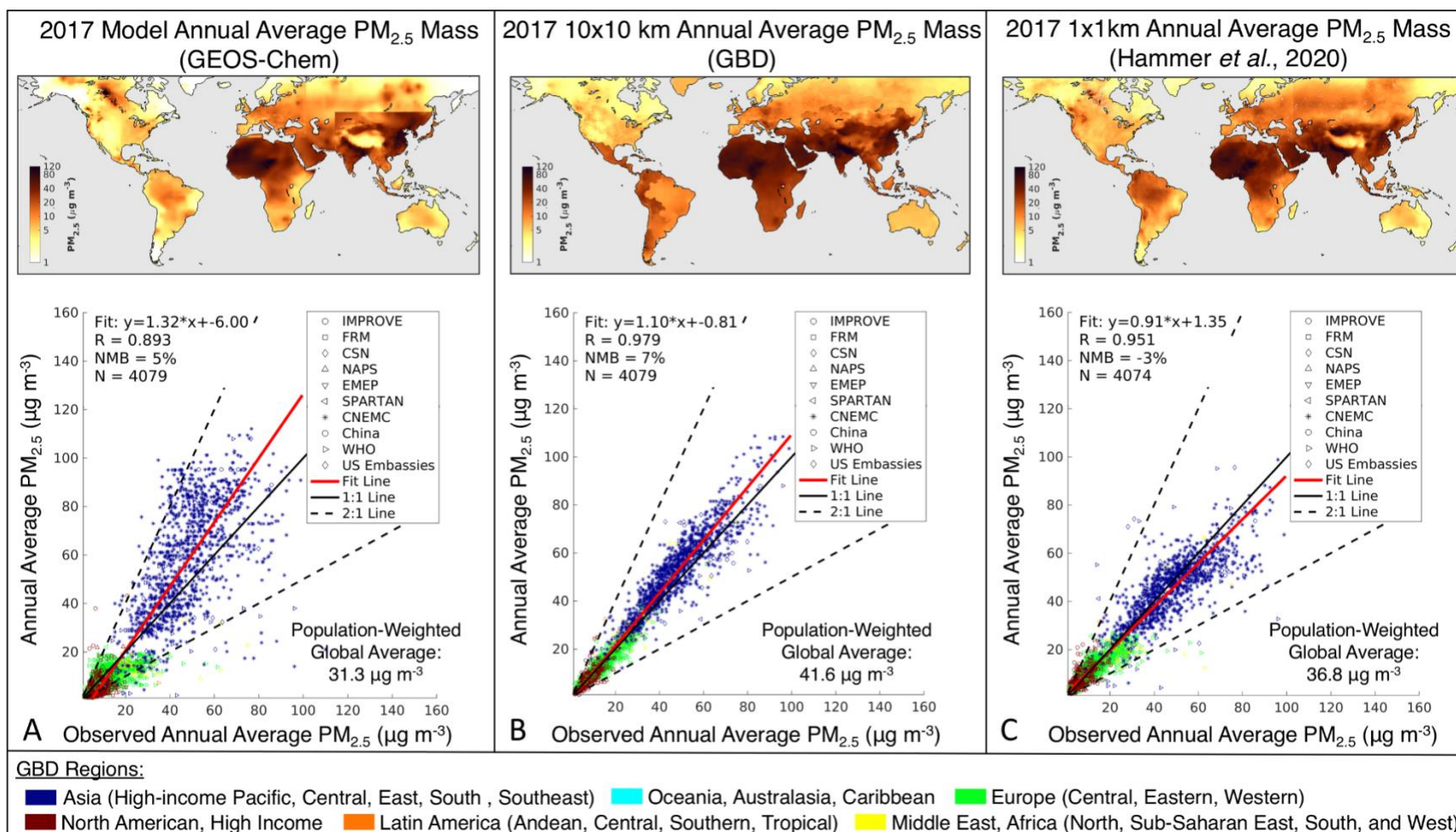
The process of spatially downscaling GBD PM_{2.5} exposure estimates using a newly available high-resolution product from Hammer, et al. ⁵ involves three steps, illustrated in Supplementary Figure 9. First, the 0.1°×0.1° GBD product is re-gridded to a 0.01°×0.01° global grid, by setting each value in the new fine-resolution grid boxes (100 boxes) to the value from the corresponding coarser grid box in the original GBD product. Second, the fractional contribution of each grid-box in the 0.01°×0.01° Hammer, et al. ⁵, product is calculated relative to the average PM_{2.5} across the surrounding 100 grid boxes. In the event that the Hammer, et al. ⁵ product does not report data for a particular grid box, the spatial fraction in that box is set to 1. Third, these resulting fractional contributions are multiplied by the GBD values from the 0.01°×0.01° PM_{2.5} product from Step 1. This process is independent of the GEOS-Chem emission sensitivity simulations.



Supplementary Figure 9: Simplified schematic of the spatial downscaling procedure. Values in each example grid box represent example PM_{2.5} mass concentrations in units of $\mu\text{g m}^{-3}$. In actuality, one of the 0.1°×0.1° grid boxes in Step 1 above corresponds to 100 grid boxes of

0.01°×0.01° resolution, not the four as shown here. In this figure ‘GWR’ refers to the high-resolution PM_{2.5} estimates from Hammer, et al. ⁵.

To assess the sensitivity of PM_{2.5} exposure estimates to the downscaling process, Supplementary Figure 10 shows maps of the gridded exposure estimates, as well as their correlations against observations for (A) the raw GEOS-Chem simulated concentrations, (B) original 0.1°×0.1° GBD PM_{2.5} product, and (C) 0.01°×0.01° Hammer, et al. ⁵ product. Fig. 1 and Supplementary Figure 10 illustrate similarly good agreement between each of the exposure estimates and the total PM_{2.5} mass observations, with correlation coefficients (r) and NMBs ranging from 0.89 to 0.979 and -3% to +11%, respectively. The added spatial information from the downscaling procedure slightly increases the NMB from +7% (Supplementary Figure 10b) to +11% (Fig. 1), but maintains a slightly higher correlation coefficient (r) than the high-resolution Hammer, et al. ⁵ product (0.977 vs 0.951). Across all four products, the 2017 global annual PWM PM_{2.5} mass ranges between 31.3 μg m⁻³ to 41.7 μg m⁻³. Differences between the GBD and Hammer, et al. ⁵ products are largely due to different methods used to calibrate geophysical estimates to surface observations.



Supplementary Figure 10: Comparison of three PM_{2.5} exposure estimates against surface observations for the year 2017. (A) GEOS-Chem annual average PM_{2.5} mass concentrations, (B) 0.1°×0.1° GBD annual average PM_{2.5} exposure estimates, (C) 0.01°×0.01° Hammer, et al. ⁵ annual average exposure estimates. Each column contains a map of the PM_{2.5} concentrations and a scatter plot comparing each product against 2017 surface observations. Colors represent world regions (Supplementary Table 1) and symbols represent observation networks (Supplementary Text 4). Red lines: correlation slope, solid black lines: 1:1 line, and dashed lines: 2:1 and 1:2 lines. The fit slope, intercept, correlation coefficient, normalized mean bias (NMB), number of observation points (N), and PWM PM_{2.5} concentrations are also provided.

Supplementary References

- 1 CIESIN (Center for International Earth Science Information Network). Gridded Population of the World Version 4. (*Palisades, NY.*), doi:doi.org/10.1128/AAC.03728-14 (2017).
- 2 Burnett, R. *et al.* Global estimates of mortality associated with long-term exposure to outdoor fine particulate matter. *P. Natl. Acad. Sci.* **115**, 9592, doi:10.1073/pnas.1803222115 (2018).
- 3 Yin, P. *et al.* Long-term Fine Particulate Matter Exposure and Nonaccidental and Cause-specific Mortality in a Large National Cohort of Chinese Men. *Environmental Health Perspectives* **125**, 117002, doi:10.1289/EHP1673.
- 4 Hystad, P., Yusuf, S. & Brauer, M. Air pollution health impacts: the knowns and unknowns for reliable global burden calculations. *Cardiovascular Research*, doi:10.1093/cvr/cvaa092 (2020).
- 5 Hammer, M. S. *et al.* Global Estimates and Long-Term Trends of Fine Particulate Matter Concentrations (1998-2018). *Environ. Sci. Technol.*, doi:10.1021/acs.est.0c01764 (2020).
- 6 Bey, I. *et al.* Global modeling of tropospheric chemistry with assimilated meteorology: Model description and evaluation. *J. Geophys. Res. Atmos.* **106**, 23073-23095, doi:10.1029/2001JD000807 (2001).
- 7 Wang, Y. X., McElroy, M. B., Jacob, D. J. & Yantosca, R. M. A nested grid formulation for chemical transport over Asia: Applications to CO. *J. Geophys. Res. Atmos.* **109**, doi:10.1029/2004JD005237 (2004).
- 8 Philip, S., Martin, R. V. & Keller, C. A. Sensitivity of chemistry-transport model simulations to the duration of chemical and transport operators: a case study with GEOS-Chem v10-01. *Geosci. Model Dev.* **9**, 1683-1695, doi:10.5194/gmd-9-1683-2016 (2016).
- 9 Park, R. J., Jacob, D. J., Field, B. D., Yantosca, R. M. & Chin, M. Natural and transboundary pollution influences on sulfate-nitrate-ammonium aerosols in the United States: Implications for policy. *J. Geophys. Res. Atmos.* **109**, doi:10.1029/2003JD004473 (2004).
- 10 Wang, Q. *et al.* Global budget and radiative forcing of black carbon aerosol: Constraints from pole-to-pole (HIPPO) observations across the Pacific. *J. Geophys. Res. Atmos.* **119**, 195-206, doi:10.1002/2013JD020824 (2014).
- 11 Kim, P. S. *et al.* Sources, seasonality, and trends of southeast US aerosol: an integrated analysis of surface, aircraft, and satellite observations with the GEOS-Chem chemical transport model. *Atmos. Chem. Phys.* **15**, 10411-10433, doi:10.5194/acp-15-10411-2015 (2015).
- 12 Jaeglé, L., Quinn, P. K., Bates, T. S., Alexander, B. & Lin, J. T. Global distribution of sea salt aerosols: new constraints from in situ and remote sensing observations. *Atmos. Chem. Phys.* **11**, 3137-3157, doi:10.5194/acp-11-3137-2011 (2011).
- 13 Duncan Fairlie, T., Jacob, D. J. & Park, R. J. The impact of transpacific transport of mineral dust in the United States. *Atmos. Environ.* **41**, 1251-1266, doi:<https://doi.org/10.1016/j.atmosenv.2006.09.048> (2007).
- 14 Zhang, L., Kok, J. F., Henze, D. K., Li, Q. & Zhao, C. Improving simulations of fine dust surface concentrations over the western United States by optimizing the particle size distribution. *Geophysical Research Letters* **40**, 3270-3275, doi:<https://doi.org/10.1002/grl.50591> (2013).
- 15 Martin, R. V., Jacob, D. J., Yantosca, R. M., Chin, M. & Ginoux, P. Global and regional decreases in tropospheric oxidants from photochemical effects of aerosols. *J. Geophys. Res. Atmos.* **108**, doi:<https://doi.org/10.1029/2002JD002622> (2003).

- 16 Koepke, P., Hess, M., Schult, I. & Shettle, E. P. Global Aerosol Dataset. (Max-Planck Institute for Meteorology, Hamburg, Germany, 1997).
- 17 Drury, E. *et al.* Synthesis of satellite (MODIS), aircraft (ICARTT), and surface (IMPROVE, EPA-AQS, AERONET) aerosol observations over eastern North America to improve MODIS aerosol retrievals and constrain surface aerosol concentrations and sources. *J. Geophys. Res. Atmos.* **115**, doi:<https://doi.org/10.1029/2009JD012629> (2010).
- 18 Latimer, R. N. C. & Martin, R. V. Interpretation of measured aerosol mass scattering efficiency over North America using a chemical transport model. *Atmos. Chem. Phys.* **19**, 2635-2653, doi:10.5194/acp-19-2635-2019 (2019).
- 19 Lee, C. *et al.* Retrieval of vertical columns of sulfur dioxide from SCIAMACHY and OMI: Air mass factor algorithm development, validation, and error analysis. *J. Geophys. Res. Atmos.* **114**, doi:<https://doi.org/10.1029/2009JD012123> (2009).
- 20 Ridley, D. A., Heald, C. L. & Ford, B. North African dust export and deposition: A satellite and model perspective. *J. Geophys. Res. Atmos.* **117**, doi:<https://doi.org/10.1029/2011JD016794> (2012).
- 21 Hammer, M. S. *et al.* Interpreting the ultraviolet aerosol index observed with the OMI satellite instrument to understand absorption by organic aerosols: implications for atmospheric oxidation and direct radiative effects. *Atmos. Chem. Phys.* **16**, 2507-2523, doi:10.5194/acp-16-2507-2016 (2016).
- 22 Fountoukis, C. & Nenes, A. ISORROPIA II: a computationally efficient thermodynamic equilibrium model for K^+ - Ca^{2+} - Mg^{2+} - NH_4^+ - Na^+ - SO_4^{2-} - NO_3^- - Cl^- - H_2O aerosols. *Atmos. Chem. Phys.* **7**, 4639-4659, doi:10.5194/acp-7-4639-2007 (2007).
- 23 Pai, S. J. *et al.* An evaluation of global organic aerosol schemes using airborne observations. *Atmos. Chem. Phys. Discuss.* **2019**, 1-39, doi:10.5194/acp-2019-331 (2019).
- 24 Lin, S.-J. & Rood, R. B. Multidimensional Flux-Form Semi-Lagrangian Transport Schemes. *Monthly Weather Review* **124**, 2046-2070, doi:10.1175/1520-0493(1996)124<2046:Mffslt>2.0.Co;2 (1996).
- 25 Wu, S. *et al.* Why are there large differences between models in global budgets of tropospheric ozone? *J. Geophys. Res. Atmos.* **112**, doi:10.1029/2006jd007801 (2007).
- 26 Lin, J.-T. & McElroy, M. B. Impacts of boundary layer mixing on pollutant vertical profiles in the lower troposphere: Implications to satellite remote sensing. *Atmos. Environ.* **44**, 1726-1739, doi:<https://doi.org/10.1016/j.atmosenv.2010.02.009> (2010).
- 27 The International GEOS-Chem User Community. GEOS-Chem 12.1.0 (Version 12.1.0). Zenodo., doi:<http://doi.org/10.5281/zenodo.1553349> (2018, November 26).
- 28 Heald, C. L. *et al.* Atmospheric ammonia and particulate inorganic nitrogen over the United States. *Atmos. Chem. Phys.* **12**, 10295-10312, doi:10.5194/acp-12-10295-2012 (2012).
- 29 Luo, G., Yu, F. & Schwab, J. Revised treatment of wet scavenging processes dramatically improves GEOS-Chem 12.0.0 simulations of nitric acid, nitrate, and ammonium over the United States. *Geosci. Model Dev. Discuss.* **2019**, 1-18, doi:10.5194/gmd-2019-58 (2019).
- 30 McDuffie, E. E. *et al.* Heterogeneous N_2O_5 Uptake During Winter: Aircraft Measurements During the 2015 WINTER Campaign and Critical Evaluation of Current Parameterizations. *J. Geophys. Res. Atmos.* **123**, 4345-4372, doi:10.1002/2018JD028336 (2018).
- 31 Shah, V. *et al.* Chemical feedbacks weaken the wintertime response of particulate sulfate and nitrate to emissions reductions over the eastern United States. *P. Natl. Acad. Sci.* **115**, 8110-8115 (2018).

- 32 McDuffie, E. E. *et al.* ClNO₂ Yields From Aircraft Measurements During the 2015 WINTER Campaign and Critical Evaluation of the Current Parameterization. *J. Geophys. Res. Atmos.* **123**, 12,994-913,015, doi:10.1029/2018JD029358 (2018).
- 33 Luo, G., Yu, F. & Moch, J. M. Further improvement of wet process treatments in GEOS-Chem v12.6.0: Impact on global distributions of aerosol precursors and aerosols. *Geosci. Model Dev. Discuss.* **2020**, 1-39, doi:10.5194/gmd-2020-11 (2020).
- 34 Snider, G. *et al.* SPARTAN: a global network to evaluate and enhance satellite-based estimates of ground-level particulate matter for global health applications. *Atmos. Meas. Tech.* **8**, 505-521, doi:10.5194/amt-8-505-2015 (2015).
- 35 Weagle, C. L. *et al.* Global Sources of Fine Particulate Matter: Interpretation of PM_{2.5} Chemical Composition Observed by SPARTAN using a Global Chemical Transport Model. *Environ. Sci. Technol.* **52**, 11670-11681, doi:10.1021/acs.est.8b01658 (2018).
- 36 Wu, H. *et al.* Probabilistic Automatic Outlier Detection for Surface Air Quality Measurements from the China National Environmental Monitoring Network. *Advances in Atmospheric Sciences* **35**, 1522-1532, doi:10.1007/s00376-018-8067-9 (2018).
- 37 Sofowote, U., Su, Y., Bitzos, M. M. & Munoz, A. Improving the correlations of ambient tapered element oscillating microbalance PM_{2.5} data and SHARP 5030 Federal Equivalent Method in Ontario: A multiple linear regression analysis. *Journal of the Air & Waste Management Association* **64**, 104-114, doi:10.1080/10962247.2013.833145 (2014).
- 38 Tortajada-Genaro, L.-A. & Borrás, E. Temperature effect of tapered element oscillating microbalance (TEOM) system measuring semi-volatile organic particulate matter. *Journal of Environmental Monitoring* **13**, 1017-1026, doi:10.1039/C0EM00451K (2011).
- 39 Rizzo, M., Scheff, P. A. & Kaldy, W. Adjusting Tapered Element Oscillating Microbalance Data for Comparison with Federal Reference Method PM_{2.5} Measurements in Region 5. *Journal of the Air & Waste Management Association* **53**, 596-607, doi:10.1080/10473289.2003.10466196 (2003).
- 40 Hand, J. L., Prenni, A. J., Schichtel, B. A., Malm, W. C. & Chow, J. C. Trends in remote PM_{2.5} residual mass across the United States: Implications for aerosol mass reconstruction in the IMPROVE network. *Atmos. Environ.* **203**, 141-152, doi:<https://doi.org/10.1016/j.atmosenv.2019.01.049> (2019).
- 41 White, W. H. Chemical markers for sea salt in IMPROVE aerosol data. *Atmos. Environ.* **42**, 261-274, doi:<https://doi.org/10.1016/j.atmosenv.2007.09.040> (2008).
- 42 Solomon, P. A. *et al.* U.S. National PM_{2.5} Chemical Speciation Monitoring Networks—CSN and IMPROVE: Description of networks. *Journal of the Air & Waste Management Association* **64**, 1410-1438, doi:10.1080/10962247.2014.956904 (2014).
- 43 Li, C. *et al.* Trends in Chemical Composition of Global and Regional Population-Weighted Fine Particulate Matter Estimated for 25 Years. *Environ. Sci. Technol.* **51**, 11185-11195, doi:10.1021/acs.est.7b02530 (2017).
- 44 Xu, Q. *et al.* Nitrate dominates the chemical composition of PM_{2.5} during haze event in Beijing, China. *Science of The Total Environment* **689**, 1293-1303, doi:<https://doi.org/10.1016/j.scitotenv.2019.06.294> (2019).
- 45 Zhao, L. *et al.* Changes of chemical composition and source apportionment of PM_{2.5} during 2013–2017 in urban Handan, China. *Atmos. Environ.* **206**, 119-131, doi:<https://doi.org/10.1016/j.atmosenv.2019.02.034> (2019).

- 46 Huang, F. *et al.* Chemical characteristics and source apportionment of PM_{2.5} in Wuhan, China. *Journal of Atmospheric Chemistry* **76**, 245-262, doi:10.1007/s10874-019-09395-0 (2019).
- 47 Zhang, H.-T. *et al.* [Spatial Temporal Characteristics and Cluster Analysis of Chemical Components for Ambient PM_{2.5} in Wuhan]. *Huan Jing Ke Xue* **40**, 4764-4773, doi:10.13227/j.hjcx.201904069 (2019).
- 48 Zhang, Q. *et al.* Drivers of improved PM_{2.5} air quality in China from 2013 to 2017. *P. Natl. Acad. Sci.* **116**, 24463, doi:10.1073/pnas.1907956116 (2019).
- 49 McNeill, J. *et al.* Large global variations in measured airborne metal concentrations driven by anthropogenic sources. *Scientific Reports* **10**, 21817, doi:10.1038/s41598-020-78789-y (2020).
- 50 Pandey, A., Shetty, N. J. & Chakrabarty, R. K. Aerosol light absorption from optical measurements of PTFE membrane filter samples: sensitivity analysis of optical depth measures. *Atmos. Meas. Tech.* **12**, 1365-1373, doi:10.5194/amt-12-1365-2019 (2019).
- 51 Dillner, A. M. & Takahama, S. Predicting ambient aerosol thermal-optical reflectance (TOR) measurements from infrared spectra: organic carbon. *Atmos. Meas. Tech.* **8**, 1097-1109, doi:10.5194/amt-8-1097-2015 (2015).
- 52 O'Brien, R. E. *et al.* Ultrasonic nebulization for the elemental analysis of microgram-level samples with offline aerosol mass spectrometry. *Atmos. Meas. Tech.* **12**, 1659-1671, doi:10.5194/amt-12-1659-2019 (2019).
- 53 Hoesly, R. M. *et al.* Historical (1750–2014) anthropogenic emissions of reactive gases and aerosols from the Community Emissions Data System (CEDS). *Geosci. Model Dev.* **11**, 369-408, doi:10.5194/gmd-11-369-2018 (2018).
- 54 McDuffie, E. E. *et al.* A global anthropogenic emission inventory of atmospheric pollutants from sector- and fuel-specific sources (1970–2017): an application of the Community Emissions Data System (CEDS). *Earth Syst. Sci. Data* **12**, 3413-3442, doi:10.5194/essd-12-3413-2020 (2020).
- 55 McDuffie, E. E. *et al.* *CEDS_GBD-MAPS_SourceCode_2020_v1.0*, (2020).
- 56 McDuffie, E. E. *et al.* CEDS_GBD-MAPS: Global Anthropogenic Emission Inventory of NO_x, SO₂, CO, NH₃, NMVOCs, BC, and OC from 1970-2017 (Version 2020_v1.0). doi:<https://doi.org/10.5281/zenodo.3754964> (2020).
- 57 Crippa, M. *et al.* Gridded emissions of air pollutants for the period 1970–2012 within EDGAR v4.3.2. *Earth Syst. Sci. Data* **10**, 1987-2013, doi:10.5194/essd-10-1987-2018 (2018).
- 58 Amann, M. *et al.* Cost-effective control of air quality and greenhouse gases in Europe: Modeling and policy applications. *Environmental Modelling & Software* **26**, 1489-1501, doi:<https://doi.org/10.1016/j.envsoft.2011.07.012> (2011).
- 59 Klimont, Z. *et al.* Global anthropogenic emissions of particulate matter including black carbon. *Atmos. Chem. Phys.* **17**, 8681-8723, doi:10.5194/acp-17-8681-2017 (2017).
- 60 Keller, C. A. *et al.* HEMCO v1.0: a versatile, ESMF-compliant component for calculating emissions in atmospheric models. *Geosci. Model Dev.* **7**, 1409-1417, doi:10.5194/gmd-7-1409-2014 (2014).
- 61 Travis, K. R. *et al.* Why do models overestimate surface ozone in the Southeast United States? *Atmos. Chem. Phys.* **16**, 13561-13577, doi:10.5194/acp-16-13561-2016 (2016).

- 62 Vinken, G. C. M., Boersma, K. F., Jacob, D. J. & Meijer, E. W. Accounting for non-linear chemistry of ship plumes in the GEOS-Chem global chemistry transport model. *Atmos. Chem. Phys.* **11**, 11707-11722, doi:10.5194/acp-11-11707-2011 (2011).
- 63 Holmes, C. D., Prather, M. J. & Vinken, G. C. M. The climate impact of ship NO_x emissions: an improved estimate accounting for plume chemistry. *Atmos. Chem. Phys.* **14**, 6801-6812, doi:10.5194/acp-14-6801-2014 (2014).
- 64 van der Werf, G. R. *et al.* Global fire emissions estimates during 1997–2016. *Earth Syst. Sci. Data* **9**, 697-720, doi:10.5194/essd-9-697-2017 (2017).
- 65 Mu, M. *et al.* Daily and 3-hourly variability in global fire emissions and consequences for atmospheric model predictions of carbon monoxide. *J. Geophys. Res. Atmos.* **116**, doi:10.1029/2011JD016245 (2011).
- 66 Philip, S. *et al.* Anthropogenic fugitive, combustion and industrial dust is a significant, underrepresented fine particulate matter source in global atmospheric models. *Environmental Research Letters* **12**, 044018, doi:10.1088/1748-9326/aa65a4 (2017).
- 67 Fairlie, D. T., Jacob, D. J. & Park, R. J. The impact of transpacific transport of mineral dust in the United States. *Atmos. Environ.* **41**, 1251-1266, doi:<https://doi.org/10.1016/j.atmosenv.2006.09.048> (2007).
- 68 Fairlie, T. D. *et al.* Impact of mineral dust on nitrate, sulfate, and ozone in transpacific Asian pollution plumes. *Atmos. Chem. Phys.* **10**, 3999-4012, doi:10.5194/acp-10-3999-2010 (2010).
- 69 Stettler, M. E. J., Eastham, S. & Barrett, S. R. H. Air quality and public health impacts of UK airports. Part I: Emissions. *Atmos. Environ.* **45**, 5415-5424, doi:<https://doi.org/10.1016/j.atmosenv.2011.07.012> (2011).
- 70 Murray, L. T., Jacob, D. J., Logan, J. A., Hudman, R. C. & Koshak, W. J. Optimized regional and interannual variability of lightning in a global chemical transport model constrained by LIS/OTD satellite data. *J. Geophys. Res. Atmos.* **117**, doi:10.1029/2012JD017934 (2012).
- 71 Hudman, R. C. *et al.* Steps towards a mechanistic model of global soil nitric oxide emissions: implementation and space based-constraints. *Atmos. Chem. Phys.* **12**, 7779-7795, doi:10.5194/acp-12-7779-2012 (2012).
- 72 Fischer, E. V., Jacob, D. J., Millet, D. B., Yantosca, R. M. & Mao, J. The role of the ocean in the global atmospheric budget of acetone. *Geophysical Research Letters* **39**, doi:10.1029/2011GL050086 (2012).
- 73 Millet, D. B. *et al.* Global atmospheric budget of acetaldehyde: 3-D model analysis and constraints from in-situ and satellite observations. *Atmos. Chem. Phys.* **10**, 3405-3425, doi:10.5194/acp-10-3405-2010 (2010).
- 74 Breider, T. J. *et al.* Multidecadal trends in aerosol radiative forcing over the Arctic: Contribution of changes in anthropogenic aerosol to Arctic warming since 1980. *J. Geophys. Res. Atmos.* **122**, 3573-3594, doi:10.1002/2016JD025321 (2017).
- 75 Riddick, S. N. *et al.* Global ammonia emissions from seabirds (NERC Environmental Information Data Centre). doi:<https://doi.org/10.5285/c9e802b3-43c8-4b36-a3a3-8861d9da8ea9> (2012).
- 76 Croft, B. *et al.* Contribution of Arctic seabird-colony ammonia to atmospheric particles and cloud-albedo radiative effect. *Nature Communications* **7**, 13444, doi:10.1038/ncomms13444 <https://www.nature.com/articles/ncomms13444#supplementary-information> (2016).

- 77 Carpenter, L. J. *et al.* Atmospheric iodine levels influenced by sea surface emissions of inorganic iodine. *Nature Geoscience* **6**, 108-111, doi:10.1038/ngeo1687 (2013).
- 78 Guenther, A. B. *et al.* The Model of Emissions of Gases and Aerosols from Nature version 2.1 (MEGAN2.1): an extended and updated framework for modeling biogenic emissions. *Geosci. Model Dev.* **5**, 1471-1492, doi:10.5194/gmd-5-1471-2012 (2012).
- 79 Liang, Q. *et al.* Finding the missing stratospheric Br_y: a global modeling study of CHBr₃ and CH₂Br₂. *Atmos. Chem. Phys.* **10**, 2269-2286, doi:10.5194/acp-10-2269-2010 (2010).
- 80 Ordóñez, C. *et al.* Bromine and iodine chemistry in a global chemistry-climate model: description and evaluation of very short-lived oceanic sources. *Atmos. Chem. Phys.* **12**, 1423-1447, doi:10.5194/acp-12-1423-2012 (2012).
- 81 Lelieveld, J. *et al.* Effects of fossil fuel and total anthropogenic emission removal on public health and climate. *P. Natl. Acad. Sci.* **116**, 7192, doi:10.1073/pnas.1819989116 (2019).
- 82 Marais, E. A. *et al.* Air Quality and Health Impact of Future Fossil Fuel Use for Electricity Generation and Transport in Africa. *Environ. Sci. Technol.* **53**, 13524-13534, doi:10.1021/acs.est.9b04958 (2019).
- 83 Lacey, F. G. *et al.* Improving present day and future estimates of anthropogenic sectoral emissions and the resulting air quality impacts in Africa. *Faraday Discussions* **200**, 397-412, doi:10.1039/C7FD00011A (2017).
- 84 Chafe, Z. A. *et al.* Household Cooking with Solid Fuels Contributes to Ambient PM_{2.5} Air Pollution and the Burden of Disease. *Environmental Health Perspectives* **122**, 1314-1320, doi:10.1289/ehp.1206340 (2014).
- 85 Wu, R. *et al.* Air quality and health benefits of China's emission control policies on coal-fired power plants during 2005–2020. *Environmental Research Letters* **14**, 094016, doi:10.1088/1748-9326/ab3bae (2019).
- 86 GBD MAPS Working Group. *Burden of Disease Attributable to Coal-Burning and Other Major Sources of Air Pollution in China. Special Report 20.* (Health Effects Institute [Available at: <https://www.healtheffects.org/publication/burden-disease-attributable-coal-burning-and-other-air-pollution-sources-china>], 2016).
- 87 GBD MAPS Working Group. *Burden of Disease Attributable to Major Air Pollution Sources in India. Special Report 21.*, (Health Effects Institute [Available at: <https://www.healtheffects.org/publication/gbd-air-pollution-india>], 2018).
- 88 Zheng, B. *et al.* Trends in China's anthropogenic emissions since 2010 as the consequence of clean air actions. *Atmos. Chem. Phys.* **18**, 14095-14111, doi:10.5194/acp-18-14095-2018 (2018).
- 89 Zhang, Z. *et al.* The contribution of residential coal combustion to PM_{2.5} pollution over China's Beijing-Tianjin-Hebei region in winter. *Atmos. Environ.* **159**, 147-161, doi:<https://doi.org/10.1016/j.atmosenv.2017.03.054> (2017).
- 90 Liu, J. *et al.* Air pollutant emissions from Chinese households: A major and underappreciated ambient pollution source. *P. Natl. Acad. Sci.* **113**, 7756, doi:10.1073/pnas.1604537113 (2016).
- 91 Lelieveld, J., Evans, J. S., Fnais, M., Giannadaki, D. & Pozzer, A. The contribution of outdoor air pollution sources to premature mortality on a global scale. *Nature* **525**, 367, doi:10.1038/nature15371 (2015).
- 92 Gu, Y. *et al.* Impacts of sectoral emissions in China and the implications: air quality, public health, crop production, and economic costs. *Environmental Research Letters* **13**, 084008, doi:10.1088/1748-9326/aad138 (2018).

- 93 Hu, J. *et al.* Premature Mortality Attributable to Particulate Matter in China: Source Contributions and Responses to Reductions. *Environ. Sci. Technol.* **51**, 9950-9959, doi:10.1021/acs.est.7b03193 (2017).
- 94 Meng, J. *et al.* Source Contributions to Ambient Fine Particulate Matter for Canada. *Environ. Sci. Technol.* **53**, 10269-10278, doi:10.1021/acs.est.9b02461 (2019).
- 95 Caiazzo, F., Ashok, A., Waitz, I. A., Yim, S. H. L. & Barrett, S. R. H. Air pollution and early deaths in the United States. Part I: Quantifying the impact of major sectors in 2005. *Atmos. Environ.* **79**, 198-208, doi:<https://doi.org/10.1016/j.atmosenv.2013.05.081> (2013).
- 96 Fann, N., Fulcher, C. M. & Baker, K. The Recent and Future Health Burden of Air Pollution Apportioned Across U.S. Sectors. *Environ. Sci. Technol.* **47**, 3580-3589, doi:10.1021/es304831q (2013).
- 97 Penn Stefani, L. *et al.* Estimating State-Specific Contributions to PM_{2.5}- and O₃-Related Health Burden from Residential Combustion and Electricity Generating Unit Emissions in the United States. *Environmental Health Perspectives* **125**, 324-332, doi:10.1289/EHP550 (2017).
- 98 Thakrar, S. K. *et al.* Reducing Mortality from Air Pollution in the United States by Targeting Specific Emission Sources. *Environ. Sci. Tech. Lett.*, doi:10.1021/acs.estlett.0c00424 (2020).
- 99 Bond, T. C. *et al.* A technology-based global inventory of black and organic carbon emissions from combustion. *J. Geophys. Res. Atmos.* **109**, doi:10.1029/2003JD003697 (2004).
- 100 Butt, E. W. *et al.* The impact of residential combustion emissions on atmospheric aerosol, human health, and climate. *Atmos. Chem. Phys.* **16**, 873-905, doi:10.5194/acp-16-873-2016 (2016).
- 101 Crippa, M., Janssens-Maenhout, G., Guizzardi, D., Van Dingenen, R. & Dentener, F. Contribution and uncertainty of sectorial and regional emissions to regional and global PM_{2.5} health impacts. *Atmos. Chem. Phys.* **19**, 5165-5186, doi:10.5194/acp-19-5165-2019 (2019).
- 102 Giannadaki, D., Pozzer, A. & Lelieveld, J. Modeled global effects of airborne desert dust on air quality and premature mortality. *Atmos. Chem. Phys.* **14**, 957-968, doi:10.5194/acp-14-957-2014 (2014).
- 103 Pozzer, A., Tsimpidi, A. P., Karydis, V. A., de Meij, A. & Lelieveld, J. Impact of agricultural emission reductions on fine-particulate matter and public health. *Atmos. Chem. Phys.* **17**, 12813-12826, doi:10.5194/acp-17-12813-2017 (2017).
- 104 Guo, H. *et al.* Effectiveness of ammonia reduction on control of fine particle nitrate. *Atmos. Chem. Phys.* **18**, 12241-12256, doi:10.5194/acp-18-12241-2018 (2018).
- 105 Anenberg, S., Miller, J., Henze, D. & Minjares, R. A global snapshot of the air pollution-related health impacts of transportation sector emissions in 2010 and 2015. *The International Council on Clean Transportation (ICCT)*. [Available at: <https://theicct.org/publications/health-impacts-transport-emissions-2010-2015>] (2019).
- 106 Chambliss, S. E., Silva, R., West, J. J., Zeinali, M. & Minjares, R. Estimating source-attributable health impacts of ambient fine particulate matter exposure: global premature mortality from surface transportation emissions in 2005. *Environmental Research Letters* **9**, 104009, doi:10.1088/1748-9326/9/10/104009 (2014).
- 107 Silva Raquel, A., Adelman, Z., Fry Meridith, M. & West, J. J. The Impact of Individual Anthropogenic Emissions Sectors on the Global Burden of Human Mortality due to Ambient

- Air Pollution. *Environmental Health Perspectives* **124**, 1776-1784, doi:10.1289/EHP177 (2016).
- 108 Tsimpidi, A. P., Karydis, V. A. & Pandis, S. N. Response of Fine Particulate Matter to Emission Changes of Oxides of Nitrogen and Anthropogenic Volatile Organic Compounds in the Eastern United States. *Journal of the Air & Waste Management Association* **58**, 1463-1473, doi:10.3155/1047-3289.58.11.1463 (2008).
- 109 McDonald, B. C. *et al.* Volatile chemical products emerging as largest petrochemical source of urban organic emissions. *Science* **359**, 760, doi:10.1126/science.aag0524 (2018).
- 110 Corbett, J. J. *et al.* Mortality from Ship Emissions: A Global Assessment. *Environ. Sci. Technol.* **41**, 8512-8518, doi:10.1021/es071686z (2007).
- 111 Sofiev, M. *et al.* Cleaner fuels for ships provide public health benefits with climate tradeoffs. *Nature Communications* **9**, 406, doi:10.1038/s41467-017-02774-9 (2018).

Description of Additional Supplementary Data Files

File Name: Supplementary Data 1

Description: Global, regional, national, and sub-national PM_{2.5} exposure estimates and sector and disease-specific fractional contributions. Provides downscaled population weighted mean (PWM) national-level PM_{2.5} exposure estimates for 200 sub-national areas, 204 countries and territories, and 21 world regions. This table also provides the total attributable deaths and the number of neonatal incidences associated with PWM PM_{2.5} exposure levels in each country and region. Burden results are provided from both the 2019 Global Burden of Disease (GBD2019) concentration response relationships and the Global Exposure Mortality Model (GEMM). Also includes the fractional contributions (units of percent) of each source sector and disease to the total GBD2019 and GEMM disease burden estimates.

File Name: Supplementary Data 2

Description: Global, regional, national, and sub-national PM_{2.5} exposure estimates and combustion fuel-type fractional contributions. Includes relative fuel-type contributions from the combustion of coal, solid biofuel, and the sum of oil and gas.

File Name: Supplementary Data 3

Description: Global, regional, national, and sub-national PM_{2.5} exposure estimates for the year 2019.

Data File 1: PM_{2.5} Exposure Estimates, Sectoral Source Contributions, Total Attributable Mortality
 McDuffie et al., 2021 -
 Last Updated: March 23, 2021

Name Legend:

Regions Countries *Sub-national regions*

Country Name	Population Weighted Annual Average PM_{2.5} ($\mu\text{g m}^{-3}$)	Agriculture Contribution (%)	Energy Coal Contribution (%)
Central_Asia	27.5	5.1	6.1
Armenia	31.9	12.8	5.2
Azerbaijan	23.9	8	3.2
<i>Baku</i>	<i>31.5</i>	<i>5.4</i>	<i>2.7</i>
Georgia	17.8	8.4	5.7
Kazakhstan	19	4.5	5.3
<i>Shymkent</i>	<i>38.1</i>	<i>3.4</i>	<i>4.3</i>
Kyrgyzstan	22.9	3.9	7.4
Mongolia	36.7	13.1	10.5
<i>Ulaanbaatar</i>	<i>81.4</i>	<i>13.5</i>	<i>12.8</i>
Tajikistan	35.9	3.6	6.2
Turkmenistan	25.5	4.2	2.3
Uzbekistan	32.5	3.6	7.1
<i>Bukhara</i>	<i>26.6</i>	<i>2.8</i>	<i>4.5</i>
<i>Tashkent</i>	<i>50.8</i>	<i>3.6</i>	<i>6.9</i>
Central_Europe	20.5	18.6	10.7
Albania	19.8	12.8	11.6
Bosnia_and_Herzegovina	29.8	16	17.8
Bulgaria	19.7	12.7	13.6
Croatia	18	15.4	8.6
Czech_Republic	16.8	23.3	7.9
Hungary	16.5	16.1	8.2
<i>Budapest</i>	<i>19.5</i>	<i>14.8</i>	<i>7.4</i>
Macedonia	31.6	13.2	18.4
Montenegro	21.6	10.5	14.5
Poland	22.7	24.6	8
<i>Warsaw</i>	<i>24.3</i>	<i>24.7</i>	<i>7.4</i>
Romania	15.9	12.8	11.2
Serbia	26.5	10.9	19.7
<i>Belgrade</i>	<i>25.7</i>	<i>10.6</i>	<i>26.3</i>
Slovakia	18.4	20.1	7.7
Slovenia	16.9	17.4	5

Eastern_Europe	11.8	11.5	7.4
Belarus	16.3	21.2	6.7
<i>Gomel</i>	<i>20.9</i>	<i>19.2</i>	<i>8</i>
Estonia	5.7	12.5	2.9
Latvia	11.7	15.3	3.8
Lithuania	10.2	18.8	4.7
<i>Kaunas</i>	<i>12</i>	<i>17.3</i>	<i>4.6</i>
Moldova	13.1	14.2	9.8
Russian_Federation	10.9	9	6.2
<i>Saint_Petersburg</i>	<i>8.2</i>	<i>9.2</i>	<i>3.3</i>
<i>Astrakhan</i>	<i>12.1</i>	<i>4.4</i>	<i>5.6</i>
<i>Moscow</i>	<i>13.8</i>	<i>7.8</i>	<i>5.2</i>
<i>Tyumen</i>	<i>13.4</i>	<i>9.9</i>	<i>4.7</i>
<i>Berezniki</i>	<i>13.9</i>	<i>9.6</i>	<i>5.4</i>
<i>Dzerzhinsk</i>	<i>11.6</i>	<i>10.7</i>	<i>5.5</i>
Ukraine	14	14.8	10.5
<i>Nikolaev</i>	<i>14.2</i>	<i>13.5</i>	<i>10.8</i>
<i>Rovno</i>	<i>19.9</i>	<i>19.5</i>	<i>8.4</i>
Australasia	6.9	9.3	7
Australia	7	8.8	8.1
<i>Sydney</i>	<i>7.6</i>	<i>12.6</i>	<i>14.4</i>
New_Zealand	6.6	12.5	0.7
<i>Auckland</i>	<i>6.5</i>	<i>10.5</i>	<i>0.6</i>
High_income_Asia_Pacific	17.3	18.6	5.3
Brunei	7.6	2.9	4
Japan	13.5	19.5	4
<i>Tokyo</i>	<i>15.1</i>	<i>20.4</i>	<i>3.1</i>
<i>Osaka</i>	<i>15.1</i>	<i>19</i>	<i>4.2</i>
<i>Fukuoka</i>	<i>17.7</i>	<i>18.1</i>	<i>5.1</i>
<i>Okayama</i>	<i>13.3</i>	<i>20.5</i>	<i>4.7</i>
<i>Yamaguchi</i>	<i>12.6</i>	<i>18.2</i>	<i>5</i>
South_Korea	26.6	18.5	6.1
<i>Seoul</i>	<i>27.4</i>	<i>17.5</i>	<i>6</i>
<i>Busan</i>	<i>24.3</i>	<i>18.9</i>	<i>5.6</i>
<i>Cheonan</i>	<i>28.6</i>	<i>19.3</i>	<i>6.5</i>
<i>Gwangju</i>	<i>27</i>	<i>19.8</i>	<i>6.3</i>
<i>Jinju</i>	<i>27.7</i>	<i>19.7</i>	<i>6.1</i>
<i>Pyongyang</i>	<i>52.9</i>	<i>16.4</i>	<i>5.8</i>
Singapore	18.5	4.2	16.9
High_income_North_America	7.8	10.2	6.6
Canada	7.3	12	3.1

<i>Montreal</i>	9.1	10.9	1.6
<i>Victoria</i>	6.3	6.5	0.6
Greenland	5.3	13.1	4
United_States	7.8	10	7
<i>Raleigh</i>	7.6	11.7	13
<i>New_York</i>	7.7	6.4	4.2
<i>Philadelphia</i>	8.6	10.5	5.8
<i>Houston</i>	9.9	6.9	7.7
<i>Minneapolis</i>	7.4	13.3	8.1
<i>Portland</i>	8	10.5	1.6
<i>Los_Angeles</i>	10.6	3.4	1.2
<i>Cleveland</i>	8.8	14.8	8.6
<i>Chicago</i>	9	12.3	7.9
<i>Springfield</i>	6.5	8.3	3.9
<i>Gainesville</i>	6.5	5.9	7.4
<i>Killeen</i>	7.4	11.7	8.9
<i>Modesto</i>	12.1	11.3	1
Southern_Latin_America	15.3	5.8	2.7
Argentina	13	5.7	1.6
<i>Buenos_Aires</i>	11.5	8.2	1.2
<i>Cordoba</i>	13.9	3	1.5
Chile	21.9	5.8	4.5
<i>Santiago</i>	28.9	4.6	4.7
Uruguay	9.8	7.5	1.7
Western_Europe	11.7	21.7	3.7
Andorra	8.8	16.3	2.6
Austria	12.1	20.7	5.1
<i>Vienna</i>	14.5	19.9	5.8
Belgium	12.8	29.2	2.4
<i>Antwerp</i>	14.1	28.4	2.7
Cyprus	15.2	7.8	16.6
Denmark	10.2	26.1	3.2
Finland	5.2	11.8	2.4
France	11.6	21.4	1.8
<i>Paris</i>	14	18.7	1.3
<i>Le_Mans</i>	13.6	25.5	1.4
Germany	11.9	28.5	4.9
<i>Berlin</i>	16	29.7	5.3
<i>Halle</i>	14.6	28.7	5.9
<i>Oldenburg</i>	13.2	33.3	3.7
Greece	14.6	9.8	14.7

<i>Thessaloniki</i>	15.9	13.8	16.5
Iceland	5.6	13.6	0.3
Ireland	7.7	25.6	1.4
Israel	19.7	9.9	10.2
<i>Tel_Aviv</i>	21.6	9.9	10.6
Italy	15.6	18.4	3.7
<i>Palermo</i>	15	5.7	5
<i>Milan</i>	23.4	21.6	1.9
Luxembourg	9.9	29	2.9
Malta	12.4	5.8	4.3
Netherlands	12.4	29.3	3.2
<i>Zwolle</i>	11.8	31.5	3.5
Norway	6.5	10.2	1.6
Portugal	8.6	14.2	1.8
Spain	9.9	13.5	2.7
<i>Madrid</i>	10.1	9.9	2.1
<i>Toledo</i>	8.5	14.8	8.1
Sweden	5.7	16.2	2.4
Switzerland	10.2	20.1	2.4
<i>Lausanne</i>	12.3	19.2	2.2
United_Kingdom	10.5	26.6	1.8
<i>Sheffield</i>	11.6	27.5	2.2
<i>London</i>	13	25.3	1.6
<i>Manchester</i>	11	26.8	1.8
Monaco	11.4	23.5	2.3
San_Marino	9.8	20.6	4.4
Andean_Latin_America	25.9	7.5	0.4
Bolivia	26	2.5	0.4
<i>Cochabamba</i>	26.2	1.7	0.3
Ecuador	18.8	8.7	0.1
<i>Quito</i>	17.6	8.6	0
Peru	29.6	8.7	0.5
Caribbean	16.5	2.8	1.5
Antigua_and_Barbuda	16.2	1.2	0.7
The_Bahamas	13.9	1.4	2.5
Barbados	19.6	0.1	0
Belize	19.3	1.5	0.8
Bermuda	7	0.8	3.3
Cuba	17.5	2.2	1.2
<i>Holguin</i>	15.5	2.7	0.9
Dominica	16.8	1.3	0.9

Dominican_Republic	16.8	4.1	2.2
Grenada	19.4	0.1	0
Guyana	20.5	0.1	0
Haiti	17.8	3.2	1.8
Jamaica	15.2	2.6	1
Puerto_Rico	7	2.4	0.6
Saint_Lucia	19.4	0.1	0.1
Saint_Vincent_and_the_Grenadines	19.4	0.1	0
Suriname	21.9	0	0
Trinidad_and_Tobago	19.5	0.1	0
Virgin_Islands_US	8.8	1	0.6
Saint_Kitts_and_Nevis	8.4	1.4	0.7
Central_Latin_America	20.8	5.8	2.3
Colombia	21.3	2.7	1.2
<i>Bogota</i>	<i>30.5</i>	<i>3.7</i>	<i>1.6</i>
<i>Valledupar</i>	<i>22.2</i>	<i>3.2</i>	<i>0.4</i>
Costa_Rica	17.3	6.2	0.2
El_Salvador	22.6	5.6	2.7
<i>San_Salvador</i>	<i>22.9</i>	<i>5.6</i>	<i>3</i>
Guatemala	27.3	3.1	1.3
<i>Guatemala_City</i>	<i>33.5</i>	<i>4.2</i>	<i>1.6</i>
Honduras	22.3	4.3	0.8
Mexico	20.1	8.5	3.6
<i>Culiacan</i>	<i>18.6</i>	<i>1.1</i>	<i>2.7</i>
<i>Guadalajara</i>	<i>18.9</i>	<i>9.1</i>	<i>3.2</i>
<i>Mexico_City</i>	<i>24.3</i>	<i>9.7</i>	<i>3</i>
<i>Reynosa</i>	<i>20.2</i>	<i>5.6</i>	<i>6.4</i>
<i>Tijuana</i>	<i>17.6</i>	<i>4.8</i>	<i>1.2</i>
Nicaragua	19.1	5	0.3
<i>Leon</i>	<i>19.9</i>	<i>4.9</i>	<i>0.2</i>
Panama	13.7	3.6	0.3
Venezuela	20.3	2.5	0.1
<i>Caracas</i>	<i>19.4</i>	<i>3.2</i>	<i>0</i>
<i>Cabimas</i>	<i>21.6</i>	<i>3.1</i>	<i>0.1</i>
Tropical_Latin_America	11.8	4.1	1
Brazil	11.8	4.2	1
<i>Sao_Paulo</i>	<i>15.3</i>	<i>5.5</i>	<i>1</i>
<i>Curitiba</i>	<i>8.9</i>	<i>5.8</i>	<i>0.8</i>
<i>Florianopolis</i>	<i>12.8</i>	<i>8.9</i>	<i>5.4</i>
<i>Belo_Horizonte</i>	<i>13.2</i>	<i>8.2</i>	<i>0.7</i>
<i>Palmas</i>	<i>10.4</i>	<i>0.3</i>	<i>0.1</i>

<i>Ilheus</i>	13.6	1.1	0.2
<i>Jequie</i>	13.3	1.8	0.3
<i>Ribeirao_Preto</i>	14.5	6.2	1
Paraguay	12.5	1.4	0.5
North_Africa_and_Middle_East	44.1	5.7	4.4
Afghanistan	50.8	5.2	6.6
<i>Kabul</i>	64.5	5.9	11.9
Algeria	31.6	4.6	1.6
<i>Algiers</i>	34	4.1	1.8
<i>Tebessa</i>	33.3	6.6	1.8
Bahrain	60.8	2.9	1.1
Egypt	65.8	5.6	5.4
<i>Cairo</i>	80.9	6.3	5.3
<i>Alexandria</i>	56.7	6.5	7.4
Iran	38.3	8.1	1.7
<i>Tehran</i>	36.3	11.4	1.4
<i>Ahvaz</i>	71.1	5.3	1.8
<i>Gorgan</i>	39.6	11.8	1.8
<i>Qom</i>	41.6	10.3	1.5
Iraq	48.6	5.1	3.4
<i>Baghdad</i>	58.2	4.9	3.3
Jordan	32.1	8.9	8.9
Kuwait	63.1	3.5	1.5
Lebanon	28.5	8.7	9.2
Libya	36.2	1.5	2.1
Morocco	34	3.4	1.8
<i>Marrakesh</i>	44	1.7	1.1
Palestine	32.6	9.8	9.7
Oman	42.6	1.7	0.9
Qatar	71.6	2.8	1
Saudi_Arabia	61.5	2.7	1.6
<i>Riyadh</i>	67.7	2.6	1.2
Sudan	50	0.7	1.1
<i>Khartoum</i>	61.2	0.5	1.1
Syria	31.1	8.9	9.1
Tunisia	29.3	3.8	2.2
<i>Kairouan</i>	35.4	4.5	2.1
Turkey	26.1	15.3	14.7
<i>Istanbul</i>	26	14.7	13.3
<i>Malatya</i>	32.7	15.2	16
<i>Kayseri</i>	37.5	16.2	12.5

United_Arab_Emirates	42.7	2.8	0.7
Yemen	44.1	2.2	1.5
<i>Sana</i>	44.7	2.2	1.5
South_Asia	76.1	9.5	6.5
Bangladesh	61.9	11.8	6.4
<i>Rajshahi</i>	55.8	11.8	8.2
<i>Dhaka</i>	69.6	11.9	6.2
<i>Saidpur</i>	61.4	12.2	6.1
Bhutan	38.8	10.2	4.7
India	80.2	9.4	7
<i>Jaipur</i>	102.8	8.7	5.3
<i>Ahmedabad</i>	131.5	6.1	7.5
<i>Kanpur</i>	152.3	9.4	6.8
<i>Kolkata</i>	85.8	8.9	7.4
<i>Mumbai</i>	60	7	7.6
<i>Pune</i>	57	9.4	6.5
<i>Hyderabad</i>	47.6	6.6	8.5
<i>Belgaum</i>	44.6	6.7	8.4
<i>Coimbatore</i>	41.2	6.2	6.3
<i>Hindupur</i>	41.3	6.3	9.2
<i>Jalna</i>	52.8	8.4	10.1
<i>Kozhikode</i>	34.8	3.7	5.1
<i>Malegaon</i>	57	7.8	10.3
<i>Parbhani</i>	41.7	8.3	10.6
<i>Singrauli</i>	153.2	11.6	13.9
<i>Sitapur</i>	136.5	10.9	6.5
<i>Vijayawada</i>	56.2	6.4	9.4
Nepal	79.3	9.2	4.4
<i>Pokhara</i>	74.6	8.1	3.8
Pakistan	59.7	8.5	2.8
<i>Karachi</i>	70.8	3.9	2.4
<i>Lahore</i>	72.5	9.1	2.2
<i>Sialkot</i>	66	10.7	2.9
East_Asia	49.3	11.1	4.7
China	49.8	11	4.7
<i>Chengdu</i>	63.9	10.4	2
<i>Qingdao</i>	46.8	13.5	5.9
<i>Taipei</i>	22	10.4	4
<i>Shanghai</i>	46.2	9.4	3.5
<i>Wuhan</i>	64.6	10.4	3.3
<i>Hangzhou</i>	54.1	9.9	3.5

<i>Guangzhou</i>	39.9	6.2	3.7
<i>Beijing</i>	71.8	13.7	5.4
<i>Tangshan</i>	73.4	14.2	6
<i>Tianjin</i>	71.7	12.4	5.5
<i>Jinan</i>	70.4	12.9	5.8
<i>Zhengzhou</i>	82.7	11	4.7
<i>Hong_Kong</i>	23.5	4.3	4.2
<i>Anqing</i>	55.4	11.1	4
<i>Bicheng</i>	54.4	8.9	3.1
<i>Changzhi</i>	72.2	13	6.2
<i>Changzhou</i>	56.1	9.4	3.9
<i>Chengguan</i>	37.3	10.4	6.6
<i>Gaoyou</i>	54.7	12.1	4.6
<i>Guixi</i>	48.9	7.9	2.8
<i>Haikou</i>	22.4	4.9	4.3
<i>Kaiping</i>	39	8.1	4.5
<i>Leshan</i>	58.8	10.2	2.4
<i>Pingxiang</i>	54.3	9.1	3.3
<i>Shenzhen</i>	32.4	4.4	4.1
<i>Suining</i>	51.2	8.2	3.4
<i>Xingping</i>	68.4	8.8	4.6
<i>Xucheng</i>	56.1	13	4.7
<i>Yanggu</i>	73.6	12.7	5.8
<i>Yiyang</i>	51.1	9.9	3.5
<i>Yucheng</i>	34.9	10.4	4.6
<i>Zhuji</i>	49.4	9.6	3.3
<i>Zunyi</i>	45.4	10.6	3.9
<i>Yulin</i>	40.7	7.6	3.3
North_Korea	41.8	16.7	6.4
Taiwan	23.9	11.5	4.1
Oceania	12.7	0.6	0.4
American_Samoa	6.1	0.2	0
Federated_States_of_Micronesia	9.1	0	0.1
Fiji	9.8	1.9	0.2
<i>Suva</i>	-	-	-
Guam	7.6	0	0.1
Kiribati	7.6	0	0
Marshall_Islands	8.6	0	0.1
Northern_Mariana_Islands	7.8	0.1	0.2
Papua_New_Guinea	13.3	0.6	0.4
Samoa	9.6	0.3	0

Solomon_Islands	10.7	0.2	0.3
Tonga	9.6	0.2	0.2
Vanuatu	11.1	0.9	0.8
Niue	6.4	0	0.1
Cook_Islands	6.1	0.1	0.1
Nauru	5.6	0	0
Palau	6.7	0.4	3.3
Tokelau	7	0	0
Tuvalu	5.7	0	0
Southeast_Asia	20.1	4.5	5.9
Cambodia	21.2	1.3	2.3
Indonesia	18	6.6	8.3
<i>Medan</i>	<i>34.6</i>	<i>2.5</i>	<i>3.1</i>
<i>Palembang</i>	<i>25.6</i>	<i>2.3</i>	<i>8.6</i>
<i>Cirebon</i>	<i>21.4</i>	<i>8.7</i>	<i>12.1</i>
<i>Parepare</i>	<i>14.4</i>	<i>1.3</i>	<i>2.5</i>
<i>Pematangsiantar</i>	<i>25.2</i>	<i>3.3</i>	<i>3.7</i>
Laos	18.5	4.9	3.8
Malaysia	16.2	3.3	7.6
<i>Ipoh</i>	<i>17.5</i>	<i>7.1</i>	<i>8</i>
<i>Rawang</i>	<i>17.2</i>	<i>4.5</i>	<i>6.6</i>
Maldives	9.9	2.6	5
Mauritius	14.7	0.8	2.6
Myanmar	28.5	3.6	5.4
<i>Myeik</i>	<i>22.7</i>	<i>2.2</i>	<i>3.3</i>
Philippines	18.4	3.4	5.8
<i>Manila</i>	<i>27.4</i>	<i>4</i>	<i>5.1</i>
<i>Bacolod</i>	<i>19.7</i>	<i>1.5</i>	<i>5.8</i>
<i>Cebu_City</i>	<i>22.4</i>	<i>2.6</i>	<i>7</i>
Sri_Lanka	19.6	2.4	4.5
Seychelles	15.4	0.2	1.2
Thailand	26.4	2.7	3.6
<i>Bangkok</i>	<i>30.4</i>	<i>1.7</i>	<i>2.7</i>
Timor_Leste	15.3	2.2	0.8
Vietnam	20	4.3	3.7
<i>Vinh_Long</i>	<i>23.7</i>	<i>2.3</i>	<i>2.5</i>
<i>Ho_Chi_Minh_City</i>	<i>27.1</i>	<i>1.9</i>	<i>2.7</i>
Central_Sub_Saharan_Africa	32.2	0.2	0.4
Angola	27	0.3	1.3
<i>Luanda</i>	<i>31.2</i>	<i>0.2</i>	<i>0.8</i>
Central_African_Republic	41.3	0.5	0.2

Congo	35.2	0.1	0.2
Democratic_Republic_of_the_Congo	33	0.2	0.3
<i>Kinshasa</i>	<i>39.4</i>	<i>0.1</i>	<i>0.2</i>
<i>Lubumbashi</i>	<i>27.4</i>	<i>0.8</i>	<i>0.7</i>
Equatorial_Guinea	41.3	0	0.1
Gabon	33.3	0	0.1
Eastern_Sub_Saharan_Africa	28.5	0.5	1.2
Burundi	31.5	0.1	0.2
Comoros	16.1	0.4	1.7
Djibouti	41.1	2.2	1.5
Eritrea	41.6	1.9	1.3
Ethiopia	32.6	0.9	0.8
<i>Addis_Ababa</i>	<i>31.5</i>	<i>0.6</i>	<i>0.7</i>
Kenya	24.4	0.2	0.6
<i>Nakuru</i>	<i>23.8</i>	<i>0.1</i>	<i>0.5</i>
Madagascar	17.5	0.4	1.9
Malawi	23.1	0.7	2.5
Mozambique	21.4	0.9	7
<i>Beira</i>	<i>24.2</i>	<i>0.6</i>	<i>7.8</i>
Rwanda	33.8	0.2	0.2
<i>Kigali</i>	<i>34.8</i>	<i>0.2</i>	<i>0.2</i>
Somalia	28.8	0.8	1.2
South_Sudan	36.4	0.3	0.4
Tanzania	24.6	0.2	0.9
<i>Arusha</i>	<i>23.1</i>	<i>0.1</i>	<i>0.9</i>
Uganda	36.7	0.2	0.3
<i>Kampala</i>	<i>48.5</i>	<i>0.1</i>	<i>0.2</i>
Zambia	24.9	0.8	2.4
<i>Ndola</i>	<i>26</i>	<i>0.9</i>	<i>1.4</i>
Southern_Sub_Saharan_Africa	27	4.6	18.3
Botswana	24.3	3.4	21.1
Lesotho	29.4	5.5	15.6
Namibia	24.4	1.1	7.5
South_Africa	28.8	5.5	20.5
<i>Port_Elizabeth</i>	<i>23.9</i>	<i>3.1</i>	<i>5.9</i>
<i>Johannesburg</i>	<i>40.2</i>	<i>6.7</i>	<i>26.1</i>
Eswatini	23.1	6.5	32.4
Zimbabwe	21.7	1.1	8.9
Western_Sub_Saharan_Africa	59.4	0.1	0.2
Benin	42.6	0.1	0.1
Burkina_Faso	50.4	0	0.2

Cameroon	58.9	0.1	0.2
Cape_Verde	46.4	0.1	0.1
Chad	55.3	0.2	0.5
Cote_d'Ivoire	52.1	0.1	0.1
The_Gambia	58.6	0.1	0.1
Ghana	54	0.1	0.1
<i>Accra</i>	<i>64.3</i>	<i>0.1</i>	<i>0.1</i>
Guinea	50.4	0.1	0.1
Guinea_Bissau	54.6	0.1	0.1
Liberia	46.5	0.1	0.1
Mali	56.5	0	0.2
<i>Bamako</i>	<i>56.3</i>	<i>0</i>	<i>0.2</i>
Mauritania	64.3	0	0.1
Niger	70.9	0.1	0.2
Nigeria	64.2	0.1	0.2
<i>Ibadan</i>	<i>38.9</i>	<i>0.2</i>	<i>0.1</i>
<i>Lagos</i>	<i>34.2</i>	<i>0.1</i>	<i>0.1</i>
<i>Gombe</i>	<i>79.1</i>	<i>0.1</i>	<i>0.2</i>
<i>Oyo</i>	<i>41.1</i>	<i>0.2</i>	<i>0.1</i>
Sao_Tome_and_Principe	29.5	0	0.3
Senegal	60.5	0.1	0.1
Sierra_Leone	48.2	0.1	0.1
Togo	44.4	0.1	0.1
Global	41.7	8.3	5.1

mortality Estimates, and Fractional Disease Contributions

Energy NonCoal Contribution (%)	Industry Coal Contribution (%)	Industry NonCoal Contribution (%)	NonRoad Transport Contribution (%)	Road Transport Contribution (%)
4.8	2.1	4.8	0.2	5.3
4.6	1.3	8.2	0.2	9
5.4	0.7	4.9	0.2	7.2
4.9	0.5	3.6	0.2	5.5
3.3	2.1	5.2	0.2	7.4
5	3	6	0.2	5.1
4.8	2.4	3.9	0.2	4.9
4.2	2.7	5.1	0.2	6.6
4.7	5.3	4.7	0.7	3.7
4.7	5.9	4.9	0.7	3.5
4.3	1.3	3.4	0.1	4.5
4.3	0.4	3.7	0.1	5.1
5	2.2	4.7	0.2	4.8
5.4	0.7	2.8	0.1	3.5
5	4.3	7.2	0.2	5.6
5.7	1.7	4.8	0.7	7.7
2.5	1.4	4.2	0.9	6.6
4.2	1.1	3.5	0.6	6.6
3.4	1.3	5.7	0.5	6.1
5	1	5.1	1	9.8
7.8	1.9	5.6	0.9	8.8
7.4	1.4	4.9	0.7	8.8
7.4	1.4	4.9	0.7	8.3
2.4	1	4	0.4	4.6
2.6	0.8	3	0.5	5
6.9	2.1	4.8	0.8	8.5
5.3	2.5	4.6	0.7	8.8
4.8	1.4	4.9	0.6	6.8
3.1	1.1	3.7	0.4	5
3.2	1.3	3.9	0.3	4.5
7.8	2	5.2	0.7	8.3
6	0.9	6.6	1.2	12.6

8.8	1.3	5.5	0.6	6
10.7	2.7	4.4	1.1	8.3
8.4	2.3	5	1	7.8
14.2	0.8	6.7	0.8	5.7
12.9	1	5.4	1.1	7.1
17.6	1.3	4.1	1.1	8
24.5	1.3	3.7	0.9	7.5
5.6	1.6	3.9	0.7	7.3
8.7	1	6.2	0.5	5.4
13.8	0.8	9.3	0.8	6.6
5	0.8	3.2	0.2	3
12.2	0.4	9.6	0.3	4.6
8.7	0.9	7.2	0.3	6.1
9.1	0.6	6.1	0.3	5.5
7.5	0.5	4.9	0.7	7.3
8	1.7	4	0.6	6.6
8.3	1.6	3.9	0.8	5.9
5.8	2.1	4.2	0.7	8.6
1.1	1.2	6.2	0.4	4.3
1.1	1	6.6	0.4	4
1.6	1	7.6	0.3	3.7
1	2.9	3.8	0.3	6.5
1.6	2.8	4.4	0.3	6
6	7.3	8.4	1.5	8.9
4.2	1.5	3.4	0.6	12.5
6.3	6.1	7.8	1.7	8
6.8	5.2	8.9	1.5	8.3
6.3	6.6	8.8	1.7	7.9
5.5	7.6	7.1	1.9	7.1
6.7	7	6.9	1.7	8.3
5.9	7.5	7.3	1.6	7.4
5.4	9.2	9.4	1.4	9.3
5.3	9.7	9.8	1.2	9
5.7	8.4	10.9	1.7	8.9
5.6	8.9	9.1	1.3	9.7
5.6	8.9	8.5	1.5	10.8
5.4	8.7	7.8	1.6	10.7
5	15.1	8	1.2	7.6
9.3	1.5	3.5	0.2	18.3
5.1	2	9.1	3.2	11.7
7.5	0.6	10.2	2.2	7.6

8.7	0.7	13.8	1.8	7.4
5.8	0.7	12.3	2.9	7.2
2.3	0.8	2.5	2.1	7.6
4.9	2.1	9	3.3	12.1
4.6	2	6.5	3.6	14
4.4	2.4	15.9	2.8	10.5
6.3	1.9	11.2	3.3	11.7
10.4	2	8.1	2.8	11.8
5.7	1.4	7.1	5.4	14.6
1.6	2.1	13	2.8	10.1
3.2	3.9	18.3	1.4	8.6
5.7	1.7	8	4	11.7
5.8	2	10.7	4.9	12.6
4	1.5	10.2	2.9	12.8
3.5	1.8	6.8	3.1	11.9
7.1	2.1	6.5	3.2	15.3
2.6	4.2	10.3	1.9	8.5
3.1	0.3	11.6	0.3	7.7
3.7	0.2	11.1	0.4	9
5.5	0.2	17.7	0.4	10.5
2.5	0.2	6.8	0.2	10.2
2.1	0.2	11.7	0.3	5.6
2.6	0.3	16.8	0.1	5.7
5.6	0.4	18.3	0.3	10
6.3	1.1	7.1	1.5	10.4
4.1	0.7	6.7	1.5	11.6
8.4	1.5	8.2	1.1	12
8	1.4	8.1	0.9	10.2
9.1	1.3	8.1	1.5	9.6
11.8	1.2	7.7	1.5	9.2
3.3	2.3	4.4	0.5	5.4
7.1	0.8	5.7	2.3	8.4
9.8	1	9.8	0.7	5.4
5	1.2	7.2	1.4	11.8
4.2	1.6	9.4	1.1	9.9
4.2	0.9	5.5	2	12.4
7.9	1.7	8.7	1.5	10.7
6.5	1.8	9.3	1.7	9.5
8.6	1.7	8.2	1.6	11.3
7.8	1.1	6	1.7	8.5
3.3	1.4	5.1	1.1	5.6

3.4	1.2	4.8	0.8	6.1
0.7	0.5	6	0.3	1.6
2.7	0.4	3.8	1.3	6.2
9.7	1.1	4.5	0.3	7.1
9.6	1.1	4.6	0.4	7.2
5	0.6	4.9	1.6	12.8
3.3	0.7	3.7	1.2	7
4.5	0.5	5.5	1.3	14.3
6	1.8	8.8	1.4	13.3
2.7	0.5	2.8	0.8	5.7
7.6	1.2	7.6	1.8	10.6
6.8	1.1	7	1.9	10.7
5	1	8.3	1.1	4.4
3.8	0.2	7.1	0.7	6.8
4.9	0.5	9.5	2	9.4
4.3	0.8	16.5	1.2	9.5
6.1	1.5	8.1	4.9	12.4
10	0.8	8.8	1.4	6.5
6.9	1.5	8.2	1.3	14.7
10.7	1.3	7.5	1.2	14.2
6.8	1.1	6.8	1.7	8.9
8.6	1.3	7	1.4	8.4
6.1	1.2	8.2	1.6	9.6
7.7	1.2	6.3	1.5	8.3
4.2	0.7	5.1	1.2	12.5
5	0.7	5.2	2.3	12.3
3.5	0.4	22.5	0.1	8.2
0.5	0.1	12.7	0	3.1
0.4	0	11.4	0	2.8
11.8	0.2	8.8	0.2	17.9
12.7	0.2	8	0.6	18.7
1.7	0.5	30.1	0.1	6.5
9.7	0.4	9.1	0.4	5.5
3.6	-0.1	1.5	0.1	5.5
6.1	1	5.1	1	6.3
0.5	0	0.2	0	0.8
5.2	0.5	4.1	0.3	6.3
2.7	0.8	3.3	1.1	5.9
9.9	0.5	19.7	0.6	5.7
16.7	0.3	11.6	0.4	4.8
3.8	-0.1	1.7	0.1	5.7

9.6	0.5	7.8	0.6	6.5
0.5	0	0.2	0	1
0.6	0	0.4	0.1	0.8
13	0.3	4	0.4	5.6
15.3	0.4	7.1	0.2	8.1
3	-0.2	2.1	0.1	4.5
0.8	0	0.3	0.1	1
0.7	0	0.3	0.1	1
0.6	0	0.4	0.1	0.8
0.7	0	0.3	0	1.4
3.3	-0.2	1.5	0.1	4.9
3.7	-0.1	1.6	0.1	5.5
8.5	2.4	7.1	0.3	9.8
3.4	7.9	9.1	0	9.1
2.8	12.3	12.4	0	8.5
5.5	0.8	6.5	0	10.8
2.8	0.1	5.6	0.1	6.9
11.2	0.1	4.3	0.1	6.5
11.1	0.1	4.4	0	6.5
5.4	0.1	4.2	0	5.5
4.6	0.1	7.1	0	5
8.8	0.4	4.8	0.1	7.8
12.4	1.6	8.1	0.5	12.3
5	0.9	3.5	1	17.2
9.1	1.9	10.3	0.2	15.8
10.9	1.8	12.1	0.2	12.2
11.7	1.6	5	2.6	12
2.9	2.9	11.7	2	11
7.1	0.1	2.1	0.2	5.5
8.3	0.1	1.9	0.3	5.9
3.4	0.2	2.6	0	8
4	0.4	4.6	0	6.6
4.3	0.2	5.1	0	4.9
5.4	0.3	5.9	0	10.7
4.6	1.7	25.2	0.2	6.3
4.6	1.8	25.6	0.2	6.3
8.4	2.3	42.1	0.2	6.8
6.9	2.6	35.8	0.3	8.2
8.3	1.7	24.6	0.3	7.9
3.6	3.6	40.7	0.2	5.5
0.6	0.5	3.6	0.1	2.4

1.1	0.6	6.5	0	3.6
1.5	1.3	12.6	0.1	5
4.9	2.3	30.7	0.3	10.3
2.8	0.6	13.4	0.2	7.5
7.4	0.8	4.4	0.3	7
5	2.2	2.7	0.1	6.2
4.8	2.8	2.3	0.1	6.7
3	0.2	3.9	0.6	17.1
3.4	0.2	6	0.8	23.3
2.7	0.2	3.5	0.5	14.3
22.9	0.4	5.7	0	6.9
6.3	0.6	4.7	0.5	5.8
6.9	0.6	5.2	0.5	6.3
6.7	0.8	4.5	0.6	5
9.8	0.4	5.2	0.1	11
7.8	0.4	6.7	0.1	14.4
15.9	0.3	4.1	0.1	8.6
7.5	0.4	6.2	0.1	12.2
8.8	0.4	6	0.1	13.8
11.1	0.6	3.7	0.1	9
11.4	0.5	3.9	0.1	8.9
9.4	1	4.4	0.3	6.8
15.2	0.3	3.6	0	6.1
11.6	1.4	4.2	0.3	6
1.2	0.2	1.1	0.2	3.3
1.6	0.1	2.7	0.3	5.4
0.8	0	1.8	0.1	3.5
9.4	1	4.5	0.3	7.1
8.5	0.8	4.4	0	3.6
20.9	0.4	5.4	0	6.4
13.8	0.4	6.8	0.1	5.1
13.6	0.3	6.9	0	5.8
4.4	0.2	2.4	0.1	2.4
4.3	0.2	2.6	0.1	2.4
8.3	1.7	4.2	0.3	6.7
3.4	0.3	4.1	0.5	9.6
3.2	0.3	3.8	0.5	10.6
3.2	3	5.2	0.5	7.4
3.1	4.4	7.5	0.7	6.8
3.5	1.9	3.3	0.4	7.9
2.7	2.8	4.5	0.3	8.1

14.6	1	5.9	0	5.3
11.7	0.8	5	0.1	3.9
12.5	0.8	5.1	0.1	4
5.5	8	6.3	1	6
6	6.7	5.6	1.6	7.2
6.2	7.8	7.3	1.1	5.2
5.6	6.2	5.2	2	7.5
4.4	7.8	6.7	1	6.1
3.5	8.2	5.7	1.1	4.3
5.5	8.2	6.6	1	5.7
4.8	7.4	4.8	1.3	8
6.1	6.2	5.5	0.8	6
4.7	8.1	6.1	1.2	6
6.3	10.7	12	0.6	3.4
5.6	10.2	9.9	1	4.3
4.2	9.8	10.1	1	4.5
4.6	8.5	6.6	1.3	5
5	7.6	5	1.6	7.6
4	8.5	7.5	0.7	5.4
5.7	7.5	4.7	1.6	6
5.2	7.6	5.2	1.4	5.5
4.1	8.8	7.1	1	5.1
6.1	7.3	5.2	1.2	5.3
5.5	7.8	5.2	1.5	5.4
12.4	5.5	4.2	0.9	3.9
4.5	7.4	5.1	1	6.6
6.5	8.7	7	1.4	4.5
3.3	8.3	4.5	0.7	5.3
2.8	6	3	0.7	5.4
5.7	7.5	4.1	0.7	8.6
6.6	7.7	6.9	0.5	6.5
5.2	9.1	6.5	0.9	9.5
4.9	8.6	4.4	1	9.9
4.9	9.1	5.2	1.4	6.2
4.8	9.1	5.2	1.4	6.2
2.3	13.5	4.8	0.9	5.5
4.1	11.2	4.6	1.4	7.1
7.6	8.1	6.3	0.8	8.1
7.5	11.3	10.1	0.6	5.4
6.2	11.3	5.7	1.6	6
4.2	8.7	7.3	0.6	6.9

3.3	9	4.8	1.5	6.9
6.3	9.8	4.4	1.2	8.8
5	9.1	4.1	1.2	7.9
4.6	8.8	4.2	1.4	8.7
4.1	10.5	4.4	1.5	6.1
4.9	8.8	4.5	1.1	5.5
3.2	9.1	6.1	0.8	6.8
4.6	9.3	5.9	1.7	5.8
3.5	10.4	3.4	1.8	6.9
9	7.2	4	1	5.2
3.8	8.5	6.6	1	6.4
4.1	6.5	3.7	1.5	4.3
4	9.9	5.8	1.8	6.8
3.2	7.7	3.3	2.7	6.3
4.5	8.7	4.4	1.4	6.6
3.6	8.4	4.6	1.8	8.4
2.9	12.8	4.2	1.2	6.2
5.6	11.2	4.8	1.7	5
3.1	9.3	5.1	0.8	6.1
3	9.3	3.4	1.4	6.2
3.5	7.1	4.9	0.8	6.8
4	10.2	5.7	1.8	6.7
4.1	10.3	4.2	1.8	5.8
4.6	10.2	4.5	3	5.2
3.7	7.4	7.1	0.3	5.1
4	9.1	7.2	0.6	7.3
5	8.3	3.6	1.7	5.3
4	10.8	5.3	2.3	5.5
5.6	12.2	7.1	1.3	7
12.6	7.8	5.6	0.9	8.4
1.5	0.2	0.6	0.2	2.4
0.4	0	0.2	0.1	0.3
0.4	0.1	0.1	0.1	0.5
2.2	0.1	1.1	0.2	0.6
-	-	-	-	-
0.5	0.3	0.4	0.1	0.8
0.2	0	0.1	0	0.5
0.3	0.1	0.1	0.1	0.5
0.7	0.5	0.6	0.2	1
1.6	0.2	0.7	0.2	2.6
0.5	0	0.2	0.1	0.4

1	0.1	0.3	0.1	0.7
0.5	0	0.3	0.1	0.4
0.8	0.3	0.4	0.1	0.7
0.3	0	0.1	0	0.3
0.4	0	0.2	0	0.3
0.3	0	0.1	0	0.4
2.3	1.2	1.9	0.4	11.8
0.3	0	0.1	0	0.3
0.2	0	0.1	0	0.4
4.1	4.6	7.5	0.6	8.4
4.6	2.8	2.9	0.5	5
1.5	2.8	6.7	0.3	12.1
1.9	3.2	7.4	0.5	14.5
2.1	2.3	4.5	0.6	10.8
1.6	3.4	8.4	0.1	10.7
0.3	1	1.8	0.1	18.1
1	1.7	6	0.1	13.2
4.5	4.4	6.7	0.9	5.7
4.5	1.7	3.2	0.3	16.6
2.8	2	4.5	0.3	14.9
6.6	1.6	4.5	0.2	21.3
6.7	6.4	4.3	1.8	5.7
4.8	0.2	0.9	0.1	1.7
4.9	5.4	5	1	4.4
10.3	6	10.1	1	6.8
4	8.2	8.9	0.7	5
5.9	15.6	16.3	0.4	4
2.1	3.9	5.1	1.1	5.6
2.7	5.2	6.5	2.3	5
5	3.3	15.8	0.4	5.8
2.9	1.6	2.4	0	2.7
11.8	5.8	14.4	0.8	8.3
18	7.2	29.2	0.6	8.6
0.2	0.3	1.7	0.3	9.1
2.6	5.3	4.2	0.7	5.5
1.5	3.1	2.3	0.3	4.4
1.5	4.4	3.6	0.2	4.7
1.8	0.1	4.5	0	1.5
2.5	0.1	5.7	0	1.8
3.8	0.1	5.5	0	1.9
1.8	0.1	0.9	0	1.2

2.3	0	4.6	0	2.3
1.5	0.1	4.3	0	1.4
2.4	0	7.8	0	2.5
2.3	0.1	21.7	0.2	0.9
3	0	4.5	0	1.9
1.9	0	10.3	0	1.6
5.7	0.8	3.3	0	3.5
2.6	0.2	2.5	0	3.4
2.2	0.6	1.3	0	1.9
10.7	0.8	4.8	0.1	3.6
9.1	0.5	4.4	0.1	3.3
9.3	0.8	3.7	0	3.3
11.1	0.9	4.1	0	3.5
7.3	1.7	2.9	0	6.1
7.9	1.9	2.5	0	7.2
2.2	1.7	2.5	0	2.3
1.2	0.4	2	0	2.3
1.3	0.7	1.9	0	2.8
1.1	0.7	1.9	0	2.6
3	0.3	3.1	0	3.8
3.2	0.3	3.2	0	4.1
4.9	1.1	2.6	0	2.3
3.9	0.3	1.5	0	2.4
3.9	0.9	3.5	0	3.2
6.6	2	4.4	0	4.3
4.8	0.6	2.2	0	4.5
6.7	0.8	3	0	5.7
1.9	0.3	10.7	0.1	1.8
1.9	0.2	15	0.1	1.3
1.8	2.3	4.1	0	6.1
1.5	2.2	4.9	0	6.7
1.7	3.1	3.8	0	7.7
0.9	0.8	8.2	0	3
2	2.7	4.1	0	6.5
1.3	2.1	2.9	0.1	7.2
2.6	3.1	5.1	0	6.9
1.7	1.6	2.8	0	4.9
1	1	3.6	0.1	4.4
1.5	0	1	0	2.2
1.9	0	1.4	0	3.9
0.8	0	0.5	0	1.7

2	0	1.2	0	1.7
0.1	0	0.1	0	0.4
1.7	0.1	0.9	0	1.4
1.7	0	0.6	0	2.4
0.7	0.1	0.2	0	0.9
2.1	0	1.2	0	3.1
2.5	0	1.6	0	3.4
0.8	0	0.4	0	1.2
0.7	0	0.3	0	1
1	0	0.5	0	1.7
0.6	0	0.4	0	1.1
0.7	0	0.4	0	1.2
0.2	0	0.2	0	0.5
0.7	0	0.4	0	1.2
1.7	0	1.3	0	2.6
2.3	0	2	0	4.6
2.6	0.1	2.1	0	4.4
1	0	0.6	0	2.1
2.1	0	2	0	4.8
1.5	0	2.3	0	1.4
0.6	0.1	0.2	0	0.7
0.9	0	0.5	0	1.3
2	0	1.4	0	3.6
5.1	6	5.7	0.9	6

Residential Coal Combustion Contribution (%)	Residential Biofuel Combustion Contribution (%)	Residential Other Combustion Contribution (%)	Commercial Combustion Contribution (%)	Other Combustion Contribution (%)
0.5	9.2	0.3	0.4	0.4
1	5.1	0.3	1.3	0.8
0.4	7.3	0.4	0.6	0.7
0.2	6.7	0.3	0.4	0.5
0.8	8.3	0.2	1	0.6
0.4	3.8	0.7	0.4	0.3
0.6	6.5	0.9	0.4	0.3
0.6	10.7	0.2	0.3	0.2
2.8	8.6	-1.2	0.8	1.3
3.1	8.9	-1.3	0.7	1.3
0.5	24	0.1	0.1	0.3
0.1	2	0.2	0.3	0.2
0.4	8.1	0.4	0.3	0.3
0.1	2.2	0.2	0.2	0.2
0.4	6.2	0.6	0.3	0.3
3.6	15.8	0.5	1.6	2.1
0.9	10.4	0.6	2.6	1.4
2.4	15	0.4	1.4	1.2
1.8	15.5	0.3	1.2	1.1
1.7	23.1	0.7	1.3	2.1
4.2	16.7	0.6	1.7	2.1
3	21.8	0.8	1.4	2.2
3.2	25.6	0.8	1.5	2.2
1.4	12.7	0.3	2.1	0.8
1.6	12.9	0.3	1.6	0.9
5.7	12.2	0.5	1.7	3
7.1	12.4	0.5	1.8	3.5
1.8	21.7	0.5	0.9	1.4
2.5	16.4	0.4	1.9	1
2.7	15.4	0.4	1.3	0.9
3.8	16.4	0.7	1.6	2.3
0.9	22	0.9	1.3	2.5

1.4	8.4	0.6	1.4	1.3
3.2	8.2	0.6	1.8	2.7
2.6	7.4	0.6	1.6	2.3
1.6	16.8	0.1	1.5	2.1
2.1	17.1	0.5	2.5	2.4
2.7	12.3	0.5	1.6	2.1
2.7	11.7	0.4	1.5	1.9
2.3	16.3	0.5	1.1	1.7
0.8	7.9	0.6	1.4	0.9
0.9	14.5	1	2.6	1.6
0.4	2.9	0.2	0.5	0.4
0.6	15.3	1.4	3	1.3
0.3	5.3	0.8	1	0.5
0.3	6.2	0.8	1.1	0.6
0.8	10.7	1	1.9	1.4
2.2	8.4	0.6	1	1.7
1.6	7.8	0.5	0.9	1.4
3.8	9.5	0.6	1.4	2.3
0	2.5	0.1	0.3	0.9
0	2.7	0.1	0.2	0.8
0	3.3	0.1	0.3	0.9
0.1	1.6	0	0.4	1.4
0.1	1.9	0	0.4	1.4
3.1	6.9	-0.6	1.6	1.5
0.6	10.5	-0.4	1	0.8
3	6.7	-1	1.4	1.4
2.1	4.9	-0.5	1.5	1.3
3	7.1	-0.9	1.4	1.3
4.1	8.5	-1.4	1.3	1.3
3.2	7.3	-1	1.2	1.3
3.8	8.4	-1.3	1.2	1.3
3.4	6.8	-0.2	1.9	1.9
3.3	6.6	-0.1	2	1.9
3.4	7.1	-0.4	1.7	1.8
3.2	6.4	0.1	2	2
3.4	7	-0.5	1.5	1.7
3.6	7.2	-0.5	1.7	1.8
3.4	7.5	-1	1	1.4
0.4	12.1	-0.2	0.3	0.3
0.3	7.5	1.4	2.3	5.7
0.8	14	0.1	0.8	4.3

0.8	22.7	0	1	5.2
0.5	14.6	2	1.6	5.6
6.1	2.2	-6.1	0.6	1.8
0.2	6.8	1.5	2.4	5.9
0.1	6	1.4	2.8	6.1
0.3	13.6	2.9	4.5	9.1
0.3	10.2	2.2	3.4	7.8
0.1	7	0.7	2.5	5.1
0.6	5.3	0.9	2.1	4
0.3	5.6	1.9	2.2	4.1
0.1	14.8	2.5	4.8	11.2
0.4	6	1.6	1.8	5.4
0.4	6.9	1.6	2.5	5.8
0.5	9.8	2.1	2.7	7.9
0	5	0.7	1.9	5.2
0.1	5.7	0.2	2	4.8
0.2	5.2	2	2.6	5.8
0	7.6	0.3	0.6	2.2
0	5	0.4	0.5	2.9
0	5.6	0.6	0.7	4.6
0	3.5	0.2	0.4	2.1
0	11.4	0.2	0.7	1.1
0	15	0.2	0.9	1.5
0	5.8	0.4	0.5	3.6
1	9.9	1	2	2.3
0.5	8	1.1	1.8	2.3
1.8	15	1.1	2	2.5
2.5	18.6	0.9	1.7	2.8
0.9	7.2	1.1	2.1	2.1
0.9	6.8	0.9	2.1	2.2
0.9	2.4	0.4	1.3	0.7
1.3	9.4	0.5	1.5	2.5
1.4	14.1	0.1	1.7	3.7
0.7	12.5	1.4	2.5	2.6
0.6	20.5	1.7	3.3	3.2
0.7	8.6	1.2	2.1	2.7
1.2	8.1	1	2.8	1.4
1.8	8.2	0.8	2.6	1.4
1.4	7.7	1	2.6	1.3
1.1	4.8	0.6	1.7	1.4
1.1	8	0.6	1	0.9

1.2	9.3	0.6	1.1	0.9
1.7	1.1	-1.4	0.2	2.4
2.9	1.9	0.2	1.2	1.3
0.4	1.7	0.2	0.5	0.3
0.4	1.7	0.2	0.6	0.3
0.5	16.7	1.4	1.3	3
0.6	9.7	0.7	0.7	1.3
0.3	23	2	2	4.7
0.8	6.7	1.3	2.2	1.9
0.3	5.3	0.7	0.6	0.8
1.1	6.2	0.8	2.1	2.4
1.2	5.4	0.7	1.9	2.1
1.4	10	-0.6	1.3	2.3
0.3	6.7	0.2	0.7	1.5
0.4	8	1	1.6	2.7
0.5	14.3	1.6	2.6	4.2
0.4	6.1	1.4	1.9	5.1
1.5	10.2	0	1.5	2.6
0.6	11.8	2.2	5.2	2.5
0.5	10.6	2.1	4.7	2.5
2.4	5.6	0.7	1.9	2.8
2.9	5.7	0.7	2	2.8
2.5	7.5	0.9	2.3	3.2
2.8	5.2	0.5	1.9	2.6
0.4	14.6	1.3	1.6	2.7
0.8	13.6	1.1	1.1	2.4
0	6.4	0.1	0.5	0.5
0	2.1	0.1	0.1	1.1
0	1.9	0.1	0	1.2
0	4.1	0.2	1.2	0.2
0	3.9	0.2	1.3	0.2
0	8.5	0	0.4	0.4
0.5	15.1	-0.4	0.4	0.6
1.9	14.5	-1.6	0.3	0.2
0.6	4.8	-0.4	0.8	2.5
0	0.9	0	0.1	0.1
0.5	6.6	-0.3	0.5	0.7
0.1	4	0	0.6	3
0.4	5.1	-0.2	0.5	1.5
0.5	7.4	-0.5	0.3	1
1.8	15.6	-1.7	0.2	0.1

0.8	13	-0.7	0.2	0.4
0	1	0	0.1	0.1
0	1.7	0	0.1	0.2
0.5	34	-0.4	0.4	0.3
0.6	14.4	-0.7	1.6	0.3
1.8	10.8	-1.6	0.1	0.2
0	0.9	0	0.1	0.1
0	0.9	0	0.1	0.1
0	1.5	0	0.1	0.2
0	1.1	0	0.1	0.1
1.9	11.9	-1.6	0.1	0.2
1.8	13.9	-1.6	0.2	0.2
0.1	15.4	0.1	0.4	1.2
0.3	11	0.1	0.1	0.7
0.4	13.6	0.1	0	0.9
0.1	4	0.1	0.2	0.2
0	4.7	0	0.6	0.3
0	29.2	0	0.9	0.1
0	30.3	0	0.9	0.1
0.1	46.1	0	1.2	0.2
0.1	54.2	0	1.4	0.1
0.2	23	-0.2	1.2	0.2
0	14.6	0.2	0.3	2
0	12.7	0.3	0	1.9
0	18.1	0.2	0.1	2
0	25.3	0.2	0.2	2.4
0.1	7.1	0.4	1.4	3.2
0.1	12.5	1.3	2.8	8.6
0	11.5	0	0.6	0.3
0	12.1	0	0.6	0.3
0	3.8	0	0.2	0.1
0	1.8	0.1	0.2	0.1
0	1.5	0.1	0.2	0
0	2	0.1	0.2	0.1
0	4.4	0.1	0.1	2.6
0	4.2	0.1	0.1	2.6
0	5	0.1	0.1	3.2
0	4.9	0.1	0.1	3.3
0	4	0.1	0.1	2.6
0	3.8	0.1	0.1	2.5
0	1.4	0	0	0.8

0	3.4	0.1	0.1	2.1
0	4.7	0.1	0.1	3.2
0	4.7	0.1	0.1	3.2
0	8.3	0.1	0.2	2.1
0.3	2.6	0.3	0.5	0.4
0	7.3	0.2	0.2	0.1
-0.1	8.7	0.2	0.1	0.1
0.1	2.5	0.4	0.4	0.5
0.2	3.1	0.4	0.5	0.5
0.2	3.2	0.5	0.4	0.6
0.1	0.4	0.1	0.1	0.1
0.2	3.5	0.3	0.3	0.5
0.2	4	0.3	0.3	0.5
0.3	3.4	0.3	0.4	0.5
0.1	1	0.4	0.4	0.6
0.1	1.1	0.7	0.6	0.9
0.1	0.5	0.2	0.2	0.3
0.1	1.3	0.9	0.6	0.8
0.1	0.9	0.6	0.5	0.7
0.2	0.7	0.3	0.3	0.3
0.2	0.7	0.2	0.3	0.2
0.3	1.5	0.2	0.5	0.3
0.1	0.4	0.1	0.2	0.1
0.5	1.8	0.2	0.6	0.4
0.2	1.6	0.7	0.2	0.2
0	2.6	0.1	1.4	0.5
0	1.9	0.1	1.1	0.3
0.3	1.7	0.2	0.5	0.3
0.1	1.4	0.1	0.1	0.1
0.1	0.4	0.1	0.1	0.1
0.1	0.9	0.1	0.1	0.1
0.1	0.6	0.1	0.1	0.1
0.1	2.3	0.1	0.5	0.1
0.1	1.8	0.1	0.6	0.1
0.7	1.7	0.4	0.9	0.6
0.2	5.3	1	0.5	1
0.2	5.4	1.1	0.5	1.1
1.8	4.1	0.5	2.1	1.2
2.5	7.4	0.9	2.5	1.6
1.6	2.6	0.5	1.9	1
1.8	2.9	0.4	2.2	1.2

0	0.7	0.1	0.1	0.1
0.1	2	0.1	0.2	0.1
0.1	1.8	0.1	0.2	0.1
1.2	23.4	1.7	1.8	2.9
0.9	25.9	1.4	0.9	3.4
1.1	23.2	1.5	1	3.5
0.7	27.5	1.3	0.7	3.4
1.2	27.4	1.8	1.2	4
1.3	30.1	1.4	1.3	2.6
1.4	22.5	1.8	2	3.1
1.4	22.3	1.8	2.2	2.9
1.4	21.6	1.5	1.9	2.2
1.6	24.5	2.2	2.3	3.8
1.5	22.7	1.7	1.8	3
1.2	18.9	1.5	2	2.3
1.3	19.4	1.6	2.2	2.4
1.5	18.8	1.7	2.4	2.5
1.5	18.6	1.8	2.5	2.7
1.8	21.3	1.3	2.2	1.9
1.6	18.4	1.7	2.6	2.6
1.4	18.9	1.8	2.4	2.8
1.7	22.2	1.5	2.6	1.9
1.3	19.2	1.7	2.1	2.5
1.4	18.2	1.8	2.3	2.8
0.9	15.1	1.5	1.5	2.5
1.4	24.4	2.1	2	3.8
1.4	18.1	1.7	2.2	2.6
1	36.6	1.4	1.6	2.7
0.7	37.6	1.2	1.4	2.2
0.2	26.9	0.9	1	0.9
0.1	27.4	0.5	0.6	0.5
0.3	33.9	1.2	1.2	1.2
0.8	27.3	1.7	1.7	2
5.3	12.6	-0.1	1.8	1.3
5.3	12.7	0	1.8	1.3
6.7	14.7	0.4	2.5	1.5
4.9	11.4	-0.2	1.7	1.4
5.3	10	-2.1	1.5	1
4.2	10.8	-0.3	1.3	0.8
5.4	13.6	0.3	1.8	1.2
4.8	12.1	-0.2	1.4	0.9

6.4	14.7	0.1	2.2	1.3
5.2	12.4	-0.1	1.6	1.3
4.7	11.1	-0.2	1.5	1.3
5.4	12.9	0	1.9	1.5
5.5	13.1	0.2	1.9	1.4
5.3	13.1	0.4	1.8	1.1
6.7	15.3	-0.1	2.2	1.2
5.2	13	0	1.7	1.1
7.1	15.7	0.6	2.8	1.8
3.5	8.8	0.2	1.2	0.9
4.7	11.5	-0.2	1.5	1
6.5	13.4	0.4	2.6	1.8
5.2	12.6	-0.1	1.8	1.3
8	17	0.5	3.1	2
7.1	16.3	0.3	2.6	1.6
6	14.2	0.3	2.1	1.3
6.8	14.9	0.4	2.5	1.6
5.8	13.9	0.2	2	1.3
7.2	16.4	0	2.5	1.4
7.8	16.7	0.5	2.9	1.9
5.6	14	0.3	1.9	1
5.2	12.8	0	1.8	1.3
5.6	13.4	0.4	2.1	1.5
5.7	14.2	0.4	2.1	1.4
5.7	13.5	-0.9	1.4	0.7
4.9	12.3	-0.2	1.4	0.9
6.7	13.9	0.5	2.8	1.9
6.8	15.6	0.4	2.4	1.5
3.9	8.6	-1.3	1.1	1.5
4.4	8.4	-1.6	1.4	0.9
1	7.7	-0.9	0	0.2
0	0.4	0	0	0
0.1	0.6	0	0	0
0	2	0	0	0.1
-	-	-	-	-
0.3	1.6	0	0.1	0.1
0	0.5	0	0	0
0.1	0.5	0	0	0.1
0.5	1.9	0	0.2	0.1
1.1	8.6	-1	0	0.2
0	0.6	0	0	0

0	1.5	0	0	0
0	0.3	0	0	0
0	0.7	0	0	0.1
0	0.2	0	0	0
0	0.2	0	0	0
0	0.4	0	0	0
2.5	17.4	-1.9	0.5	0.5
0	0.2	0	0	0
0	0.3	0	0	0
1.9	25	0.1	1.3	1.2
3.2	24.7	0	1.1	1.1
0.3	32.7	0.1	0.4	0.5
0.5	39	0.6	0.8	0.9
0.4	31.3	0	0.5	0.5
0	35.7	0.2	0.3	0.5
0.8	39.7	-0.5	0.4	0.6
0.3	44.9	0.2	0.4	0.6
3.8	15.8	0.3	1.6	1.6
0.6	13.4	0.2	0.7	0.9
0.4	11.3	0.4	0.9	1.2
0.2	11.9	0.1	0.6	0.9
1.4	16.5	1.9	2.6	2.2
0.1	0.7	0.1	0.1	0.1
2	28.1	0.5	1.6	1.9
2.2	14	0.9	1.5	1.6
1	15.5	-0.4	2.8	0.4
0.7	16.8	-0.2	3.1	0.4
1	16.7	-0.5	3.1	0.3
0.8	15.3	-0.3	2.4	0.4
0.9	19.5	0.4	1.2	0.6
0.6	9.2	0.2	0.5	0.2
2.5	11.8	0.4	1.3	1.5
1.2	7.3	0.3	0.7	1.1
0	8.9	0	0.1	0.1
6.6	30.2	0.2	2.3	3
6.7	37	0.2	2.3	3.5
7.7	41.4	0.1	2.6	4
0.1	9.6	0.2	0.3	0.3
0.2	4.9	0.1	0.3	0.2
0.1	4.9	0.1	0.3	0.1
0	3.6	0.1	0.2	0.1

0	7.6	0.2	0.7	0.1
0	11.5	0.2	0.3	0.4
0	10.6	0.3	1.3	0.2
0.1	8	0	0.2	0.2
0	8	0.3	1	0.1
0	5.8	0.2	0.4	0.1
0.2	19.3	1	0.6	0.8
0	29.5	0.6	0.8	2
0.3	7.2	0.2	0.4	0.5
0.1	3.9	0.2	0.3	0.2
0.1	4	0.2	0.4	0.1
0.1	21.3	0.6	0.6	0.2
0.1	28.1	0.8	0.6	0.2
0.1	23	3.6	0.3	0.7
0.1	27.2	5	0.2	0.6
0.3	7.8	0.7	0.9	1.2
0.3	9.7	0.1	1.1	0.9
1.1	7.9	0.2	1.2	0.7
1.1	6.7	0.2	1.1	0.6
0	34.2	0.8	1	2.3
0	36.1	0.9	1.1	2.5
0.2	5.5	0.2	0.3	0.3
0.1	7.6	0.2	0.3	0.2
0.2	19.1	0.9	0.3	1.8
0.2	20.6	2.1	0.2	1.8
0.1	28.3	1.5	0.7	1.3
0.1	34.2	2.1	0.8	1.6
0.3	9.5	0.1	0.4	0.5
0.2	8.3	0	0.3	0.3
5.4	9.6	0.6	2.3	1.2
4.1	8.5	0.4	1.7	1
6.4	9.6	0.6	2.7	1.1
0.9	5.1	0.1	0.5	0.7
6.5	8.8	0.7	2.7	1
5.2	5.5	0.4	2.1	0.8
7	9.6	0.9	2.9	1.1
4.1	8	0.5	1.9	0.7
1.1	13.9	0.5	0.8	1.9
0	7.5	0.3	0.7	0.1
0	8.9	0.5	0.9	0
0	3.7	0.1	0.3	0.1

0	8.1	0.4	1.4	0.1
0	0.3	0	0	0
0	2.3	0.1	0.3	0.1
0	6.2	0.3	0.7	0.1
0	1.4	0.1	0.1	0.1
0	6.3	0.3	0.6	0.1
0	6.8	0.4	0.6	0.1
0	3.5	0.1	0.2	0.2
0	2.2	0.1	0.1	0.1
0	5	0.2	0.4	0.2
0	2.3	0.1	0.2	0.1
0	2.5	0.1	0.2	0.1
0	0.6	0	0.1	0
0	3	0.1	0.2	0
0	10.4	0.5	0.9	0
0	12.7	0.7	1.2	0
0	12.5	0.7	1.2	0
0	5.5	0.2	0.6	0
0	12.6	0.6	1.2	0
0.1	5.1	0.1	0.3	0.1
0	1	0.1	0.1	0.1
0	4.4	0.2	0.3	0.2
0	8	0.5	0.8	0
2	16.4	0.8	1.5	1.8

Solvent Contribution (%)	Waste Contribution (%)	International Shipping Contribution (%)	Agricultural Waste Burning Contribution (%)	Other Open Fire Contribution (%)	AFCID Dust Contribution (%)
0	6.1	0.2	0.4	1.8	4
-0.2	2.2	0.3	0.7	1.1	6.3
-0.1	2.4	0.2	0.6	1	5
-0.1	2.3	0.1	0.4	0.9	4.2
-0.1	2.8	0.4	1.4	2.2	6.6
0	4.3	0.3	1	3.8	5.7
0.1	6.4	0.4	0.3	1.5	5.3
-0.1	7.8	0.1	0.2	1.4	2.9
0.2	3	0.4	0.8	10.4	6.2
0.2	3.4	0.4	0.7	8.2	6.4
-0.1	7.1	0.2	0	0.5	2.5
-0.1	2.1	0.1	0.2	0.9	2.3
0	8.5	0.3	0.2	1	3.4
-0.1	4.6	0.1	0.2	1	2.6
0.2	11.2	0.4	0.3	1.1	4.2
-0.1	1.5	1.1	1	0.8	6.9
-0.2	2.8	1.5	2	2.1	7.1
-0.2	2.4	0.9	1.3	1.7	4.9
-0.2	2	0.6	3	1.2	8
-0.3	1	1.4	1	1.3	5.3
-0.1	0.5	1.2	0.2	0.5	5.4
-0.2	0.9	0.8	0.5	0.6	6.8
-0.1	0.8	0.8	0.4	0.5	6.3
-0.2	2.7	0.7	1.9	1.6	8.6
-0.2	3.6	0.9	2.7	3.8	6.5
-0.1	0.9	1.5	0.2	0.4	7
0	1	1.3	0.2	0.4	7.4
-0.2	1.8	0.6	2	0.7	8.1
-0.1	3.9	0.5	2	1.1	6.2
-0.1	3.7	0.4	2.4	0.6	5.1
-0.2	0.8	0.8	0.4	0.7	7.6
-0.3	0.5	1.5	0.4	1.4	5.2

-0.2	3.2	0.6	2.3	3.2	14.6
-0.3	1.5	1	0.7	0.7	9.9
-0.4	1.9	0.8	1.4	1.1	11.5
-0.2	1.1	1.7	0.2	0.7	11.3
-0.3	1.7	1.7	0.3	0.6	8.1
-0.3	1.4	1.6	0.4	0.5	7.5
-0.2	1.4	1.3	0.4	0.4	6.9
-0.4	2.8	0.7	2.7	0.8	11.8
-0.1	3.6	0.4	2.1	4.5	15.9
0	4.2	0.7	0.2	0.6	15.5
-0.1	1.5	0.1	1.5	3.2	7.2
0.1	4	0.4	0.4	0.4	18.8
-0.1	5	0.1	1.5	5.8	19.3
-0.1	3.5	0.1	0.9	4.7	17.4
-0.2	4.2	0.9	1	0.9	17.5
-0.3	2.8	0.7	3.3	0.8	13.5
-0.3	3	1	4.9	0.8	13
-0.4	2.2	0.8	1.1	0.6	12.6
0	0.4	3.2	1.1	10.8	2.6
0	0.4	3	1.3	12.1	2.9
0	0.7	1.7	0.5	9.1	2.4
-0.1	0.3	4.2	0.2	2.9	1
-0.1	0.4	4.2	0.1	1.9	0.8
0.2	4.2	1.6	0.9	1.9	9.5
0.4	3.4	2.7	0.6	4	11.9
0.4	3.7	2.1	1.1	2.4	9.5
0.8	2.7	2.4	1.1	2.1	11.7
0.3	4.5	1.9	1.1	2.3	7.8
-0.1	5.3	2.5	0.7	1.4	8.5
0	4.3	1.5	1.2	2.4	7.8
-0.1	5.2	1.7	0.8	1.8	8.6
0.1	4.7	1	0.6	1.2	9.6
0.1	4.8	0.8	0.6	1.1	11
0	4.9	1.4	0.7	1.3	7
0.2	4.2	1	0.6	1.1	9.2
-0.1	4.3	1.4	0.6	1.1	7.3
-0.1	4.4	1.2	0.7	1.4	7.4
0	6.8	0.5	0.6	1	10.9
0.1	5.9	3.1	0.1	2.6	7.1
0.1	2.9	1.5	1.2	12.2	2.7
0.1	1.3	2.3	0.4	18.5	3.1

0.1	1.3	3.4	0.3	7.2	2.6
0.1	2.2	1.5	0.2	19	4.1
-0.2	1	9.4	0.7	19.6	2.7
0.1	3.1	1.4	1.3	11.6	2.7
0	3.7	1.1	0.6	6	2.1
0.4	3.4	1.3	0.2	4.8	2.9
0.4	3.8	1.3	0.2	5.2	3.9
-0.1	3.2	2.6	1.2	5.3	1.3
0	2.2	0.6	0.6	13.9	3.5
0	3.3	1.2	0.5	24.2	2
0.4	4.8	0.7	1.2	8.7	4.6
0.1	2.7	3.4	0.3	9.7	2.6
0.2	2.5	1.9	0.6	7.8	2.5
0.1	3.8	1.1	0.2	8.9	4.4
-0.2	3.2	2.3	1.4	12.6	2.6
-0.1	3	1.1	0.9	6	3.3
0.2	3.5	1.2	3.3	25.9	2.8
0	2.6	0.7	1.3	19.4	4.5
0	2.8	0.8	0.9	12.9	4.5
0	3.3	1.7	0.4	6	5.4
0	2.9	0.2	1.1	16.8	4.3
0	2.5	0.5	2.1	30	4.3
-0.1	3	0.4	2	27.5	5.4
-0.1	2.2	1.9	0.4	7	5.6
-0.1	0.9	4.5	0.4	1.5	5.1
-0.5	0.8	3.8	0.9	4.3	6.2
-0.3	0.5	1.3	0.2	0.6	5.6
-0.1	0.5	1.1	0.3	0.5	5.6
0.3	0.4	5	0.1	0.6	5
0.4	0.4	4.9	0.1	0.6	5
-0.2	1.6	1.4	0.5	0.3	6.6
0	0.5	8.5	0.1	0.6	4.4
-0.2	0.9	1.8	0.1	0.9	12.1
-0.1	0.7	5.1	0.5	1.5	5.5
0.1	0.7	3.6	0.1	0.6	5.2
-0.2	0.6	6.8	0.1	0.9	5.1
0	0.3	3.7	0.1	0.6	4.6
0	0.4	4.4	0.1	0.5	4.4
0	0.3	2.8	0.1	0.5	4.6
0.3	0.3	11.6	0.1	0.6	3.2
-0.2	1.2	1.6	1.7	1.4	6.4

-0.2	1.4	1	2	4.1	8.8
0	0.2	7.7	0.1	2.2	2.4
-0.1	0.3	16.5	0.1	1	2.1
-0.2	3.8	1.2	0.3	0.1	5.2
-0.2	3.9	1.2	0.3	0.1	5.3
-0.3	1	2.9	0.9	1.6	4.8
-0.4	1.2	4	1.2	1.6	5.7
-0.1	0.8	1.8	0.5	2.1	4.1
0.1	0.4	3.2	0.1	0.6	5.9
-0.3	1	6.4	1.2	1.3	4.6
0.3	0.4	5.4	0.1	0.6	4.9
0.3	0.3	6.1	0.1	0.6	4.5
-0.1	0.6	5.3	0.2	1.4	10.6
0	0.7	12.6	0.7	15.9	5.6
-0.2	0.9	6.4	0.5	3.7	5
0.1	0.7	3.5	0.3	2.8	4.4
0.1	2.6	2.6	0.4	9.5	2.7
-0.2	0.8	4.4	0.1	1.1	9.2
-0.4	0.7	1.8	0.2	0.9	5.8
-0.4	0.7	2.1	0.2	0.8	5.5
0	1.5	6.1	0.1	0.7	4.3
0.1	1.6	4.8	0.1	0.7	4.1
0.1	2	4.9	0.1	0.7	5
0	1.4	5.9	0.1	0.7	4.4
-0.2	1	9.2	0.5	1.8	4.3
-0.4	1	3.9	0.7	1	5.2
-0.1	3.7	1	0.3	14.2	2.9
0	1.2	0	0.5	37.1	3
0	1	0	0.5	41.2	3
0	4.8	1.9	0.5	7.4	3.7
0	4.8	1.6	0.4	6.5	4.1
-0.1	4.1	0.9	0.2	9.4	2.6
-0.1	5.4	4.9	1	2.6	1.7
0	2.6	2.4	0	3.4	1.3
-0.1	2.4	12.2	0.9	4.1	1.5
0	0.4	1.5	0.2	1.6	0.5
0	2.8	5.6	1.6	16.9	2
0	1.4	8.9	-0.5	4.6	1.5
-0.2	3.5	7.1	3	3.7	2.5
-0.1	3.9	7.4	1.2	2.4	2.1
0	2.8	1.9	0.3	2.7	1.2

-0.1	7.3	4.6	0	1.9	1.6
0	0.4	1.8	0.2	1.8	0.5
0	1.1	1	0.6	4.3	0.8
0	8.1	3.5	0.2	1.3	1.3
-0.1	4.5	6.3	0.3	1.8	1.5
0	3.3	4.3	-0.3	3.4	1.2
0	0.5	1.5	0.2	1.4	0.5
0	0.5	1.6	0.2	1.5	0.5
0	0.5	0.8	0.4	4.9	0.6
0	1.4	1.7	0.4	3.4	0.6
0	2.6	3.8	-0.2	3.5	1.3
0	2.9	2.7	0	3.4	1.3
-0.1	4.8	1.4	1.1	7.4	3.6
0	3.6	1	0.3	6.4	4.2
0	4	0.2	0.2	6.8	4.8
0	3	2.4	0.4	3.8	2.4
0	3.8	4.1	0.7	2.1	2
0	6	1	0.6	3.9	2.1
0	6.1	1	0.6	3.7	2.1
0	6.8	0.9	0.8	6.4	1.9
0	6.7	0.5	0.3	3.1	1.3
0	5.3	2.8	1.1	6.3	2.1
-0.2	5.3	1.3	1.7	9.1	4.3
-0.1	4.3	1.6	3	13	3.5
-0.3	4.7	0.3	1.4	11.7	3.5
-0.3	7.3	0.4	0.9	3.2	4
-0.1	3.9	2.9	1.6	7	4.3
0.3	7	2	0.8	9.6	4.3
0	3.2	2.6	0.5	3.1	1.5
0	3.3	2.5	0.5	3.1	1.5
0	2.3	6.2	0.3	1.9	1.3
0	3.2	1.7	0.6	5.9	2.2
0	3.4	1.9	0.5	5.3	2.3
0	3.5	2	0.8	5.2	2.6
0	2.6	2	0.6	11.4	7.7
0	2.6	2	0.6	10.7	7.7
-0.1	3	1.4	0.4	3.4	8.9
-0.1	3	1.8	0.5	5.6	9.1
-0.1	2.6	2.2	0.4	5.5	7.9
0	2.8	1	0.1	6.6	7.9
0	0.7	0.5	0.6	57.4	3.4

0	1.8	6.7	0.2	7.1	7.6
0	2.6	5.4	0.2	6.7	10.7
-0.1	3.4	0.6	2.1	9.7	8.8
0	1.6	0.2	0.9	30.3	5.5
-0.1	3.4	1.3	0.3	0.5	6.4
-0.2	3.9	0.1	0	0.5	5.1
-0.2	5.7	0.1	0	0.4	7.3
-0.2	4.7	5.5	0.5	2.4	13.1
-0.2	4.9	7.1	0.5	2.4	14.8
-0.2	3.8	3.7	0.4	1.6	17.4
-0.1	1.1	0.1	0	0	1.3
-0.2	5.8	1.9	0.3	0.1	11.8
-0.2	6.5	2	0.3	0.1	14
-0.2	4.8	2.4	0.3	0.1	10.5
0	2.6	0.3	0.2	0.5	3.8
0.1	3.6	0.3	0.2	0.7	5.5
-0.1	2.6	0.2	0.1	0.2	2.7
0	2.1	0.2	0.3	0.8	4.4
0	2.9	0.3	0.2	0.5	4.2
-0.1	3.8	0.3	0.2	0.2	4.3
-0.1	4.2	0.3	0.1	0.1	4.6
-0.2	3.4	0.9	0.2	0.1	4.6
-0.1	2.2	0.2	0.1	0.1	1.6
-0.1	3.9	0.9	0.3	0.1	4.9
-0.1	0.6	0.9	0.3	0.5	1.9
-0.1	2	3.3	0.1	0.6	3.3
-0.1	1.5	1.1	0.1	0.4	2.2
-0.2	3.9	1.2	0.3	0.1	5.6
-0.1	0.7	0.9	0	0.1	1.3
-0.1	1	0.1	0	0	1.3
-0.1	1.3	0.5	0.1	0.1	1.6
-0.1	1.1	0.2	0.1	0.1	1.2
0	1.1	0.4	0.2	1.3	2.1
0	1.1	0.3	0.1	0.3	2.2
-0.2	4.5	0.8	0.5	0.2	6.9
-0.2	2.8	4.9	0.4	1.1	16.4
-0.2	3.3	4.4	0.4	1	24.5
-0.1	2.6	1.1	0.9	0.5	7.9
-0.1	3.9	1.5	1.4	0.6	7.7
-0.2	2.2	0.5	0.4	0.3	6.9
-0.2	2	0.6	0.5	0.4	9.4

-0.1	0.8	0.5	0	0.1	1.4
-0.1	2.2	1.1	0.1	0.2	2.1
-0.1	2.3	0.9	0.1	0.2	2
0.4	4.4	0.6	0.9	0.9	10.9
-0.2	6.1	0.1	0.2	0.6	9
-0.2	4.6	0	0.1	0.1	12.1
-0.3	6	0.1	0.1	0.2	9.2
-0.4	5.2	-0.1	0.1	0.3	8.9
-0.2	3.8	0	0.2	3.5	10.6
0.4	4.2	0.7	1	1	11.5
0.6	4.9	0.9	1.1	0.8	10.8
0.3	4.9	0.7	0.5	0.4	14.7
0.5	4	0.7	1	0.7	9.9
0.1	2.9	0.1	0.2	0.3	11.8
0.6	4.8	1.1	0.8	0.7	10.2
0.6	5	1.4	0.9	0.9	11.4
0.9	4.4	1.1	1.1	1.2	16.9
0.9	4.9	1.5	1.2	1.3	12.7
0.4	5.3	1.2	0.6	1.4	17.1
1.2	4.7	1.5	1.4	1.6	14.5
0.8	5.3	1.2	1.1	1	11.3
0.8	4.8	2.5	0.9	1.5	13.3
0.6	5.4	1	0.9	0.8	12.4
0.9	4.9	1.1	1.2	1.1	11.7
0.5	3.5	0.6	0.7	0.6	14.6
0.4	4.1	0.6	1.3	1.7	9.8
0.8	4.3	1	1.1	1.3	15.7
0.2	3.1	0.4	0.8	2.7	7.6
0.3	2.4	0.5	0.8	3.5	11.1
0.4	5.3	0.7	0.9	0.7	8.6
0.2	4.3	1	0.4	0.4	9.4
0.6	4.2	0.7	1.5	0.8	5.1
0.5	5.1	0.8	1	1	7
0.2	8.8	0.4	0.5	0.9	12.7
0.2	8.9	0.3	0.5	0.9	12.8
0.4	8.3	0.2	0.5	0.5	11.5
0.3	7.7	0.6	0.6	0.8	14.8
-0.3	4.8	3.5	0.4	1.3	13.3
0.2	7.2	0.8	0.4	0.5	18.7
0.4	11.9	0.2	0.4	0.5	11.4
0.2	10.1	0.3	0.6	1.1	19.7

0.6	8.1	0.7	0.4	1.2	22.2
0.6	6	0.1	0.3	0.6	11.4
0.5	6.7	0.3	0.5	0.7	16.2
0.7	7	0.4	0.6	0.8	14.1
0.5	8.1	0.3	0.5	0.6	13.4
0.6	8	0.2	0.3	0.4	18.5
0	7.9	1.3	0.2	0.9	21.7
0.2	13.4	0.2	0.6	0.6	12.9
0.5	10.1	0.4	0.8	0.8	10.6
0.1	7.1	0.1	0.3	0.5	16
0.4	8.1	0.4	0.6	0.6	24.2
0	10.8	0.4	0.5	1.5	11.2
0.4	10.3	0.6	0.8	0.7	12.8
0	11.2	0.4	0.6	0.8	8.4
0.1	10.3	1.1	0.6	1.8	13.9
0.6	10.7	0.8	0.4	1.2	15.9
0.2	9.8	0.2	0.5	0.6	10.4
-0.1	12.8	0.2	0.4	0.9	14.1
0.2	8	1.1	0.3	1.1	22.2
-0.2	10.4	0.3	0.6	0.6	7.7
0.1	9.2	0	0.1	0.3	9.2
0.4	11	0.5	0.6	0.7	11.2
0.6	8	0.4	0.6	0.7	11.3
0.2	14	0.3	0.6	0.7	10.8
-0.3	12.1	1.5	0.2	0.6	17.3
0.2	11.3	0.3	0.8	2	16.8
0	10.2	0.5	0.6	1.1	10.9
-0.1	12	0.5	0.5	1.8	12.1
0	6.5	0.5	0.7	1.3	10.4
-0.3	4	4.1	0.3	1.2	13.2
0	5.8	2.8	1.5	14.7	0.6
0	0.4	2.4	0	0.4	0.1
0.1	0.2	1.3	0	0.5	0.4
0	2	2	0	1.2	0.1
-	-	-	-	-	-
0.1	0.3	7	0	0.6	1.9
0	0.1	2	0	0.9	0.4
0.1	0.1	1	0	0.5	0.5
0.1	0.4	6.1	0.1	0.7	2.5
0	6.4	2.8	1.6	16.5	0.7
0	0.7	2.3	0	0.4	0.1

0.1	0.5	3.1	0.1	0.9	0.1
0	0.1	2.4	0	1	0.1
0	0.6	2.7	0.1	1.9	0.1
0	0.1	2.7	0	0.7	0.1
0	0.1	2.7	0	0.8	0.1
0.1	0.1	1	0	0.5	0.2
0.2	1.9	3.6	0.4	3.6	6.4
0	0.1	2	0	0.4	0.1
0	0.1	1.1	0	0.4	0.2
0.1	5.3	1.2	0.7	4.9	8.9
0.1	5.4	0.9	1.3	22.2	10
0	3.2	1	0.2	4	4.7
0	3.9	4.8	0.4	1.9	6.1
0	3.1	1.1	0.4	13.3	5.1
-0.2	3	0.4	0.1	1.9	4.8
0	4.3	0.8	0.4	4.1	4.5
-0.1	5.5	3.5	0.1	1.5	5.6
0.5	5.8	0.7	1	13.4	13.1
0.1	5.8	2.6	0.5	4	16.8
0.2	6.7	1.6	0.6	3.1	20.7
0	6.1	1.6	0.5	3.9	19.4
1.5	3.4	3.1	1.8	2.6	12.1
0	1.7	5	0	1.7	1.6
0.6	4	0.8	1.2	9.1	9.2
0.7	4.4	1.1	1.6	8.2	11
-0.1	5.5	2.2	0.4	1.4	13.6
-0.2	4.1	1.6	0.4	1	10.2
-0.1	7.5	2.1	0.2	1.1	14.7
-0.1	6.9	2.2	0.1	1	12.3
0.2	18.3	2.4	0.4	1.1	7
0	1.5	2.9	0.1	1	7.2
0.4	6	0.9	1.6	5.9	11.3
0.3	4.1	0.5	1.5	2.5	7.5
0	1.3	1.4	0.2	21.1	2.2
0.2	8.1	1	1	3.2	10.2
0.1	8.7	1.3	3.7	3.1	10.5
0	7.5	1	0.8	2.3	7.6
0	1.1	0.1	1.8	55	2.5
0	0.9	0.2	1.1	67.6	1.7
0	0.9	0.4	0.9	64.2	2
0	0.7	0.1	1	41.8	1.5

0	0.8	0.2	2.4	49.5	2.3
0	1.2	0.1	2	53.9	2.7
0	1	0.1	3	53.2	2.7
0	2.1	0.1	0.4	54	1
0	0.9	0.4	1.2	22.1	3.2
0	0.5	0.3	1.6	37.5	3.1
0	2	0.6	0.7	19.3	4.6
0	3	0	1.1	32.8	5.6
0	2.1	3.3	0.4	18	2.8
-0.1	1.7	1.5	0.1	0.3	2.3
-0.1	1.6	1	0.1	0.5	2.4
0	1.9	0.6	0.3	5	4.2
0	2.2	0.6	0.2	2.1	4.9
0	2.1	0.5	0.3	6	7
0	2.4	0.3	0.2	5.3	8.2
0	3.4	1.4	0.5	31.2	3.8
0	1.9	0.4	0.5	57.6	3
0	1.6	1.5	0.5	43.9	3.1
0	1.2	2	0.4	40.8	2.7
0	3.9	0	1.2	22.8	6.9
0	4.2	0.1	1.2	20.2	7.2
0	1.1	1.3	0.1	0.9	3.4
0	1	0.3	1.5	27.4	2.6
0	1.6	0.5	0.8	27	5.2
0	1.6	0.5	0.4	9.3	6.8
0	2.1	0.1	1.6	20.6	5.5
0	2.1	0.1	1.1	11.9	5.9
0	1.5	0.2	0.6	55.2	2.4
0	1.8	0.1	0.5	56.3	1.5
-0.1	3.4	0.8	0.6	14.7	7
-0.1	2.7	0.3	0.3	17.4	5.8
-0.1	3.8	0.5	0.6	11.4	5.6
0	0.9	0.3	0.4	42.5	2.7
-0.1	3.9	0.9	0.7	8.6	7.5
-0.1	2.4	3.2	0.3	9.6	5.3
-0.1	4.1	0.2	0.6	6.2	8.6
-0.1	3.9	1	0.9	10	4.1
0	1.7	0.5	0.4	37.9	6.1
0	0.9	0.2	1	5.9	1.7
0	0.9	0.2	1.3	6.5	1.9
0	0.5	0.1	0.5	2.3	0.9

0	1.1	0.2	1.2	16	2.4
0	0.1	0.7	0	0.3	0.2
0	0.6	0.1	0.5	6.7	1.1
0	0.7	0.4	1.1	9.8	1.7
0	0.4	0.5	0.6	2.6	0.5
0	0.7	0.3	1.7	9.7	2.2
0	0.7	0.5	2	9.8	2.6
0	0.5	0.3	0.6	11.2	0.7
0	0.4	0.4	0.6	5.4	0.5
0	0.7	0.8	0.9	12	1.1
0	0.4	0.1	0.4	2.3	0.6
0	0.4	0.1	0.5	3	0.7
0	0.1	0.2	0.1	0.6	0.2
0	0.4	0.1	0.2	0.6	0.7
0	1.1	0.1	1.2	4.8	2.2
0	1.4	0.2	1.6	7.5	2.6
0	1.2	0.3	1.7	8.1	2.5
0	0.7	0.1	0.7	1.7	1.4
0	1.4	0.2	1.6	7	2.7
0	0.5	0.7	1.1	35.5	2
0	0.3	0.4	0.5	1.7	0.4
0	0.6	0.6	0.8	12.2	0.9
0	0.8	0.2	1.7	8.1	1.9
0.2	4.8	0.7	0.7	3.4	9.3

Windblown Dust Contribution (%)	Remaining Sources Contribution (%)	Total Attributable Mortality (Deaths)		
		GBD2019 CRF	Lower 95% Confidence Interval (CRF)	Upper 95% Confidence Interval (CRF)
44.3	3.9	60999	38899	83661
35.7	4.2	3037	2012	4034
49.1	2.9	7590	4617	10689
58.5	2.6	-	-	-
38.2	5.1	3162	1792	4737
43.2	7	9606	5643	14051
48.8	4.7	-	-	-
41.7	4.1	2378	1442	3374
17.8	6.3	1989	1418	2532
15	6.8	-	-	-
37.9	3.5	4459	3049	5822
70.2	1.3	3462	2164	4806
46.5	3.2	25316	16762	33617
67.3	1.7	-	-	-
38.2	4	-	-	-
8.4	6.8	92306	54865	133818
20.7	8.3	1580	938	2310
11.4	7.5	3666	2440	4874
14	8.2	9265	5472	13561
8.9	6.5	3024	1726	4502
5	6	6263	3414	9521
7.7	6.2	7200	3958	10902
7.1	5.9	-	-	-
15.1	8	2845	1957	3718
20.4	8.2	599	370	850
4.5	6.5	27725	16919	39238
4.1	6.3	-	-	-
11.3	6.8	14936	8195	23045
12.6	7.7	10974	7110	14947
9	8	-	-	-
7.1	6.4	3420	1909	5135
8	6	808	457	1215

12.7	9.6	123227	57686	205136
6.7	8.3	8681	4578	13454
8.5	9	-	-	-
9.3	10.3	136	9	323
7.8	8.9	1100	513	1849
5.8	8.4	1274	534	2229
4.7	7.1	-	-	-
9.4	7.2	2074	1009	3377
14.5	10.4	68482	30672	117145
6.9	7.5	-	-	-
55.3	4.7	-	-	-
5.8	8.3	-	-	-
9.5	13.2	-	-	-
13.7	14.1	-	-	-
11	11.7	-	-	-
10.7	8.4	41480	20371	66759
12.1	8.7	-	-	-
8.6	7.6	-	-	-
15.1	33.6	2147	597	4218
16.6	30	1802	516	3516
15.3	24.5	-	-	-
5.8	54.5	346	81	702
5.5	57.3	-	-	-
6.6	6.8	59889	34089	90490
1	34.4	35	11	68
7.9	8.2	38942	20649	61823
6.3	9.5	-	-	-
8	7.8	-	-	-
9.5	6.1	-	-	-
8.5	6.6	-	-	-
9.6	6	-	-	-
5.5	4.4	19685	12741	26753
4.8	4.3	-	-	-
6.6	4.5	-	-	-
5	4.6	-	-	-
6	4.7	-	-	-
6.7	4.5	-	-	-
4.8	4	-	-	-
0.4	13.8	1226	688	1846
2.2	11.9	50594	17329	93521
0.9	10.4	3686	1157	6967

0.5	10.1	-	-	-
1.5	11	-	-	-
8.9	21	3	0	8
2.4	12.1	46904	16172	86546
0.6	14.2	-	-	-
0.4	9.6	-	-	-
0.4	10.1	-	-	-
1.1	20	-	-	-
0.9	9.8	-	-	-
1.4	11.5	-	-	-
3.8	2.3	-	-	-
0.6	11.1	-	-	-
0.6	10.5	-	-	-
0.7	13.7	-	-	-
1.1	23.8	-	-	-
1.7	16.5	-	-	-
1.3	6.4	-	-	-
9	20.2	18377	9779	28513
13.2	24.4	12197	6138	19540
8.5	19.7	-	-	-
13.6	30.5	-	-	-
3.2	14.1	5409	3295	7651
2.5	6.9	-	-	-
7.2	21.6	772	345	1322
10.1	9.4	114536	56831	185059
15.4	11.9	10	4	17
6.8	6.2	2358	1136	3824
5.5	5.9	-	-	-
4.9	8.8	3458	1798	5471
4.9	8.5	-	-	-
35.8	8.1	378	201	577
5.7	11.4	1348	633	2236
12	10.5	280	6	741
7.5	9.8	13251	6545	21491
5.5	8.5	-	-	-
8.7	10.8	-	-	-
4.6	7.6	26869	13026	43657
4.2	7.5	-	-	-
4.6	7.2	-	-	-
3.7	8.6	-	-	-
25.2	10.2	5592	3019	8723

14.4	8.9	-	-	-
20.7	39.5	14	1	32
11.5	19.8	496	171	922
38.1	5.5	2161	1263	3119
37.1	5.8	-	-	-
10.7	8.4	24366	13450	37014
28.1	18.8	-	-	-
4	5.1	-	-	-
5.7	8	85	38	144
39.1	16.4	135	65	220
5.1	9.5	4574	2378	7212
4.5	9.7	-	-	-
18	18	384	90	783
8.6	11.9	2202	884	3989
16.9	10.5	9026	4145	15201
13	7.8	-	-	-
0.6	10.5	-	-	-
10.5	12.1	614	51	1445
6.2	7.1	1398	627	2367
6.7	7.6	-	-	-
8.2	11.9	15518	7290	25840
7.7	10.6	-	-	-
6.6	10.5	-	-	-
8.9	12	-	-	-
5.9	7.3	15	7	24
11.3	7.7	5	2	9
6.1	21.7	15247	9354	21463
7.8	27.8	3393	2108	4722
5.7	28.8	-	-	-
8.6	19.7	3853	2181	5678
10.8	17.5	-	-	-
4.7	20.6	8000	5064	11064
10.8	28.1	14258	7804	21590
13.1	49.5	28	15	42
4.9	42.4	84	43	132
72.4	20.6	155	89	225
2.4	42.1	76	43	110
4.7	53.8	8	2	15
3.5	29.7	5918	3323	8889
4.7	32.2	-	-	-
11.8	49.9	29	16	44

6	33.6	3453	1883	5241
70.8	21.5	47	27	68
68.3	19.8	402	235	577
3.2	19.3	1504	846	2248
4.4	30.3	893	479	1356
11.8	52.4	430	104	857
69.8	22.6	71	42	103
70.1	22.3	57	32	83
70.9	18.3	253	153	357
69.5	19.1	813	459	1173
12.5	52.7	30	11	54
12.8	49.4	8	3	16
13.9	14.8	65630	38150	94095
23.2	15.8	11818	7074	16861
16.7	11.1	-	-	-
40.3	16	-	-	-
26.8	33	888	494	1331
10.7	15	1803	1064	2571
10	14.4	-	-	-
1.8	14.2	3338	2051	4644
0.6	9.3	-	-	-
7.8	23.1	1581	976	2221
2.7	11.8	34259	19616	49136
9	19.7	-	-	-
0.5	8.2	-	-	-
0.2	6.2	-	-	-
1.9	21.5	-	-	-
8.7	5.4	-	-	-
25.5	30.8	863	487	1264
23.3	31.2	-	-	-
35	30.9	643	328	1013
49.3	16.6	10436	6060	15054
50.7	16.3	-	-	-
43	15	-	-	-
4.8	20.8	42973	20585	70359
4.9	20.8	41992	20110	68776
0.6	7.5	-	-	-
1.3	10	-	-	-
1.9	15.7	-	-	-
0.8	12.1	-	-	-
3.6	23.8	-	-	-

2.8	54.8	-	-	-
2.6	41.1	-	-	-
1	10.5	-	-	-
3	21.3	981	475	1583
50.8	3.5	317861	227116	404247
51.8	2.8	7110	5208	8918
39.5	3.8	-	-	-
30.9	8.3	19437	12897	25909
15.8	10.4	-	-	-
28.9	10.1	-	-	-
55.7	1.1	551	412	671
42	4.7	87957	67883	106168
36.1	4.6	-	-	-
39.8	5.9	-	-	-
52.9	0.9	40870	28535	52551
41.2	2.5	-	-	-
58.3	-1.5	-	-	-
46.3	2.2	-	-	-
46.9	1.4	-	-	-
56.6	-0.1	22830	16961	28159
56.5	-0.4	-	-	-
44	4.6	2622	1745	3466
66.2	-1.4	1370	1046	1666
39.3	5.7	3240	2037	4445
77.4	6.1	3030	2093	3925
66.3	4.5	25152	17055	32982
80.2	2.4	-	-	-
38.9	5.3	1695	1132	2234
73.5	2	1617	1149	2053
58.8	1.1	459	354	552
63.7	1.1	16992	13138	20453
66.8	-0.7	-	-	-
78	2.8	13005	9667	16117
80.4	1.9	-	-	-
38.9	4.9	10039	6572	13454
33	9.7	6946	4507	9394
24	9.4	-	-	-
21.9	6.3	41149	26190	56294
11.8	7.7	-	-	-
29.5	4.7	-	-	-
26.2	5.6	-	-	-

65	1	2783	2019	3475
63.2	3.6	9006	6517	11362
62.9	3.3	-	-	-
4.1	3.8	1032907	810092	1238344
1.5	4.8	63718	49507	76737
1.2	4.4	-	-	-
1.4	5	-	-	-
1.5	4.6	-	-	-
3.6	3.9	240	170	306
3.4	3.8	866566	682014	1036734
6.4	3.6	-	-	-
7.3	4.3	-	-	-
3	3.5	-	-	-
0.9	3.8	-	-	-
5.3	5.2	-	-	-
3.7	3.5	-	-	-
2.9	3.4	-	-	-
4.2	4.2	-	-	-
3.1	3.7	-	-	-
3.4	3.8	-	-	-
4.9	3.6	-	-	-
6.4	5	-	-	-
5.3	3.6	-	-	-
4.4	3.9	-	-	-
2.1	3.5	-	-	-
2.7	3.8	-	-	-
2.5	3.3	-	-	-
3	3.3	15905	12615	19009
4.9	3.6	-	-	-
13	2.6	86477	65786	105558
17.9	2.9	-	-	-
3.8	3	-	-	-
6	2.9	-	-	-
9.2	3.9	1418337	1075605	1738024
9.2	3.8	1386689	1053525	1696981
10.7	2.8	-	-	-
4.3	3.8	-	-	-
8	7.6	-	-	-
4.3	3.5	-	-	-
4.8	3.6	-	-	-
4.1	3.9	-	-	-

2.6	4	-	-	-
6.5	4.4	-	-	-
5	4.2	-	-	-
4.8	4.2	-	-	-
5	4.1	-	-	-
6.3	3.7	-	-	-
3.8	4.3	-	-	-
5.1	3.7	-	-	-
8.2	2.8	-	-	-
11.9	3.6	-	-	-
3.8	3.7	-	-	-
11.8	2.2	-	-	-
4.6	4	-	-	-
11.8	2.3	-	-	-
4.6	5	-	-	-
2.9	4.3	-	-	-
9.9	2.4	-	-	-
5	2.7	-	-	-
3	3.7	-	-	-
13.3	2.5	-	-	-
18.4	3.3	-	-	-
4.7	4	-	-	-
6.7	4.1	-	-	-
5.4	3.1	-	-	-
5.7	4.2	-	-	-
4.1	4	-	-	-
10.5	2	-	-	-
4.2	3.3	-	-	-
5.8	4.5	20110	14907	25011
6.5	6.9	11539	7172	16032
2.5	58.1	1381	631	2286
0.7	94.3	7	1	16
0.8	94.8	25	9	45
3.6	82.5	273	104	476
-	-	-	-	-
1.7	83.9	25	7	48
2	93.1	11	3	23
1	94.9	10	4	19
2.1	82.1	9	3	17
2.6	54.2	841	424	1330
0.7	93.6	32	13	56

1.6	89.5	80	35	137
3.5	90.8	18	7	30
4	85.7	42	19	70
2.3	93	0	0	1
2.8	92.1	2	0	4
1	95.6	1	0	2
1.3	42.3	4	1	9
0.9	95.5	0	0	0
1	96.1	1	0	3
2.8	10.6	230616	138209	332098
2.6	8	2975	1788	4291
2.4	12.2	93807	54694	137546
1.1	6.9	-	-	-
0.4	12.5	-	-	-
2.4	6	-	-	-
1.3	18.5	-	-	-
0.7	8	-	-	-
4.9	6.5	1087	631	1604
0.9	16.2	9619	5179	14843
1	12.3	-	-	-
0.3	9.1	-	-	-
7.5	10.9	37	16	64
3.3	74.8	574	293	879
4.7	6.6	21691	14555	28851
4.1	9.2	-	-	-
1.4	20.2	29306	16666	43512
0.9	9.9	-	-	-
1.3	27.5	-	-	-
1.1	26.7	-	-	-
4.8	6.4	6940	3979	10055
12.9	52.6	33	18	52
3.2	5.8	29501	18954	40308
1.6	3.4	-	-	-
15.7	34.4	183	100	283
2.8	5	34862	21336	49809
1.3	5.2	-	-	-
1	4.9	-	-	-
11.6	9	15279	10064	20591
4	7.1	3851	2425	5351
5	8.7	-	-	-
37.9	8.2	738	508	967

15.3	11.4	1367	932	1790
10.6	9.3	8344	5536	11198
6.9	7.7	-	-	-
2.4	4.8	-	-	-
44.1	9.2	288	201	371
23.4	13.1	691	462	913
24.4	11.5	31529	20012	43791
7.2	8.2	731	480	989
12.2	44.5	75	41	116
60.9	5	343	239	445
64.6	4.5	1078	747	1403
38.3	8	6473	4239	8765
32.2	7	-	-	-
25.1	12.4	5029	3101	7115
20.9	9.3	-	-	-
3.5	34.4	1768	1006	2664
4.2	11.1	1070	644	1539
5.2	18.8	1506	906	2175
4.7	23.8	-	-	-
7.5	8.7	1325	890	1762
7.2	8.2	-	-	-
61	12.9	583	365	817
42	8.2	1084	712	1469
15	15.2	4856	2961	6929
23.2	15	-	-	-
16.2	9.6	3430	2317	4545
14.7	8.8	-	-	-
3.7	7.8	2179	1363	3058
3	7	-	-	-
8	9.2	29840	18964	40735
9.2	9	803	492	1125
12.8	7.5	781	506	1056
15.8	8.6	697	429	979
8.5	8.9	25035	16073	33892
22.5	20.2	-	-	-
3.7	4.7	-	-	-
4.9	10.3	303	182	427
4.2	10.9	2221	1282	3256
74.1	2.7	94736	68733	119976
68.6	2.6	1686	1158	2216
86.2	2.1	2666	1855	3479

58.9	5.1	7777	5708	9754
93.4	4	244	175	310
80.5	2.9	1979	1396	2567
69.3	4.9	4970	3553	6359
89.4	2.3	407	302	508
67.6	3.8	10734	7908	13427
64.8	4	-	-	-
76.5	3.5	2084	1468	2698
85.1	3	291	213	365
69.7	5.7	506	360	646
89	2.1	2176	1574	2769
87.4	2.4	-	-	-
95.6	1.3	1117	835	1382
90.9	1.2	2232	1632	2812
70.6	2.3	50577	36761	63987
59.8	2.9	-	-	-
59.1	3.1	-	-	-
83.4	1.7	-	-	-
60.6	2.8	-	-	-
36.8	11.9	45	29	61
91.7	2	2732	2034	3391
72.2	4.6	1236	868	1601
67.8	2.9	1278	903	1644
16.1	5.2	3832670	2715393	4972016

GEMM	COPD Contribution (%)		DM Contribution (%)		LRI Contribution (%)	
	GBD2019 CRF	GEMM	GBD2019 CRF	GEMM	GBD2019 CRF	GEMM
75492	4.2	4.9	5	5.8	5.7	8.8
3644	8.1	9.3	8.1	9.5	3.1	4.5
8630	3.1	3.8	4.6	5.2	4.3	6.8
-						
3543	3.5	4.4	6	6.7	2.1	3.5
10602	11.6	14.1	4.7	5.1	4.2	6.7
-						
3228	7	8.6	1.8	2	3.1	5
2885	2.6	3.1	0.9	1.2	4.1	6.2
-						
7288	4.3	4.9	5.4	6.7	10.3	14.8
3728	1.7	2	3.6	4.1	5.4	8.5
31945	1.6	1.9	5.4	6.6	7	10.3
-						
-						
100703	5.5	6.6	5	5.6	3.4	5.3
1774	4.5	5.6	1.4	1.6	2.6	4.3
4710	5.3	6.2	11.3	13.3	1.5	2.3
9724	4	5	3.6	4.1	2.1	3.5
3134	7.1	8.8	5.7	6.2	1.6	2.7
6572	6.8	8.2	8.3	8.6	4.6	7.3
7529	8.8	10.8	5.1	5.3	1.4	2.3
-						
3380	4	4.8	7.2	8.8	1	1.5
652	1.9	2.4	4	4.6	1.3	2.1
31196	5.5	6.4	5	5.4	5	7.7
-						
14974	5	6.4	2.3	2.4	3.5	5.8
12615	5.3	6.4	6.1	7.1	1.9	2.9
-						
3586	3.7	4.5	3.6	3.8	5.1	8.1
857	7.7	9.1	6.3	6.4	7	10.9

117852	3	3.9	2	2.1	1.9	3.2
8560	2.8	3.5	0.6	0.7	1.1	1.8
-						
98	3.9	5.3	3.4	3.4	2.5	4.1
1023	2.5	3.3	3.3	3.5	1.7	2.9
1168	3.4	4.5	1.7	1.8	1.9	3.2
-						
2024	3.6	4.7	1.6	1.7	2.8	4.7
64298	3.4	4.5	2.9	3.1	2.3	3.8
-						
-						
-						
-						
-						
40682	2.3	3	0.7	0.8	1.4	2.4
-						
-						
2090	14.2	17.9	10.1	9.6	4.7	7.3
1757	14.2	17.8	10.5	10	4.8	7.4
-						
333	14.2	18	7.5	7.2	4.5	7
-						
67774	8.3	9.3	5.8	6.1	15.8	22.8
33	6.3	8.2	25.5	25.2	5.7	9.2
42858	8.1	9.1	2.7	2.5	18.2	26.7
-						
-						
-						
-						
-						
23414	8.9	9.7	12.2	13	10.4	15
-						
-						
-						
-						
-						
1469	5.7	6	2	1.9	24.7	34.7
49670	14.4	18	9.1	8.6	4.5	7
3632	12.6	15.6	9.1	8.6	5.4	8.2

-						
-						
3	11.8	15.4	4	3.9	3.8	6
46035	14.6	18.2	9.1	8.6	4.4	6.8
-						
-						
-						
-						
-						
-						
-						
-						
-						
-						
-						
20581	11.3	12.8	10.6	10.2	15.6	22.8
13619	11.2	12.5	10	9.3	18.9	27.6
-						
-						
6199	11.3	12.9	11.9	12.4	9	13.6
-						
763	13.7	16.7	10	9.5	8.5	13.2
118698	12.6	15.1	8.9	8.7	6.8	10.4
10	15.6	18.7	6.3	5.9	6.9	10.5
2368	10	12.3	10.9	10.8	2.8	4.4
-						
3717	15.2	17.6	5.6	5.2	10.6	15.8
-						
392	10.8	13	16.9	17.2	3.1	4.9
1403	18.3	21.6	9.1	8.5	7.8	11.7
254	6.6	8.9	3.4	3.4	2.1	3.5
13733	9.1	10.8	9.6	9.2	8.6	13.2
-						
-						
27266	10.8	13.2	8.8	8.6	4.9	7.7
-						
-						
-						
5806	9.6	11.5	3.2	3.2	7.3	11.5

-						
13	11	13.7	4.8	4.4	8.1	12.4
499	15.1	18.4	5.5	5.1	8.4	12.7
2436	10.1	11.4	19.4	19.6	7.9	11.8
-						
25517	11.6	13.8	12.1	12.3	3.8	6
-						
-						
85	12.5	15.2	6.5	6.2	6.3	9.7
138	6.8	8.2	10	9.9	7.8	12.2
4847	16.4	19.2	7.7	7.3	7.5	11.3
-						
385	15.7	19.2	6.7	6.1	9.3	13.9
2202	12.1	14.7	13.5	12.7	12	18.3
9163	19.1	22.9	9.5	9	6.3	9.5
-						
-						
583	10.2	13.1	9.4	9	5.5	8.7
1404	10.8	13.3	8.6	8.4	5.7	8.9
-						
16453	16.9	19.6	3.6	3.3	11.8	17.4
-						
-						
-						
15	7.8	9.3	2.9	2.8	8.7	13.2
5	9	11.2	6.5	6.3	5.6	8.9
21966	7.5	7.9	13.9	13.8	23.5	32.3
5522	9.2	9.7	15.5	15.9	20	27.8
-						
4518	8.5	9.6	19.6	19.6	13.1	19.6
-						
11927	6.4	6.4	10.5	10.6	30.1	39.2
19138	6.1	7	13.2	13.5	8.1	13.9
29	2.7	3.3	27.8	28.6	8.6	13.6
86	3.2	4	19.5	20.2	6.9	11.2
172	3.2	3.7	30.6	31.5	10	15.3
100	6.6	7.5	25.2	25.5	11.5	17.3
7	4.8	6.2	15.6	15.4	5	8.1
6639	8.4	9.7	5.1	5.1	10.5	16
-						
33	5.6	6.6	27.1	27.6	8.1	12.7

3951	3.9	4.9	10.7	11.5	4.6	7.6
54	3.6	4.2	24.4	25.4	9.6	14.9
472	2.4	2.9	20.6	22.3	6.3	10
4860	5.1	6	13	13.4	13.1	20.4
967	5.4	6.7	33.2	34.7	3.6	5.8
415	9.9	12.6	35.3	33.8	5.8	9.1
81	7.5	8.8	27.2	28.5	7	10.9
65	3	3.5	28.1	29.7	6.4	10.1
302	4.4	5.3	16.2	17.7	6.5	10.3
870	2.8	3.4	35.7	37.9	3.3	5.1
28	3.1	4.1	19	19.4	2.8	4.6
8	3.6	4.8	22.2	22.8	6.9	11.5
85241	11.1	12.6	22.4	23.1	7.1	11.3
14390	17.2	19.7	8.9	9.3	6.6	10
-						
-						
974	14.7	17.2	9.3	9.5	6.4	10
2502	8.4	9.3	18.6	19.1	12.5	18.2
-						
7029	5.7	5.8	22.8	22.9	24.5	32.7
-						
3250	14.1	16.7	6.3	6.8	4.3	6.8
43465	10.7	12.2	30.4	31.2	5.9	9
-						
-						
-						
-						
1616	10.1	11.7	20.2	20.8	7	10.7
-						
694	9	10.9	21.6	21.6	8	12.5
11322	7.2	8.4	15.8	16.8	5.2	8.2
-						
-						
45750	10.7	12.9	15.3	14.9	10.8	16.7
44559	10.8	13.1	15.1	14.7	10.9	16.8
-						
-						
-						
-						
-						

-						
-						
-						
1192	6.4	8	22.7	22.9	7.1	11.4
419282	6.1	6.8	6	7.7	6.1	9.6
29383	4.9	5.3	4.2	5.7	20.9	27.2
-						
22018	4.9	5.8	5.1	6.2	4.7	7.1
-						
-						
776	5.9	5.9	26.7	36.1	3.8	4.4
110679	5.4	6	5	7.9	7.4	9.6
-						
-						
48441	7.3	8.3	7.6	9.5	4.8	6.8
-						
-						
-						
27431	1.9	2.2	8.2	11.6	3.4	4.7
-						
3077	3.8	4.3	14.4	16.8	6.2	9
1754	3.3	3.7	5.3	8	12.8	16.4
3693	5	5.7	5.2	6	4.1	6.2
3535	5.3	6.2	5.7	7.1	4.8	6.9
30306	4.8	5.6	4.9	6	4.2	6.3
-						
1992	3.4	3.8	15.2	18	4.8	7
1951	3.7	4.2	9.9	12.9	5.9	8.2
625	3.4	3.5	14.9	22.7	4.4	5.2
20827	4	4.6	3.6	5.6	7.3	9.8
-						
25334	5.9	6.8	2.7	3.8	8.6	11.9
-						
11249	3.6	4.3	3.3	3.9	3.8	5.8
7808	5	5.9	5	5.8	4	6
-						
47245	12.7	14.4	9	9.9	4.9	7.3
-						
-						
-						

3331	9.1	10.4	8.4	11	4	5.6
17827	5.7	6.6	2.3	3.2	9.4	13.2
-						
2146883	24.4	25.5	4.7	7.5	10.9	13.1
158987	14.1	15.6	5.2	7.9	8.3	10.8
-						
-						
-						
524	26.7	29	7.5	9.1	7.7	10.5
1752666	26	27.2	4.5	7.2	10.8	12.9
-						
-						
-						
-						
-						
-						
-						
-						
-						
-						
-						
-						
-						
-						
39195	41.2	42.8	2.5	4	10.4	12.3
-						
195510	13.8	14.8	6.8	9.8	13.6	17.1
-						
-						
-						
2049784	18.3	20.6	2.4	3.3	2.8	3.7
1992762	18.4	20.6	2.3	3.2	2.6	3.6
-						
-						
-						
-						
-						

-						
-						
-						
-						
-						
-						
-						
-						
-						
-						
-						
-						
-						
-						
-						
-						
-						
-						
-						
-						
-						
-						
-						
-						
-						
43106	21.1	24.1	2.4	3.2	4	5.6
13916	11.6	12.5	16.5	16.7	13.8	19.6
3812	9.8	13.5	23.6	20	10.5	19
5	6.4	8.7	29.1	29.5	3.4	5.6
30	5.6	7.4	25.4	26.1	4.3	7.1
311	2.4	3.1	44	45.2	2.7	4.4
-						
22	5.1	6.8	10.3	10.4	3.5	5.8
23	3.6	4.9	28.4	29.9	3.4	5.8
12	5.6	7.4	18.4	19	5.1	8.5
8	5.6	7.5	18.4	18.8	3.3	5.5
2977	13.5	15.6	18.7	17.8	14.5	21.9
46	7.9	10.2	20.6	21	5.2	8.5

260	5.2	6.6	14.4	14.7	8.5	13.9
21	7.6	9.6	32.4	31.8	6.4	10.2
90	7.6	9.8	12.6	13	5.9	9.7
0	5.7	7.6	33.1	33.2	3.8	6.3
2	4.9	6.4	39.8	39	6.1	9.8
1	3.4	4.8	20.5	21.4	5.3	9.1
4	6.2	8.1	23.5	23.1	8	12.9
0	7.3	9.7	22.7	22.9	4.7	7.7
1	6.2	8.5	24.2	24.7	4.1	6.9
326462	8.3	10.2	11.7	12.5	7.6	12
7983	6.9	7.7	8.1	8.2	19.4	28.5
119054	7.3	9.1	13.1	14.3	3.5	5.8
-						
-						
-						
-						
-						
2831	8.1	9.5	8.5	8.8	12.9	20
10569	6.1	7	4.3	4.3	17.5	26.4
-						
-						
37	12.2	15.7	9.9	10.1	3.5	5.7
595	4.6	5.6	41.5	42.7	3.5	5.6
46930	14.6	16.6	10.3	11.7	8.2	12.1
-						
43218	6.5	7.5	10.4	10.6	14.2	21.7
-						
-						
-						
9675	7.5	8.8	24.3	25.6	5.3	8.2
37	6.8	7.8	10	9.7	17.6	26.4
38193	9.9	10.9	10.7	11.5	12.6	18.2
-						
386	9.4	11.2	6.5	6.6	12.4	19.4
46955	8.4	10.3	10.1	11.1	5	8.1
-						
-						
53321	7.4	8	8.9	8.8	26.6	36.7
8764	5.4	5.7	9.8	10	26.6	36.4
-						
4423	6.1	6.1	6.4	7.3	37.4	46.3

2589	6.5	7	10.9	12.6	17.4	23.7
36180	8.6	8.9	7.6	8.1	28.2	37.1
-						
-						
439	7.5	7.7	13.5	15.9	22.3	28.4
927	5.9	6.3	16.7	18.7	16	21.8
131540	6.4	6.5	9.3	9.4	29.7	40.7
4539	7.9	8.2	7.6	8.1	28.5	37.9
205	6.2	7	11.9	11.5	20.9	31
592	4.5	4.6	8.8	10.4	27.6	35.3
3668	5.7	5.8	7.6	8.8	33.6	42.1
33633	7.4	7.5	9.5	10	31.9	41.2
-						
12872	7.6	8	9.9	9.9	26.2	36.5
-						
6616	6.1	6.9	6.4	6.4	21.1	31.8
4842	5.5	5.8	10.5	10.2	29.1	40.2
8492	4.2	4.7	10.3	10.4	23.3	34
-						
4827	8.7	9	9.4	10.3	26	34.4
-						
9549	5	4.9	6.5	6.3	42.6	53.9
4609	5.1	4.9	6.8	7.1	46.2	55.7
18021	4.7	4.8	9.8	9.6	31.8	43.1
-						
13648	7.1	7.2	9.5	10.4	31.6	40.3
-						
5427	5.2	5.6	9.6	9.8	24.8	35
-						
45500	8.3	8.5	21.3	21.6	17.7	25.5
1213	6.4	6.9	18.9	19.2	19	27
1800	9.9	10.4	18.1	19	20.9	28.4
1128	9.4	10.1	15.4	15.7	20	28.4
34898	8.7	9.2	22.3	23.5	16.2	22.3
-						
-						
561	6.4	6.8	26.3	26.2	19.1	27.1
5900	3.7	3.8	12.5	11.7	31.3	42.5
320839	5	4.9	5.8	7.3	43.4	51.5
7039	5	4.9	6.1	7	40.1	48.9
16949	3.3	3.1	5.1	6.1	49.5	57.5

19088	5.4	5.4	8	10.8	34.7	40.9
393	5.7	6	8.7	11.1	18.9	24.3
13333	4.6	4.4	3.9	4.9	54	61.3
16003	4.9	4.9	6.3	8	38.6	46
1538	6.7	6.9	6.2	8.5	29.3	35.6
22565	5.9	6.1	7.9	10.6	25.5	31.7
-						
11118	5.6	5.4	5.5	6.8	44.1	52
1400	5.8	5.9	6.5	8.7	29.4	36.1
2170	4.8	5	7.9	9.9	27.3	34.4
14124	7.6	7.5	5.7	7.4	41	48
-						
2501	6	6.1	7.6	10.7	29.3	34.7
19482	4.6	4.4	3.3	4.6	57	62.9
152639	4.6	4.4	5	6.8	49.9	56.4
-						
-						
-						
-						
98	12	12.8	3.3	3.5	21.6	29.8
9924	7	7.2	7.6	10.6	27.5	33.1
6034	5	5	5.1	6.2	40.9	49.2
4440	5.5	5.7	6.3	7.6	28.9	36.7
6222380	16.1	18.2	5.2	6.7	7.7	12.3

LC Contribution (%)		IHD Contribution (%)		Stroke Contribution (%)		Pre-Term Birt
GBD2019 CRF	GEMM	GBD2019 CRF	GEMM	GBD2019 CRF	GEMM	GBD2019 CRF
3.4	3.8	54.3	52.8	27.5	23.9	17558
8.6	9.7	54.5	51.7	17.6	15.2	504
4.6	5.2	57.7	56.7	25.7	22.3	1411
6.5	7.5	44.8	45.4	37.1	32.5	323
4.8	5.4	39.9	39.1	34.8	29.6	1351
2.8	3.2	57.5	57.1	27.7	24.2	1082
5.3	6.5	42.1	41.8	45	41.3	907
2	2.3	51.7	48.6	26.2	22.7	2453
1.9	2.2	55.3	54.8	32.2	28.4	1164
1.8	2.1	60.8	58.6	23.3	20.5	8362
12.6	14.1	43.7	42.6	29.8	25.7	7243
9.1	10.4	42.1	42.6	40.3	35.5	219
11.2	12.9	36	34.9	34.6	30.4	192
7.1	8.1	43.7	44.3	39.6	34.9	432
12.5	14	44.7	44.2	28.3	24.1	130
12	13	50	47.9	18.2	15	575
15	16.5	50	48.7	19.6	16.4	494
8.5	10.1	31.9	31.8	47.4	43	222
13	15.1	34.5	35.2	45.5	40.7	48
17.5	19.1	43.9	41.9	23.2	19.5	2429
8.5	9.6	44.5	44.6	36.3	31.2	1012
11.6	13.3	37.3	36.9	37.7	33.3	1010
9.7	10.7	56.5	54.9	21.4	18	382
19	20.3	34.9	33	25.1	20.4	97

5	5.7	60.4	61.3	27.8	23.8	8485
4.7	5.4	67.9	68.7	22.9	19.9	308
12.9	14.4	59.7	58.3	17.5	14.5	10
7	8	54.7	55.6	30.8	26.6	49
7.1	8	62.8	62.9	23.1	19.6	56
4.7	5.3	61.2	61.4	26.2	22.3	147
5.6	6.5	53.9	54.6	32	27.5	5955

3.9	4.5	69.6	70.3	22	19	1960
-----	-----	------	------	----	----	------

17.3	18.2	36.8	33.8	16.8	13.2	524
17.7	18.5	36.1	33.1	16.7	13.1	457

15.7	16.6	40.8	37.6	17.4	13.7	67
------	------	------	------	------	------	----

20.3	20.6	23.3	20.7	26.5	20.6	6093
10.9	11.8	33.7	31.4	17.9	14.2	14
20.7	20.5	24.7	21.8	25.7	19.4	2761

19.9	21	19.8	17.9	28.8	23.3	2880
------	----	------	------	------	------	------

15.5	14.9	37.3	31.6	14.8	10.9	439
17.7	18.6	40.5	37.1	13.8	10.7	8634
22.5	23.5	37.1	33.7	13.3	10.4	593

26.4	28.4	31	28.3	22.9	18	1
17.4	18.2	40.8	37.3	13.8	10.8	8041

10.5	10.6	30.1	26.7	21.9	16.8	4440
10.1	10	30.5	26.5	19.2	14.2	2780

10.8	11.4	29.5	27.3	27.4	22.3	1521
------	------	------	------	------	------	------

14.2	14.8	28.9	26.5	24.8	19.3	140
18.1	18.8	34.3	31.7	19.4	15.3	14863
24.3	24.8	31.6	28.4	15.3	11.7	1
15.1	16.2	46.8	44.5	14.5	11.7	310

20.6	20.8	29.5	26.4	18.5	14.1	585
------	------	------	------	------	------	-----

12.9	13.8	39.1	37	17.4	14.2	163
21	21.3	26.3	23.5	17.6	13.4	154
12.8	14.2	54.3	52.7	20.8	17.3	21
24.2	25	29.1	26.6	19.5	15.2	2556

16.2	17.2	42.1	39.5	17.1	13.7	2929
------	------	------	------	------	------	------

16	17.1	36.8	34.7	27.1	22	595
----	------	------	------	------	----	-----

18.8	19.5	43.2	39	14.2	11	3
17.3	17.7	38.5	34.5	15.1	11.6	87
15.6	16.2	29.6	27	17.5	13.9	1253
16.9	18.1	33.1	31.4	22.5	18.3	2191
20.7	21.7	34.6	31.9	19.5	15.3	20
12.1	12.8	46.7	43.7	16.7	13.3	14
24.3	24.8	25.7	23.2	18.4	14.1	596
17.2	17.5	33.6	29.9	17.5	13.3	49
10.9	11.3	22.9	20.8	28.6	22.1	175
17.6	18.1	28.6	25.9	19	14.7	868
13.3	14.2	42.7	39.9	18.8	15.1	68
17.9	18.8	40.4	37.5	16.5	13.1	220
18.4	18.3	32.7	28.8	16.7	12.5	2002
31.1	32	31.8	29	17.7	13.8	1
23.2	24.7	31.2	29.3	24.5	19.6	1
5.9	6	29	24.7	20.1	15.4	9906
4.5	4.6	28	24.4	22.8	17.7	2353
4.9	5.1	32.8	29.7	21.1	16.5	1949
7	6.9	27.5	22.9	18.5	14	5604
8	7.5	39.2	36.3	25.3	21.8	3143
3.8	4	29.8	28.3	27.3	22.2	6
6	6.6	37.6	36.1	26.7	21.9	21
3.9	4.2	25.7	23.8	26.6	21.5	22
5.1	5.3	29.9	27.2	21.8	17.2	46
14.4	15.7	42.1	40	18	14.6	1
13.6	14.2	40.7	37.5	21.8	17.3	445
6.1	6.5	27.8	26.1	25.3	20.4	5

4.3	4.9	48.2	47.3	28.3	23.9	1294
4.3	4.6	30.3	28.4	27.7	22.5	10
1.8	1.9	37.3	36	31.8	26.8	103
2.1	2.3	33.7	31.4	32.8	26.4	723
6.4	7	20.8	20.2	30.6	25.5	198
6.4	6.8	30.9	28.5	11.8	9.2	44
4.7	5	22.3	21.1	31.3	25.7	13
3.1	3.4	33.5	31.9	25.9	21.4	11
4.9	5.5	33.4	32.1	34.4	29.1	71
3.2	3.5	34.9	33.4	20.1	16.8	124
7.8	8.8	50.1	49	17.1	14.2	4
3.4	3.8	28.3	27.7	35.6	29.5	2
5	5.1	37.9	34.5	16.5	13.4	28834
7.1	7.5	41.4	38.4	18.8	15.2	9034

6.3	6.7	45	42	18.4	14.8	446
4.5	4.6	40.5	36.4	15.5	12.3	815
2.8	2.7	28	23.6	16.3	12.3	2494
6.9	7.6	37.3	35.8	31.1	26.3	1018
3.7	3.9	35.5	32.6	13.8	11	10363

3.2	3.4	41.8	39	17.8	14.4	567
6.1	6.5	31.5	29.5	23.7	19	373
7.1	7.8	44.1	41.8	20.5	17	3723

6.6	6.9	32.2	29.5	24.5	19.1	15130
6.6	6.9	32.1	29.4	24.5	19.1	14740

6.1	6.6	33.2	31.4	24.5	19.8	390
4.5	4.8	54.3	50.7	23	20.4	177440
1.6	1.9	43.8	39.2	24.6	20.8	7496
3.3	3.8	55.8	54.1	26.1	23.1	14103
6.1	6.9	42.8	35.3	14.6	11.4	283
1.9	2.5	62.1	58	18.2	16.1	58393
4.7	5.5	52.1	49.3	23.6	20.6	12173
4.4	5.4	49.3	46.9	32.8	29.3	16200
6.4	7.1	43.9	41	25.3	21.6	4901
4.3	5.3	54.2	49.3	20.1	17.4	1224
8.4	9.4	67.4	64.2	9.8	8.4	1070
6.4	7.5	54.2	51.6	23.6	20.8	1512
4.1	4.8	56.5	54.7	25.5	22.7	10153
5.9	6.7	45.2	42.5	25.4	21.9	1416
2.3	2.7	58.2	54.5	20	17.5	1094
6.6	8	54.6	47.3	16.1	13.3	257
2.3	3	55.1	52.1	27.7	24.9	3525
1.8	2.3	53.2	50.5	27.8	24.8	16343
2.7	3.1	66.7	65.1	19.9	17.7	2820
6.7	7.7	54.8	53.1	24.5	21.4	2645
12.8	13.9	39.4	36.8	21.3	17.7	12340

3.8	4.6	48.9	45.7	25.8	22.7	552
2.1	2.6	53.6	50.8	26.8	23.7	8942

2.1	2.7	36	32.2	21.9	19.2	589379
2.1	2.6	28.8	26.7	41.5	36.4	51595

2.3	2.6	35.3	31.8	20.5	17.1	119
2	2.5	36.5	32.8	20.3	17.4	474772

1.9	2.3	24.8	22.1	19.2	16.4	3935
-----	-----	------	------	------	------	------

3.4	4	37.6	33.4	24.9	21	58958
-----	---	------	------	------	----	-------

11.6	13.9	26.5	24.7	38.4	33.7	178666
11.6	14	26.6	24.9	38.5	33.7	174361

6	7.1	22.9	21.7	43.5	38.4	3040
16.6	16.9	20.6	18.2	20.7	16.1	1265
2.9	3.1	32.4	27.9	20.8	16.6	576
5.7	6.4	34.1	32.5	21.3	17.3	2
3.5	4	37.8	36.2	23.4	19.1	4
1.3	1.5	35.8	34.4	13.9	11.4	49
9.6	10.7	55	52.8	16.6	13.5	6
1.9	2.2	32.3	31.7	30.4	25.4	3
3.7	4.2	41.1	39.5	26.2	21.4	2
10.3	11.6	39	37.4	23.5	19.2	1
3.1	3.1	28.5	25.2	21.8	16.4	459
2	2.2	39.1	37.5	25.3	20.6	8

2.5	2.7	42.5	40.2	27	21.8	22
6.4	6.9	30.2	28	17	13.5	6
3.2	3.5	42.6	41	28.1	23	13
4.9	5.4	33.9	32.3	18.7	15.2	0
7.3	8	26.3	24.4	15.6	12.4	0
3.1	3.6	43.2	41.2	24.5	19.9	0
6.2	6.8	36.9	34	19.1	14.9	0
4.8	5.3	37.1	35.4	23.5	19	0
3.7	4.2	38	36.4	23.8	19.4	0
6.2	6.7	28.2	26.4	38	32.2	67696
6	6.2	24.8	22.2	34.7	27.3	1356
5.1	5.8	29.5	29.2	41.6	35.8	23142

4.7	5	29.9	27.8	35.9	29	525
5.9	6.1	41.1	36.9	25	19.4	3304

3.9	4.3	46.4	44.6	24.2	19.7	17
3.5	3.8	28.2	26.9	18.7	15.3	87
4.7	5.2	19	17.9	43.2	36.5	6259

4.4	4.6	35.5	32.5	29.1	23.1	18547
-----	-----	------	------	------	------	-------

3.8	4.1	36.7	34.7	22.5	18.6	1289
5.9	6	35.3	31.4	24.3	18.6	11
12	12.7	24.9	22.6	29.8	24.1	7418

4.8	5.1	30.3	28.3	36.7	29.4	111
7.4	8.4	21.8	21.5	47.2	40.6	5631

3.4	3.2	24.7	20.7	29	22.5	20528
3.8	3.8	24.8	21.3	29.6	22.8	7075

2.1	2.2	21	17.3	27	20.9	720
-----	-----	----	------	----	------	-----

4.1	4.5	29.8	26.5	31.3	25.8	1467
3	3	24	20.5	28.7	22.4	10131
5.3	5.7	23.5	20.1	27.9	22.2	563
5.5	5.9	27.9	24.7	28	22.7	573
2	1.9	21.3	18	31.3	23.5	48729
1.7	1.8	23.7	20.3	30.6	23.8	1243
2.3	2.3	27.7	24.6	31	23.6	50
3	3.2	26	22.3	30.1	24.1	458
1.9	2	21.1	17.7	30.2	23.7	1324
1.7	1.8	22.1	18.6	27.4	21	12659
1.9	1.9	21.9	18.9	32.5	24.8	5106
1.3	1.4	24.7	22.2	40.4	31.4	1965
1.7	1.6	23.2	19.7	30.1	22.6	1337
1.8	1.8	20	17.7	40.4	31.5	2155
2.5	2.6	19.9	17.2	33.4	26.4	1771
1	0.9	19	15.2	25.9	18.7	841
2.2	2.1	16.7	13.2	23	16.9	1677
2.5	2.4	21.3	17.9	29.9	22.3	10517
2.1	2.1	20.1	16.9	29.6	23	4383
2.5	2.6	19.3	16.8	38.6	30.1	3244
5.7	5.6	22.9	20.2	24.1	18.7	16252
4.7	4.8	25	21.9	26	20.2	432
3.2	3.3	19	16.4	28.8	22.5	333
1.9	2	24.3	21.4	28.9	22.5	513
6.2	6.3	22.3	19.5	24.2	19.1	12668
3.6	3.6	20.7	18	24	18.4	207
3.2	3	29.8	24.7	19.5	14.2	2099
2	2.2	20.3	16.4	23.5	17.7	137091
2.3	2.4	20.6	16.9	26	19.9	2150
1.9	2	20.9	16.7	19.3	14.6	3902

3.1	3.5	21.6	18	27.2	21.5	11120
5.3	5.9	35.6	31.3	25.9	21.3	169
1.9	2	15.8	12.6	19.9	14.9	3278
2.9	3.1	22.9	18.9	24.5	19.1	7652
1.7	2	28.4	24.5	27.7	22.5	553
2.1	2.5	24.9	21.6	33.6	27.5	11057
1.9	2	19.5	15.9	23.4	17.9	2406
2.4	2.7	26.3	22.5	29.7	24	362
2.7	2.9	28.4	24.4	28.9	23.3	779
1.6	1.8	19.7	16.2	24.4	19	4112
3.5	4.1	27	23	26.7	21.5	1564
1.5	1.6	14.9	12.1	18.8	14.4	4305
1.7	1.9	18.4	14.9	20.5	15.7	76712
4.5	4.7	29.3	25.9	29.3	23.3	35
3.5	4	26.5	22.6	27.9	22.5	3846
2.1	2.2	22.6	18.6	24.2	18.8	1456
2.8	3	27.8	23.9	28.8	23.1	1635
7.6	7.7	33.9	30.2	29.5	24.8	1361207

hs (Incidences)	Low Birth Weight (Incidences)	
GEMM	GBD2019 CRF	GEMM
24545	4811	6861
639	196	267
1775	504	613
419	108	124
1664	786	877
1641	298	432
1457	196	361
4203	563	1092
1397	274	325
11351	1886	2772
8747	3193	3516
282	63	74
267	45	65
521	251	277
152	75	78
660	343	345
575	285	290
292	104	147
60	16	19
2933	1035	1190
1168	562	559
1283	187	238
442	180	187
111	48	48

9659	3879	3455
353	214	212
9	7	4
54	27	24
61	33	27
169	54	50
6752	2759	2386

2261	786	753
------	-----	-----

580	332	236
505	289	205
74	44	30

7107	4361	4402
15	11	8
3114	2907	2691

3470	1216	1465
------	------	------

508	227	237
9552	5752	4257
656	380	275

1	1	0
8895	5371	3982

5132	2274	2216
3159	1558	1435

1821	631	712
------	-----	-----

152	85	68
16717	8533	7598

1	1	1
347	168	149

657	271	246
-----	-----	-----

186	36	35
171	81	67
24	14	9
2858	1510	1317

3279	1453	1280
------	------	------

675	279	266
-----	-----	-----

4	2	1
96	64	47
1461	623	665
2499	1166	1141
22	10	8
16	8	7
669	321	287
54	33	23
193	154	118
955	796	644
76	25	17
244	140	116
2228	1379	1155
1	1	0
1	0	0
13871	5160	7036
3740	853	1346
2358	1512	1653
7774	2795	4037
5546	1965	2889
7	3	3
25	18	17
26	11	11
63	22	28
1	1	1
526	223	234
6	3	3

1677	861	978
12	5	6
133	88	106
2507	363	1121
241	177	183
49	34	24
16	7	7
14	5	6
92	56	68
144	86	91
4	2	2
2	1	1
40086	14630	19242
11518	3289	3922

524	195	202
1147	455	610
4961	1344	2700
2270	591	1248
13743	6290	7677

1127	341	614
440	240	233
4357	1886	2036
17596	7602	6952
17066	7349	6676

531	254	276
267499	71840	149526
30910	6693	36613
17287	3450	4523
368	110	201
76699	15651	29574
15168	9012	13109
20561	6202	10254
6016	1706	2254
1597	386	718
1299	520	647
1875	519	732
13204	5709	8200
1750	573	767
1374	485	749
343	136	265
4583	3255	5989
33593	5735	15538
3452	1347	1751
3219	691	872
14839	5585	6676

694
18670

494
3581

763
9332

1257195
132821

383815
25072

1191054
91494

260
982038

54
291840

139
886289

9811
132266

5242
61606

19193
193939

267456
259102

46334
44965

90948
87927

6846	909	2490
1509	460	531
1939	302	804
1	1	1
6	3	3
66	28	28
6	5	3
7	2	3
3	2	2
1	1	1
1709	231	702
13	4	5

84	12	35
8	4	4
33	10	19
0	0	0
0	0	0
0	0	0
0	0	0
0	0	0
0	0	0
106133	43901	63644
3696	842	2144
33523	12533	16215

1460	489	1224
3780	2116	2100

20	23	20
100	75	73
14245	3512	8200
28838	15781	22051

1935	1608	2208
12	6	6
9765	3012	3956

253	51	99
8504	3854	5349

65759	10828	36436
15555	4382	9688
3980	346	2310

2766	610	1291
41883	4946	22282

816	245	431
758	300	434
198691	25250	107062

7385	712	4517
140	58	141
754	197	392
4221	568	2197
61602	6142	32395

12701	3427	8292
-------	------	------

7639	1606	5535
5809	953	3964
12261	1322	7043

6207	509	1967
------	-----	------

12421	433	6581
6321	770	3306
36897	3356	11484

16347	3619	15443
-------	------	-------

7988	1578	3805
------	------	------

25094	8910	13882
--------------	-------------	--------------

646	286	416
743	190	441
821	337	524
17266	6834	9593

377	92	161
5242	1171	2748
435067	54595	242053

8200	1518	7107
22051	1541	11514

25314	3774	12008
266	70	140
19509	1256	10230
22647	3508	13908
1994	263	1325
22366	4578	12572
11590	956	6086
1660	222	1389
3195	320	1681
24419	1563	12802
3319	572	1738
34082	1546	17839
209187	29421	114778
76	9	20
13267	1998	9710
6501	643	3728
5424	837	3477
2783970	708266	1964067

Data File 2: PM_{2.5} Exposure Estimates, Combustion Fuel-Type Source Contributions, and To

McDuffie et al., 2021 -

Last Updated: March 23, 2021

Name Legend:

Regions Countries *Sub-national regions*

Country Name	Population Weighted Annual Average PM _{2.5} ($\mu\text{g m}^{-3}$)	Total Biofuel Contribution (%)	Total Coal Contribution (%)
Central_Asia	27.5	9.9	9
Armenia	31.9	5.4	8.6
Azerbaijan	23.9	7.8	4.6
<i>Baku</i>	<i>31.5</i>	<i>7.2</i>	<i>3.7</i>
Georgia	17.8	8.8	9.5
Kazakhstan	19	4.8	9.2
<i>Shymkent</i>	<i>38.1</i>	<i>7.6</i>	<i>7.3</i>
Kyrgyzstan	22.9	11.2	11.1
Mongolia	36.7	11.4	18.2
<i>Ulaanbaatar</i>	<i>81.4</i>	<i>11.7</i>	<i>21.6</i>
Tajikistan	35.9	24.4	8.2
Turkmenistan	25.5	2.2	2.9
Uzbekistan	32.5	8.7	9.9
<i>Bukhara</i>	<i>26.6</i>	<i>2.3</i>	<i>5.4</i>
<i>Tashkent</i>	<i>50.8</i>	<i>7.1</i>	<i>11.7</i>
Central_Europe	20.5	20.8	18.7
Albania	19.8	12.5	15.5
Bosnia_and_Herzegovina	29.8	18	23.8
Bulgaria	19.7	18.1	18.5
Croatia	18	26.8	12.4
Czech_Republic	16.8	23.4	16.4
Hungary	16.5	28.2	14.4
<i>Budapest</i>	<i>19.5</i>	<i>32.4</i>	<i>13.7</i>
Macedonia	31.6	14.7	23.3
Montenegro	21.6	15.1	19
Poland	22.7	18.7	19.5
<i>Warsaw</i>	<i>24.3</i>	<i>18.9</i>	<i>21.7</i>
Romania	15.9	24.6	15.8
Serbia	26.5	19.4	25.8
<i>Belgrade</i>	<i>25.7</i>	<i>18.9</i>	<i>32.2</i>

Slovakia	18.4	23.2	16.5
Slovenia	16.9	27.4	7.2
Eastern_Europe	11.8	12.5	11.2
Belarus	16.3	14.7	15
<i>Gomel</i>	20.9	11.2	14.8
Estonia	5.7	30.8	5.6
Latvia	11.7	30.4	7.9
Lithuania	10.2	26.7	10.5
<i>Kaunas</i>	12	33	10.6
Moldova	13.1	19.2	15.3
Russian_Federation	10.9	11.7	8.5
<i>Saint_Petersburg</i>	8.2	25.3	5.3
<i>Astrakhan</i>	12.1	4.2	7.2
<i>Moscow</i>	13.8	24.5	6.5
<i>Tyumen</i>	13.4	7.5	6.4
<i>Berezniki</i>	13.9	8.5	6.8
<i>Dzerzhinsk</i>	11.6	14.3	7.1
Ukraine	14	11.7	16.7
<i>Nikolaev</i>	14.2	10.8	15.8
<i>Rovno</i>	19.9	13.2	17
Australasia	6.9	3.5	8.6
Australia	7	3.6	9.4
<i>Sydney</i>	7.6	4.8	16.2
New_Zealand	6.6	2.8	4.2
<i>Auckland</i>	6.5	3.7	4
High_income_Asia_Pacific	17.3	11	15.3
Brunei	7.6	10.9	5.6
Japan	13.5	9.2	12.4
<i>Tokyo</i>	15.1	7.4	9.5
<i>Osaka</i>	15.1	10	13.6
<i>Fukuoka</i>	17.7	11.6	16.7
<i>Okayama</i>	13.3	9.7	14.7
<i>Yamaguchi</i>	12.6	11.4	16.2
South_Korea	26.6	13	18.7
<i>Seoul</i>	27.4	13.2	19.1
<i>Busan</i>	24.3	14.1	17.4
<i>Cheonan</i>	28.6	12.8	18.6
<i>Gwangju</i>	27	12.3	18.8
<i>Jinju</i>	27.7	11.8	18.4
<i>Pyongyang</i>	52.9	11.2	24.3
Singapore	18.5	14.5	19.1

High_income_North_America	7.8	13.2	9.1
Canada	7.3	17.1	3.9
<i>Montreal</i>	9.1	26.4	2.5
<i>Victoria</i>	6.3	20.5	1.6
Greenland	5.3	3.1	5.1
United_States	7.8	12.8	9.7
<i>Raleigh</i>	7.6	11.4	15.6
<i>New_York</i>	7.7	23.7	7.4
<i>Philadelphia</i>	8.6	17.4	8.4
<i>Houston</i>	9.9	12.6	10.2
<i>Minneapolis</i>	7.4	10.2	10.2
<i>Portland</i>	8	11.9	4.1
<i>Los_Angeles</i>	10.6	27.2	5.8
<i>Cleveland</i>	8.8	10.8	11.1
<i>Chicago</i>	9	13.3	10.7
<i>Springfield</i>	6.5	15.6	6
<i>Gainesville</i>	6.5	9.2	9.5
<i>Killeen</i>	7.4	9.2	11.3
<i>Modesto</i>	12.1	12.8	5.6
Southern_Latin_America	15.3	15.5	3
Argentina	13	13	1.9
<i>Buenos_Aires</i>	11.5	19.3	1.4
<i>Cordoba</i>	13.9	7.7	1.6
Chile	21.9	18.5	4.8
<i>Santiago</i>	28.9	25.6	5.2
Uruguay	9.8	21	2.1
Western_Europe	11.7	14.3	6
Andorra	8.8	10.4	3.6
Austria	12.1	22.8	9.1
<i>Vienna</i>	14.5	26.8	10.9
Belgium	12.8	13.5	4.6
<i>Antwerp</i>	14.1	14	4.7
Cyprus	15.2	3.2	21.9
Denmark	10.2	15.7	5.4
Finland	5.2	28.2	5.2
France	11.6	16.8	3.6
<i>Paris</i>	14	25.6	3.5
<i>Le_Mans</i>	13.6	11.4	2.9
Germany	11.9	14.1	8.1
<i>Berlin</i>	16	13.5	9.5
<i>Halle</i>	14.6	13.3	9.5

<i>Oldenburg</i>	13.2	8.9	6
Greece	14.6	9.7	18.5
<i>Thessaloniki</i>	15.9	11.1	20.4
Iceland	5.6	1.7	1
Ireland	7.7	4.1	4.1
Israel	19.7	2.1	12.3
<i>Tel_Aviv</i>	21.6	2.1	12.8
Italy	15.6	19.4	5.1
<i>Palermo</i>	15	11.6	6.7
<i>Milan</i>	23.4	25.7	2.8
Luxembourg	9.9	11.3	5.6
Malta	12.4	6.5	5.5
Netherlands	12.4	11.6	5.5
<i>Zwolle</i>	11.8	10	5.9
Norway	6.5	15.5	3.3
Portugal	8.6	9.6	2.1
Spain	9.9	10.5	3.5
<i>Madrid</i>	10.1	17.9	3.2
<i>Toledo</i>	8.5	10.9	10.4
Sweden	5.7	22.7	4.6
Switzerland	10.2	20.9	4.6
<i>Lausanne</i>	12.3	22.6	4.1
United_Kingdom	10.5	10.3	5.4
<i>Sheffield</i>	11.6	11.7	6.6
<i>London</i>	13	12.7	5.5
<i>Manchester</i>	11	9.7	5.7
Monaco	11.4	17.2	3.4
San_Marino	9.8	16.4	6.4
Andean_Latin_America	25.9	8.5	0.8
Bolivia	26	5.1	0.5
<i>Cochabamba</i>	26.2	4.9	0.3
Ecuador	18.8	6.1	0.3
<i>Quito</i>	17.6	6.2	0.3
Peru	29.6	10.3	1.1
Caribbean	16.5	20.6	1.9
Antigua_and_Barbuda	16.2	17.3	0.6
The_Bahamas	13.9	7.5	3.5
Barbados	19.6	1.2	0.1
Belize	19.3	9.1	1.3
Bermuda	7	5.7	4.1
Cuba	17.5	14.5	1.7

<i>Holguin</i>	15.5	15.1	1.2
Dominica	16.8	18.5	0.8
Dominican_Republic	16.8	19.6	2.7
Grenada	19.4	1.2	0.1
Guyana	20.5	2.2	0.1
Haiti	17.8	36.5	2.1
Jamaica	15.2	19.5	1.5
Puerto_Rico	7	13.6	0.4
Saint_Lucia	19.4	1.2	0.1
Saint_Vincent_and_the_Grenadines	19.4	1.2	0.1
Suriname	21.9	1.9	0.1
Trinidad_and_Tobago	19.5	1.3	0.1
Virgin_Islands_US	8.8	14.2	0.4
Saint_Kitts_and_Nevis	8.4	16.7	0.6
Central_Latin_America	20.8	19.2	4.8
Colombia	21.3	16.2	9.5
<i>Bogota</i>	30.5	20.9	14.3
<i>Valledupar</i>	22.2	5.8	1.3
Costa_Rica	17.3	9.6	0.3
El_Salvador	22.6	35.4	2.9
<i>San_Salvador</i>	22.9	36.6	3.1
Guatemala	27.3	50.2	1.5
<i>Guatemala_City</i>	33.5	59	1.6
Honduras	22.3	29.3	1.2
Mexico	20.1	18.1	5.3
<i>Culiacan</i>	18.6	14.3	3.6
<i>Guadalajara</i>	18.9	21.5	5.2
<i>Mexico_City</i>	24.3	30	4.9
<i>Reynosa</i>	20.2	11.5	8.2
<i>Tijuana</i>	17.6	20.2	4.6
Nicaragua	19.1	15.3	0.4
<i>Leon</i>	19.9	16.8	0.4
Panama	13.7	5.4	0.5
Venezuela	20.3	2.9	0.5
<i>Caracas</i>	19.4	2.6	0.2
<i>Cabimas</i>	21.6	3	0.4
Tropical_Latin_America	11.8	23	2.8
Brazil	11.8	23.1	2.8
<i>Sao_Paulo</i>	15.3	37	3.5
<i>Curitiba</i>	8.9	29.8	3.5
<i>Florianopolis</i>	12.8	21.5	7.2

<i>Belo_Horizonte</i>	13.2	29.7	4.4
<i>Palmas</i>	10.4	3.7	0.5
<i>Ilheus</i>	13.6	8.7	0.9
<i>Jequie</i>	13.3	14.1	1.6
<i>Ribeirao_Preto</i>	14.5	25.4	3.5
Paraguay	12.5	19.4	1.1
North_Africa_and_Middle_East	44.1	3.3	6
Afghanistan	50.8	7.9	9.2
<i>Kabul</i>	64.5	9.3	15.5
Algeria	31.6	3.2	1.9
<i>Algiers</i>	34	4	2.2
<i>Tebessa</i>	33.3	3.9	2.2
Bahrain	60.8	0.5	1.6
Egypt	65.8	4.8	6.6
Cairo	80.9	5.5	6.5
<i>Alexandria</i>	56.7	4.7	9.1
Iran	38.3	1.2	2.4
<i>Tehran</i>	36.3	1.5	2.1
<i>Ahvaz</i>	71.1	0.7	2.4
<i>Gorgan</i>	39.6	1.6	2.4
<i>Qom</i>	41.6	1.2	2.1
Iraq	48.6	0.9	4.5
<i>Baghdad</i>	58.2	0.9	4.3
Jordan	32.1	1.9	10.7
Kuwait	63.1	0.5	2
Lebanon	28.5	2.2	11.9
Libya	36.2	1.9	2.6
Morocco	34	4.2	1.9
<i>Marrakesh</i>	44	3	1.2
Palestine	32.6	2.3	11.6
Oman	42.6	1.6	1.8
Qatar	71.6	0.5	1.5
Saudi_Arabia	61.5	1.1	2.1
<i>Riyadh</i>	67.7	0.7	1.7
Sudan	50	3.1	1.4
<i>Khartoum</i>	61.2	2.9	1.4
Syria	31.1	2	12.7
Tunisia	29.3	6.1	2.8
<i>Kairouan</i>	35.4	6.2	2.6
Turkey	26.1	4.7	23
<i>Istanbul</i>	26	8.4	24.1

<i>Malatya</i>	32.7	2.9	22.4
<i>Kayseri</i>	37.5	3.3	20.8
United_Arab_Emirates	42.7	0.8	1.8
Yemen	44.1	2.4	2.4
<i>Sana</i>	44.7	2.2	2.4
South_Asia	76.1	29.2	16.2
Bangladesh	61.9	29.5	14.7
<i>Rajshahi</i>	55.8	28.9	18
<i>Dhaka</i>	69.6	30.6	13.9
<i>Saidpur</i>	61.4	31.7	16.1
Bhutan	38.8	33.7	14.9
India	80.2	28.8	17.1
<i>Jaipur</i>	102.8	26.8	14
<i>Ahmedabad</i>	131.5	29	15.6
<i>Kanpur</i>	152.3	30.6	16.9
<i>Kolkata</i>	85.8	33	20.7
<i>Mumbai</i>	60	27.7	19.6
<i>Pune</i>	57	27	18.9
<i>Hyderabad</i>	47.6	24.8	18.7
<i>Belgaum</i>	44.6	23.3	17.7
<i>Coimbatore</i>	41.2	26.8	17.6
<i>Hindupur</i>	41.3	23.1	18.3
<i>Jalna</i>	52.8	24.1	19.6
<i>Kozhikode</i>	34.8	28.1	16.2
<i>Malegaon</i>	57	25.4	19.5
<i>Parbhani</i>	41.7	23.6	20.2
<i>Singrauli</i>	153.2	27.2	20.8
<i>Sitapur</i>	136.5	29.5	15.7
<i>Vijayawada</i>	56.2	24.5	19.5
Nepal	79.3	39.8	14.1
<i>Pokhara</i>	74.6	40.2	10.6
Pakistan	59.7	30.5	10.3
<i>Karachi</i>	70.8	34	10.1
<i>Lahore</i>	72.5	40.2	11.4
<i>Sialkot</i>	66	31.1	12.2
East_Asia	49.3	13.3	22.7
China	49.8	13.3	22.7
<i>Chengdu</i>	63.9	14.7	26.9
<i>Qingdao</i>	46.8	12.2	24.6
<i>Taipei</i>	22	11.1	17.6
<i>Shanghai</i>	46.2	11.3	22.4

Wuhan	64.6	14	24.4
Hangzhou	54.1	12.5	21.2
Guangzhou	39.9	15	23.4
Beijing	71.8	13.4	23.4
Tangshan	73.4	12.1	22.3
Tianjin	71.7	13.8	22.8
Jinan	70.4	13.8	25.8
Zhengzhou	82.7	13.5	23.5
Hong_Kong	23.5	15.7	24
Anqing	55.4	13.5	23
Bicheng	54.4	15.7	25.1
Changzhi	72.2	9.3	20.6
Changzhou	56.1	12	20.7
Chengguan	37.3	13.7	25
Gaoyou	54.7	13.2	23.4
Guixi	48.9	17.1	23.1
Haikou	22.4	17.2	23.4
Kaiping	39	14.6	23.2
Leshan	58.8	14.9	26.5
Pingxiang	54.3	14.3	24.4
Shenzhen	32.4	16.7	24.9
Suining	51.2	16.8	25
Xingping	68.4	14.2	22
Xucheng	56.1	13.3	24.1
Yanggu	73.6	14	25.7
Yiyang	51.1	14.6	23.9
Yucheng	34.9	14.2	22.3
Zhuji	49.4	12.8	21.6
Zunyi	45.4	14	23.8
Yulin	40.7	16.1	24.5
North_Korea	41.8	11.6	22.5
Taiwan	23.9	9.4	16.4
Oceania	12.7	7.9	0.6
American_Samoa	6.1	0.4	0.1
Federated_States_of_Micronesia	9.1	3.2	1.2
Fiji	9.8	2.2	0.3
Suva	-	-	-
Guam	7.6	1.8	0.9
Kiribati	7.6	0.6	0.1
Marshall_Islands	8.6	0.6	0.2
Northern_Mariana_Islands	7.8	2.1	1.3

Papua_New_Guinea	13.3	8.8	0.7
Samoa	9.6	0.7	0.1
Solomon_Islands	10.7	1.6	0.4
Tonga	9.6	0.4	0.2
Vanuatu	11.1	0.8	1.1
Niue	6.4	0.2	0.2
Cook_Islands	6.1	0.2	0.2
Nauru	5.6	0.5	0.1
Palau	6.7	19.1	5.3
Tokelau	7	0.3	0
Tuvalu	5.7	0.4	0.1
Southeast_Asia	20.1	31.2	12.9
Cambodia	21.2	28.3	8.8
Indonesia	18	36	11.5
<i>Medan</i>	<i>34.6</i>	<i>43.2</i>	<i>6.9</i>
<i>Palembang</i>	<i>25.6</i>	<i>33.9</i>	<i>11</i>
<i>Cirebon</i>	<i>21.4</i>	<i>39.8</i>	<i>16.4</i>
<i>Parepare</i>	<i>14.4</i>	<i>40.9</i>	<i>3.5</i>
<i>Pematangsiantar</i>	<i>25.2</i>	<i>47.3</i>	<i>5.9</i>
Laos	18.5	18.7	13
Malaysia	16.2	14.6	10
<i>Ipoh</i>	<i>17.5</i>	<i>12.1</i>	<i>10.7</i>
<i>Rawang</i>	<i>17.2</i>	<i>12.4</i>	<i>8.6</i>
Maldives	9.9	21.6	11.8
Mauritius	14.7	3.5	2.9
Myanmar	28.5	31.6	12.6
<i>Myeik</i>	<i>22.7</i>	<i>25.4</i>	<i>11.8</i>
Philippines	18.4	22.6	15.6
<i>Manila</i>	<i>27.4</i>	<i>30.3</i>	<i>23.2</i>
<i>Bacolod</i>	<i>19.7</i>	<i>19.6</i>	<i>10.4</i>
<i>Cebu_City</i>	<i>22.4</i>	<i>20.3</i>	<i>12.7</i>
Sri_Lanka	19.6	35.1	8.8
Seychelles	15.4	11.5	3.6
Thailand	26.4	29.8	12.3
<i>Bangkok</i>	<i>30.4</i>	<i>44.2</i>	<i>11.2</i>
Timor_Leste	15.3	9.4	1.2
Vietnam	20	34	17.4
<i>Vinh_Long</i>	<i>23.7</i>	<i>41.1</i>	<i>13.8</i>
<i>Ho_Chi_Minh_City</i>	<i>27.1</i>	<i>46.6</i>	<i>16.5</i>
Central_Sub_Saharan_Africa	32.2	11.8	0.6
Angola	27	5.7	1.7

<i>Luanda</i>	31.2	5.5	1.1
Central_African_Republic	41.3	4.2	0.3
Congo	35.2	11.2	0.3
Democratic_Republic_of_the_Cong	33	14	0.4
<i>Kinshasa</i>	39.4	17.4	0.2
<i>Lubumbashi</i>	27.4	12.8	1
Equatorial_Guinea	41.3	12.6	0.1
Gabon	33.3	14.8	0.2
Eastern_Sub_Saharan_Africa	28.5	21.7	2.3
Burundi	31.5	34.6	0.5
Comoros	16.1	8.9	2.7
Djibouti	41.1	4.5	2.5
Eritrea	41.6	4.7	2
Ethiopia	32.6	22.2	1.8
<i>Addis_Ababa</i>	31.5	29	1.8
Kenya	24.4	25.2	2.5
<i>Nakuru</i>	23.8	28.8	2.5
Madagascar	17.5	11.1	3.9
Malawi	23.1	12.2	3.3
Mozambique	21.4	9.5	9.4
<i>Beira</i>	24.2	8	10.2
Rwanda	33.8	40.2	0.5
<i>Kigali</i>	34.8	42.5	0.5
Somalia	28.8	6.7	2.7
South_Sudan	36.4	8.4	0.8
Tanzania	24.6	23.8	2
<i>Arusha</i>	23.1	25.4	3.2
Uganda	36.7	31.5	1
<i>Kampala</i>	48.5	38.4	1.2
Zambia	24.9	12.7	3.1
<i>Ndola</i>	26	11.6	1.9
Southern_Sub_Saharan_Africa	27	11.7	31.4
Botswana	24.3	10.2	31.2
Lesotho	29.4	11.2	31.6
Namibia	24.4	6.1	9.8
South_Africa	28.8	10.9	36.5
<i>Port_Elizabeth</i>	23.9	6.5	16.2
<i>Johannesburg</i>	40.2	12.6	44.1
Swaziland	23.1	9.4	43.7
Zimbabwe	21.7	16.7	11.8
Western_Sub_Saharan_Africa	59.4	8.9	0.2

Benin	42.6	10.9	0.2
Burkina_Faso	50.4	4.3	0.2
Cameroon	58.9	10.1	0.2
Cape_Verde	46.4	0.4	0.1
Chad	55.3	2.8	0.6
Cote_d'Ivoire	52.1	7.2	0.1
The_Gambia	58.6	1.7	0.2
Ghana	54	7.6	0.1
<i>Accra</i>	<i>64.3</i>	<i>8.4</i>	<i>0.1</i>
Guinea	50.4	4.1	0.1
Guinea_Bissau	54.6	2.5	0.2
Liberia	46.5	5.8	0.1
Mali	56.5	2.7	0.2
<i>Bamako</i>	<i>56.3</i>	<i>3.1</i>	<i>0.2</i>
Mauritania	64.3	0.7	0.1
Niger	70.9	3.3	0.3
Nigeria	64.2	12.3	0.2
<i>Ibadan</i>	<i>38.9</i>	<i>15.5</i>	<i>0.2</i>
<i>Lagos</i>	<i>34.2</i>	<i>15.5</i>	<i>0.2</i>
<i>Gombe</i>	<i>79.1</i>	<i>6.4</i>	<i>0.3</i>
<i>Oyo</i>	<i>41.1</i>	<i>15.4</i>	<i>0.2</i>
Sao_Tome_and_Principe	29.5	6.4	0.5
Senegal	60.5	1.2	0.2
Sierra_Leone	48.2	5.2	0.1
Togo	44.4	9.7	0.2
Global	41.7	20	14.1

otal Attributable Mortality Estimates

Oil and Gas Contribution (%)	Total Attributable Mortality (Deaths)			
	GBD2019 CRF	Lower 95% Confidence Interval (CRF)	Upper 95% Confidence Interval (CRF)	GEMM
10.7	60999	38899	83661	75492
17.1	3037	2012	4034	3644
14.8	7590	4617	10689	8630
11.9	-	-	-	-
13.5	3162	1792	4737	3543
10.4	9606	5643	14051	10602
9.4	-	-	-	-
11.2	2378	1442	3374	3228
9.7	1989	1418	2532	2885
9.9	-	-	-	-
8.2	4459	3049	5822	7288
11.2	3462	2164	4806	3728
9.8	25316	16762	33617	31945
7.8	-	-	-	-
10.3	-	-	-	-
14.7	92306	54865	133818	100703
15.5	1580	938	2310	1774
12	3666	2440	4874	4710
11.9	9265	5472	13561	9724
18.4	3024	1726	4502	3134
16.3	6263	3414	9521	6572
16.4	7200	3958	10902	7529
16.2	-	-	-	-
10	2845	1957	3718	3380
10.1	599	370	850	652
16.2	27725	16919	39238	31196
16	-	-	-	-
13.6	14936	8195	23045	14974
9.9	10974	7110	14947	12615
8.9	-	-	-	-

15.4	3420	1909	5135	3586
22.2	808	457	1215	857
14.3	123227	57686	205136	117852
19.3	8681	4578	13454	8560
18.3	-	-	-	-
15.6	136	9	323	98
17.2	1100	513	1849	1023
17.9	1274	534	2229	1168
16.6	-	-	-	-
14.9	2074	1009	3377	2024
13.7	68482	30672	117145	64298
17.2	-	-	-	-
7.2	-	-	-	-
13.4	-	-	-	-
16.4	-	-	-	-
14.6	-	-	-	-
16.6	-	-	-	-
14.4	41480	20371	66759	40682
14.4	-	-	-	-
16.7	-	-	-	-
12.6	2147	597	4218	2090
12.2	1802	516	3516	1757
11	-	-	-	-
14.6	346	81	702	333
14.4	-	-	-	-
18.7	59889	34089	90490	67774
19.5	35	11	68	33
18.7	38942	20649	61823	42858
20.8	-	-	-	-
19.1	-	-	-	-
16.8	-	-	-	-
17.6	-	-	-	-
16.4	-	-	-	-
18	19685	12741	26753	23414
17.6	-	-	-	-
18.3	-	-	-	-
18.9	-	-	-	-
19.4	-	-	-	-
19.1	-	-	-	-
13	-	-	-	-
27.5	1226	688	1846	1469

27.3	50594	17329	93521	49670
21.3	3686	1157	6967	3632
23.6	-	-	-	-
21.4	-	-	-	-
24.1	3	0	8	3
27.9	46904	16172	86546	46035
28.3	-	-	-	-
31.8	-	-	-	-
31.1	-	-	-	-
27	-	-	-	-
28.6	-	-	-	-
21.9	-	-	-	-
28.5	-	-	-	-
31.1	-	-	-	-
31.6	-	-	-	-
30.8	-	-	-	-
26.2	-	-	-	-
29.8	-	-	-	-
22.1	-	-	-	-
15.5	18377	9779	28513	20581
17.1	12197	6138	19540	13619
23.2	-	-	-	-
15.3	-	-	-	-
12.7	5409	3295	7651	6199
15	-	-	-	-
21	772	345	1322	763
25.5	114536	56831	185059	118698
26.1	10	4	17	10
21.3	2358	1136	3824	2368
19.1	-	-	-	-
25.8	3458	1798	5471	3717
24.3	-	-	-	-
14.2	378	201	577	392
26.7	1348	633	2236	1403
15.1	280	6	741	254
28.4	13251	6545	21491	13733
27.7	-	-	-	-
29.9	-	-	-	-
23.7	26869	13026	43657	27266
22.4	-	-	-	-
23	-	-	-	-

29.3	-	-	-	-
14.1	5592	3019	8723	5806
13.4	-	-	-	-
14.4	14	1	32	13
30	496	171	922	499
20.6	2161	1263	3119	2436
20.6	-	-	-	-
25.4	24366	13450	37014	25517
17.7	-	-	-	-
29.1	-	-	-	-
28.5	85	38	144	85
18.1	135	65	220	138
27.5	4574	2378	7212	4847
28.1	-	-	-	-
17.1	384	90	783	385
26.4	2202	884	3989	2202
29.3	9026	4145	15201	9163
34.7	-	-	-	-
31	-	-	-	-
18.3	614	51	1445	583
28	1398	627	2367	1404
27.3	-	-	-	-
26.8	15518	7290	25840	16453
24.8	-	-	-	-
27.7	-	-	-	-
25	-	-	-	-
30.8	15	7	24	15
25.6	5	2	9	5
15	15247	9354	21463	21966
8.4	3393	2108	4722	5522
8.3	-	-	-	-
34	3853	2181	5678	4518
34.7	-	-	-	-
10.7	8000	5064	11064	11927
22.3	14258	7804	21590	19138
10.8	28	15	42	29
29.8	84	43	132	86
3.1	155	89	225	172
18.4	76	43	110	100
22.2	8	2	15	7
31.4	5918	3323	8889	6639

30.5	-	-	-	-
10.6	29	16	44	33
22.3	3453	1883	5241	3951
3.6	47	27	68	54
2.6	402	235	577	472
19.4	1504	846	2248	4860
29.3	893	479	1356	967
11.9	430	104	857	415
3.7	71	42	103	81
3.7	57	32	83	65
2.6	253	153	357	302
3.8	813	459	1173	870
11.8	30	11	54	28
11.5	8	3	16	8
21.1	65630	38150	94095	85241
15.7	11818	7074	16861	14390
15.2	-	-	-	-
19.7	-	-	-	-
15.7	888	494	1331	974
17.6	1803	1064	2571	2502
17.4	-	-	-	-
12	3338	2051	4644	7029
13.7	-	-	-	-
18.8	1581	976	2221	3250
27.7	34259	19616	49136	43465
27.5	-	-	-	-
30.3	-	-	-	-
29.5	-	-	-	-
28	-	-	-	-
29.5	-	-	-	-
14.5	863	487	1264	1616
15.4	-	-	-	-
19.2	643	328	1013	694
13.4	10436	6060	15054	11322
12.6	-	-	-	-
19.2	-	-	-	-
16.8	42973	20585	70359	45750
17	41992	20110	68776	44559
20.8	-	-	-	-
22.4	-	-	-	-
21	-	-	-	-

22.1	-	-	-	-
4.7	-	-	-	-
13.3	-	-	-	-
16.1	-	-	-	-
21.6	-	-	-	-
11.8	981	475	1583	1192
18.1	317861	227116	404247	419282
10.5	7110	5208	8918	29383
10.2	-	-	-	-
28.6	19437	12897	25909	22018
39.1	-	-	-	-
23.6	-	-	-	-
28.7	551	412	671	776
17.5	87957	67883	106168	110679
19.2	-	-	-	-
17.5	-	-	-	-
23.5	40870	28535	52551	48441
29.4	-	-	-	-
23.4	-	-	-	-
25.2	-	-	-	-
27	-	-	-	-
22.8	22830	16961	28159	27431
23.5	-	-	-	-
19.7	2622	1745	3466	3077
21.9	1370	1046	1666	1754
21.5	3240	2037	4445	3693
6.8	3030	2093	3925	3535
12.8	25152	17055	32982	30306
6.9	-	-	-	-
20.4	1695	1132	2234	1992
12.6	1617	1149	2053	1951
25.4	459	354	552	625
22.9	16992	13138	20453	20827
22.7	-	-	-	-
7.6	13005	9667	16117	25334
7.6	-	-	-	-
19.4	10039	6572	13454	11249
21.4	6946	4507	9394	7808
21.9	-	-	-	-
16.6	41149	26190	56294	47245
18.8	-	-	-	-

15.7	-	-	-	-
15.8	-	-	-	-
19.1	2783	2019	3475	3331
16.4	9006	6517	11362	17827
16.9	-	-	-	-
14.6	1032907	810092	1238344	2146883
19.2	63718	49507	76737	158987
16.8	-	-	-	-
19.7	-	-	-	-
17.6	-	-	-	-
13.2	240	170	306	524
14.2	866566	682014	1036734	1752666
15.4	-	-	-	-
12.8	-	-	-	-
15.8	-	-	-	-
13.8	-	-	-	-
12.1	-	-	-	-
12.3	-	-	-	-
11.6	-	-	-	-
14.4	-	-	-	-
12.6	-	-	-	-
11.5	-	-	-	-
12.7	-	-	-	-
12.3	-	-	-	-
12.5	-	-	-	-
12.5	-	-	-	-
10.5	-	-	-	-
15.9	-	-	-	-
11.5	-	-	-	-
12.3	15905	12615	19009	39195
10.9	-	-	-	-
14.5	86477	65786	105558	195510
12.7	-	-	-	-
15.7	-	-	-	-
16.6	-	-	-	-
11.1	1418337	1075605	1738024	2049784
11	1386689	1053525	1696981	1992762
9	-	-	-	-
12.2	-	-	-	-
15.9	-	-	-	-
9.6	-	-	-	-

10.5	-	-	-	-
11	-	-	-	-
11.7	-	-	-	-
14.3	-	-	-	-
13.1	-	-	-	-
13.8	-	-	-	-
11	-	-	-	-
9.6	-	-	-	-
12	-	-	-	-
10.6	-	-	-	-
11	-	-	-	-
8.9	-	-	-	-
10.5	-	-	-	-
7.4	-	-	-	-
12.1	-	-	-	-
10.8	-	-	-	-
10.4	-	-	-	-
13.7	-	-	-	-
10.2	-	-	-	-
9.3	-	-	-	-
10.6	-	-	-	-
10.1	-	-	-	-
10.7	-	-	-	-
12.1	-	-	-	-
10.8	-	-	-	-
11	-	-	-	-
10.5	-	-	-	-
11.4	-	-	-	-
8.5	-	-	-	-
10.4	-	-	-	-
12.8	20110	14907	25011	43106
16.6	11539	7172	16032	13916
7.6	1381	631	2286	3812
3.2	7	1	16	5
4.6	25	9	45	30
6.1	273	104	476	311
-	-	-	-	-
8.5	25	7	48	22
2.6	11	3	23	23
1.8	10	4	19	12
8	9	3	17	8

8	841	424	1330	2977
3.3	32	13	56	46
5.5	80	35	137	260
3.6	18	7	30	21
4.7	42	19	70	90
3.2	0	0	1	0
3.4	2	0	4	2
1.6	1	0	2	1
17.6	4	1	9	4
2.4	0	0	0	0
1.6	1	0	3	1
13	230616	138209	332098	326462
7.2	2975	1788	4291	7983
16.3	93807	54694	137546	119054
22.2	-	-	-	-
14.5	-	-	-	-
15.2	-	-	-	-
20.8	-	-	-	-
18.8	-	-	-	-
7.5	1087	631	1604	2831
23.6	9619	5179	14843	10569
22	-	-	-	-
29.2	-	-	-	-
11.1	37	16	64	37
9.8	574	293	879	595
8.9	21691	14555	28851	46930
9.6	-	-	-	-
12.9	29306	16666	43512	43218
12.7	-	-	-	-
13.8	-	-	-	-
14	-	-	-	-
12.4	6940	3979	10055	9675
8.2	33	18	52	37
11.4	29501	18954	40308	38193
12.4	-	-	-	-
11.7	183	100	283	386
9	34862	21336	49809	46955
7.8	-	-	-	-
8.4	-	-	-	-
2.5	15279	10064	20591	53321
3.3	3851	2425	5351	8764

4.3	-	-	-	-
2.7	738	508	967	4423
3.4	1367	932	1790	2589
2.2	8344	5536	11198	36180
3.5	-	-	-	-
1.6	-	-	-	-
3.7	288	201	371	439
3.3	691	462	913	927
8.5	31529	20012	43791	131540
4.7	731	480	989	4539
6.3	75	41	116	205
16	343	239	445	592
14.2	1078	747	1403	3668
11.3	6473	4239	8765	33633
11.9	-	-	-	-
13.4	5029	3101	7115	12872
15.7	-	-	-	-
6	1768	1006	2664	6616
3.5	1070	644	1539	4842
5.3	1506	906	2175	8492
5.5	-	-	-	-
5.6	1325	890	1762	4827
6	-	-	-	-
7.9	583	365	817	9549
5.5	1084	712	1469	4609
5.9	4856	2961	6929	18021
10.2	-	-	-	-
7.8	3430	2317	4545	13648
9.9	-	-	-	-
2.7	2179	1363	3058	5427
2	-	-	-	-
9.2	29840	18964	40735	45500
9	803	492	1125	1213
10.5	781	506	1056	1800
4.4	697	429	979	1128
10	25035	16073	33892	34898
12.4	-	-	-	-
10.1	-	-	-	-
7.6	303	182	427	561
6.3	2221	1282	3256	5900
3.4	94736	68733	119976	320839

5.3	1686	1158	2216	7039
2.4	2666	1855	3479	16949
3.3	7777	5708	9754	19088
1.4	244	175	310	393
3.2	1979	1396	2567	13333
3.7	4970	3553	6359	16003
1.9	407	302	508	1538
4.7	10734	7908	13427	22565
5.3	-	-	-	-
2.1	2084	1468	2698	11118
1.9	291	213	365	1400
3.1	506	360	646	2170
1.7	2176	1574	2769	14124
1.8	-	-	-	-
1	1117	835	1382	2501
1.9	2232	1632	2812	19482
3.8	50577	36761	63987	152639
6.2	-	-	-	-
6.1	-	-	-	-
3.1	-	-	-	-
6.3	-	-	-	-
2.7	45	29	61	98
1.6	2732	2034	3391	9924
2.6	1236	868	1601	6034
5	1278	903	1644	4440
13.2	3832670	2715393	4972016	6222380

Data File 3: PM_{2.5} Exposure Estimates for the year 2019

McDuffie et al., 2021 -

Last Updated: March 23, 2021

Name Legend:

Regions Countries *Sub-national regions*

Name	2019 Population Weighted Annual Average PM _{2.5} (µg m ⁻³)
Central_Asia	24.5
Armenia	30.7
Azerbaijan	24.3
<i>Baku</i>	<i>34.2</i>
Georgia	17.6
Kazakhstan	19.2
<i>Shymkent</i>	<i>37.8</i>
Kyrgyzstan	22.7
Mongolia	39
<i>Ulaanbaatar</i>	<i>86.2</i>
Tajikistan	35.6
Turkmenistan	24.6
Uzbekistan	32.3
<i>Bukhara</i>	<i>26</i>
<i>Tashkent</i>	<i>50</i>
Central_Europe	20.2
Albania	19.2
Bosnia_and_Herzegovina	29.3
Bulgaria	19.4
Croatia	18.1
Czech_Republic	16.8
Hungary	16.5
<i>Budapest</i>	<i>19.6</i>
Macedonia	30.3
Montenegro	20.9
Poland	22.6
<i>Warsaw</i>	<i>23.8</i>
Romania	15.8
Serbia	25.2
<i>Belgrade</i>	<i>24.3</i>
Slovakia	18.5
Slovenia	17.2
Eastern_Europe	11.9
Belarus	16.3

<i>Gomel</i>	20
Estonia	5.9
Latvia	11.9
Lithuania	10.3
<i>Kaunas</i>	12.1
Moldova	13.5
Russian_Federation	11
<i>Saint_Petersburg</i>	8.2
<i>Astrakhan</i>	12
<i>Moscow</i>	13.5
<i>Tyumen</i>	13.8
<i>Berezniki</i>	13.4
<i>Dzerzhinsk</i>	11.6
Ukraine	14
<i>Nikolaev</i>	14.7
<i>Rovno</i>	20.1
Australasia	6.8
Australia	6.9
<i>Sydney</i>	7.6
New_Zealand	6.6
<i>Auckland</i>	6.4
High_income_Asia_Pacific	17.4
Brunei	7.8
Japan	13.4
<i>Tokyo</i>	15
<i>Osaka</i>	15
<i>Fukuoka</i>	17.7
<i>Okayama</i>	13.1
<i>Yamaguchi</i>	12.9
South_Korea	27.2
<i>Seoul</i>	28.1
<i>Busan</i>	24.8
<i>Cheonan</i>	29.4
<i>Gwangju</i>	27.7
<i>Jinju</i>	28.4
<i>Pyongyang</i>	55.8
Singapore	18.7
High_income_North_America	7.7
Canada	7.1
<i>Montreal</i>	8.8
<i>Victoria</i>	5.9
Greenland	5.2
United_States	7.7

<i>Raleigh</i>	7.7
<i>New_York</i>	7.7
<i>Philadelphia</i>	8.4
<i>Houston</i>	9.7
<i>Minneapolis</i>	7.3
<i>Portland</i>	7.3
<i>Los_Angeles</i>	10.2
<i>Cleveland</i>	8.7
<i>Chicago</i>	9.2
<i>Springfield</i>	6.4
<i>Gainesville</i>	6.6
<i>Killeen</i>	7.3
<i>Modesto</i>	12
Southern_Latin_America	15.5
<i>Argentina</i>	12.9
<i>Buenos_Aires</i>	11.5
<i>Cordoba</i>	14.2
<i>Chile</i>	22.7
<i>Santiago</i>	30.2
<i>Uruguay</i>	9.7
Western_Europe	11.6
<i>Andorra</i>	8.7
<i>Austria</i>	12.3
<i>Vienna</i>	14.5
<i>Belgium</i>	12.7
<i>Antwerp</i>	13.9
<i>Cyprus</i>	15.6
<i>Denmark</i>	9.7
<i>Finland</i>	5.5
<i>France</i>	11.6
<i>Paris</i>	13.7
<i>Le_Mans</i>	13.5
<i>Germany</i>	11.8
<i>Berlin</i>	15.5
<i>Halle</i>	14.6
<i>Oldenburg</i>	12.7
<i>Greece</i>	14.3
<i>Thessaloniki</i>	15.2
<i>Iceland</i>	5.6
<i>Ireland</i>	7.9
<i>Israel</i>	19.3
<i>Tel_Aviv</i>	21.1
<i>Italy</i>	15.6

<i>Palermo</i>	15.1
<i>Milan</i>	23.1
Luxembourg	10.2
Malta	12.9
Netherlands	12
<i>Zwolle</i>	11.3
Norway	6.5
Portugal	8.4
Spain	9.9
<i>Madrid</i>	10.3
<i>Toledo</i>	8.9
Sweden	5.7
Switzerland	10.2
<i>Lausanne</i>	12.3
United_Kingdom	10.2
<i>Sheffield</i>	11.4
<i>London</i>	12.4
<i>Manchester</i>	10.9
Monaco	11.6
San_Marino	9.9
Andean_Latin_America	26.3
Bolivia	25.7
<i>Cochabamba</i>	26
Ecuador	19.6
<i>Quito</i>	18.4
Peru	30.1
Caribbean	16.3
Antigua_and_Barbuda	16.5
The_Bahamas	14.1
Barbados	20.1
Belize	19.5
Bermuda	6.9
Cuba	16.8
<i>Holguin</i>	15.7
Dominica	17.3
Dominican_Republic	16.8
Grenada	19.9
Guyana	18.9
Haiti	17.6
Jamaica	15
Puerto_Rico	7.1
Saint_Lucia	19.9
Saint_Vincent_and_the_Gren	19.8

Suriname	19.9
Trinidad_and_Tobago	20.1
Virgin_Islands_US	8.9
Saint_Kitts_and_Nevis	8.6
Central_Latin_America	20.6
Colombia	21.3
<i>Bogota</i>	29.6
<i>Valledupar</i>	22.7
Costa_Rica	17.2
El_Salvador	21.7
<i>San_Salvador</i>	21.9
Guatemala	27.1
<i>Guatemala_City</i>	32.8
Honduras	22.5
Mexico	19.8
<i>Culiacan</i>	18.2
<i>Guadalajara</i>	18.9
<i>Mexico_City</i>	24.1
<i>Reynosa</i>	19.5
<i>Tijuana</i>	18
Nicaragua	19.8
<i>Leon</i>	20
Panama	13
Venezuela	20.5
<i>Caracas</i>	19.8
<i>Cabimas</i>	22.3
Tropical_Latin_America	11.8
Brazil	11.7
<i>Sao_Paulo</i>	15.3
<i>Curitiba</i>	9.1
<i>Florianopolis</i>	13.3
<i>Belo_Horizonte</i>	13.3
<i>Palmas</i>	10.1
<i>Ilheus</i>	14.1
<i>Jequie</i>	14.4
<i>Ribeirao_Preto</i>	14.1
Paraguay	12.5
North_Africa_and_Middle_E:	43.9
Afghanistan	49.9
<i>Kabul</i>	62.6
Algeria	31.9
<i>Algiers</i>	33.9
<i>Tebessa</i>	34.8

Bahrain	58.4
Egypt	66.6
<i>Cairo</i>	<i>81.9</i>
<i>Alexandria</i>	<i>57.3</i>
Iran	37.4
<i>Tehran</i>	<i>35.1</i>
<i>Ahvaz</i>	<i>70.6</i>
<i>Gorgan</i>	<i>36.9</i>
<i>Qom</i>	<i>40.7</i>
Iraq	47.1
<i>Baghdad</i>	<i>57.4</i>
Jordan	30.3
Kuwait	60.7
Lebanon	28.3
Libya	36.9
Morocco	35.2
<i>Marrakesh</i>	<i>49.4</i>
Palestine	31.6
Oman	43
Qatar	67.8
Saudi_Arabia	59.3
<i>Riyadh</i>	<i>64.3</i>
Sudan	51
<i>Khartoum</i>	<i>63.4</i>
Syria	30.7
Tunisia	29.9
<i>Kairouan</i>	<i>34.7</i>
Turkey	25.9
<i>Istanbul</i>	<i>26.4</i>
<i>Malatya</i>	<i>29.1</i>
<i>Kayseri</i>	<i>32.1</i>
United_Arab_Emirates	42.5
Yemen	42.4
<i>Sana</i>	<i>42.3</i>
South_Asia	77.3
Bangladesh	62.6
<i>Rajshahi</i>	<i>54.5</i>
<i>Dhaka</i>	<i>69.1</i>
<i>Saidpur</i>	<i>66.4</i>
Bhutan	38.9
India	81.6
<i>Jaipur</i>	<i>102.4</i>
<i>Ahmedabad</i>	<i>134</i>

<i>Kanpur</i>	154.1
<i>Kolkata</i>	87
<i>Mumbai</i>	60
<i>Pune</i>	63.2
<i>Hyderabad</i>	50
<i>Belgaum</i>	46.1
<i>Coimbatore</i>	43
<i>Hindupur</i>	41.4
<i>Jalna</i>	55.3
<i>Kozhikode</i>	34.9
<i>Malegaon</i>	56.6
<i>Parbhani</i>	42.2
<i>Singrauli</i>	157.5
<i>Sitapur</i>	137.7
<i>Vijayawada</i>	56.8
<i>Nepal</i>	81.4
<i>Pokhara</i>	72.2
<i>Pakistan</i>	60.5
<i>Karachi</i>	70.9
<i>Lahore</i>	74.4
<i>Sialkot</i>	66.9
East_Asia	47.1
<i>China</i>	47.6
<i>Chengdu</i>	61.4
<i>Qingdao</i>	44
<i>Taipei</i>	20.8
<i>Shanghai</i>	44.9
<i>Wuhan</i>	61.4
<i>Hangzhou</i>	51.8
<i>Guangzhou</i>	38.1
<i>Beijing</i>	71.4
<i>Tangshan</i>	74.6
<i>Tianjin</i>	71.8
<i>Jinan</i>	67.9
<i>Zhengzhou</i>	75.2
<i>Hong_Kong</i>	23
<i>Anqing</i>	50.6
<i>Bicheng</i>	50.6
<i>Changzhi</i>	64.2
<i>Changzhou</i>	51.8
<i>Chengguan</i>	34.9
<i>Gaoyou</i>	50.9
<i>Guixi</i>	44.9

<i>Haikou</i>	21.7
<i>Kaiping</i>	37.8
<i>Leshan</i>	54.3
<i>Pingxiang</i>	51.3
<i>Shenzhen</i>	31.4
<i>Suining</i>	49.8
<i>Xingping</i>	60.1
<i>Xucheng</i>	51.5
<i>Yanggu</i>	70
<i>Yiyang</i>	47.1
<i>Yucheng</i>	33.4
<i>Zhuji</i>	47.2
<i>Zunyi</i>	43.5
<i>Yulin</i>	38.8
North_Korea	43.3
Taiwan	23.9
Oceania	12.9
American_Samoa	6.1
Federated_States_of_Micron	9.2
Fiji	9.7
<i>Suva</i>	-
Guam	8.1
Kiribati	7.5
Marshall_Islands	8.5
Northern_Mariana_Islands	8.1
Papua_New_Guinea	13.5
Samoa	9.7
Solomon_Islands	11.1
Tonga	9.5
Vanuatu	11.1
Niue	6.5
Cook_Islands	6.1
Nauru	5.6
Palau	6.6
Tokelau	7
Tuvalu	5.7
Southeast_Asia	20.5
Cambodia	21.3
Indonesia	18.7
<i>Medan</i>	33.2
<i>Palembang</i>	27.1
<i>Cirebon</i>	23
<i>Parepare</i>	15

<i>Pematangsiantar</i>	23.7
Laos	19.7
Malaysia	16.3
<i>Ipoh</i>	17
<i>Rawang</i>	17.5
Maldives	9.6
Mauritius	14.8
Myanmar	28.8
<i>Myeik</i>	23.5
Philippines	18.6
<i>Manila</i>	28.5
<i>Bacolod</i>	19.9
<i>Cebu_City</i>	21.2
Sri_Lanka	19.6
Seychelles	15
Thailand	26.9
<i>Bangkok</i>	30.2
Timor_Leste	15.2
Vietnam	20
<i>Vinh_Long</i>	23.7
<i>Ho_Chi_Minh_City</i>	27
Central_Sub_Saharan_Africa	32.6
Angola	27.4
<i>Luanda</i>	31.9
Central_African_Republic	43
Congo	36
Democratic_Republic_of_the_	33.3
<i>Kinshasa</i>	38.7
<i>Lubumbashi</i>	27.6
Equatorial_Guinea	43.6
Gabon	34.5
Eastern_Sub_Saharan_Africa	27.4
Burundi	32
Comoros	16.5
Djibouti	40.8
Eritrea	41.8
Ethiopia	32.5
<i>Addis_Ababa</i>	31.9
Kenya	21.1
<i>Nakuru</i>	20.1
Madagascar	17.3
Malawi	21.6
Mozambique	20.1

<i>Beira</i>	24.1
Rwanda	34.4
<i>Kigali</i>	35.2
Somalia	29
South_Sudan	35.4
Tanzania	24
<i>Arusha</i>	19.9
Uganda	33.6
<i>Kampala</i>	42
Zambia	24.7
<i>Ndola</i>	26.1
Southern_Sub_Saharan_Afric	26.4
Botswana	24.1
Lesotho	27.2
Namibia	23.4
South_Africa	28.6
<i>Port_Elizabeth</i>	23.9
<i>Johannesburg</i>	40.2
Eswatini	23
Zimbabwe	20.1
Western_Sub_Saharan_Afric	59.9
Benin	44
Burkina_Faso	50.6
Cameroon	61
Cape_Verde	45.2
Chad	55.1
Cote_dIvoire	52.5
The_Gambia	55.6
Ghana	52.2
<i>Accra</i>	61.7
Guinea	49.5
Guinea_Bissau	51.6
Liberia	48.6
Mali	55.7
<i>Bamako</i>	55.3
Mauritania	61.8
Niger	72.5
Nigeria	65.3
<i>Ibadan</i>	42.1
<i>Lagos</i>	35.7
<i>Gombe</i>	78.5
<i>Oyo</i>	45.2
Sao_Tome_and_Principe	30.5

Senegal	57.5
Sierra_Leone	49
Togo	44.1
Global	41.7